BNL-82 (S-7)

BROOKHAVEN NATIONAL LABORATORY

Quarterly Progress Report
July 1 - Sept. 30, 1950

Associated Universities, Inc.
under contract with the
United States Atomic Energy Commission

BROOKHAVEN NATIONAL LABORATORY

QUARTERLY PROGRESS REPORT

July 1 - September 30, 1950

Associated Universities, Inc.
under contract with the
United States Atomic Energy Commission

Printed at Upton, New York, for distribution
to individuals and organizations associated
with the national atomic energy program.

November, 1950 600 copies

FOREWORD

This is the third of a series of Quarterly Progress Reports. While most of the departments have summarized their work or used a form comparable to abstracts, the Chemistry Department has given both abstracts and complete reports on its work. The major part of the progress in the Reactor Science and Engineering Department is being presented simultaneously in a separate classified report.

CONTENTS

PHYSICS DEPARTMENT

As in previous quarterly reports, subjects are presented only when significant progress has been accomplished and the report is of definite scientific interest. In most instances, the material presented is an abstract or an abridged edition of a more complete coverage of the work which is either already submitted or is about to be submitted for publication in a scientific journal or for oral presentation before a scientific society. The items have been grouped under five general headings: 1) dynamic properties of nuclei, 2) stationary properties of nuclei, 3) high energy particle physics, 4) general physics, sometimes utilizing nuclear techniques, and 5) theoretical topics.

Dynamic Properties of Nuclei

Decay of Yb^{169}

de Benedetti and McGowan (Phys.Rev. 74, 736 (1948)) have reported that following K-capture in Yb^{169} (33-day half-life), a converted gamma ray of 400 kev is emitted, leading to an isomeric state of 1 μsec lifetime, which decays to the ground state by emission of an internally converted gamma ray of 190 kev. Recent work by Cork et al. (Phys.Rev. 78, 95 (1950)) has revealed the presence of several gamma rays. We have investigated the decay scheme by scintillation counter coincidence techniques; approximate K/L ratios for the conversion lines, obtained with a 180° permanent magnet-type spectrograph, have been used in assigning a level scheme. Only K and L X-rays of Tm, and no gamma rays or internal conversion electrons, precede the isomeric state. The lifetime of the isomeric state is 6.0×10^{-7} sec, in agreement with an independent measurement by Fuller (Proc.Roy.Soc. 63A, 1044 (1950)). The isomeric state is probably 307 kev above the ground state, and decays in three alternative ways: 1) the 307-kev transition to the ground state, 2) a 177-kev gamma ray followed by a 130-kev gamma ray, and 3) a 198-kev gamma ray followed by a 109-kev gamma ray.

Radiation of 7-hr Mo^{93} Isomer

This isomer was produced in the Columbia cyclotron by bombardment of Cb by deuterons. The lifetime-determining transition of this isomer of extraordinarily large excitation energy is found to have an energy of 256 kev and a K/L ratio of 2.8 ± 0.3, which is compatible with a 2^5 pole electric transition. The isomeric transition is followed by gamma rays of 1.5 Mev and 0.7 Mev, which have been measured with scintillation counters and by pulse height discrimination.

Radiations of Cr^{51}

This isotope was produced by neutron capture in enriched Cr^{50} at Oak Ridge National Laboratory. The previously reported conversion line

(Rev. Mod. Phys. 22, 36 (1950)) of 230-260 kev is not found in this sample.

Radiations of W^{181}(140 d)

This isotope is shown to be produced in good yield by bombarding ordinary W with slow neutrons. Among its radiations are K X-rays and gamma rays of 30, 600 and 800 kev. These radiations have been found in an aged W sample, but no direct isotopic assignment has yet been made.

High Energy Gamma Rays of Rh^{106}

The gamma rays of Rh^{106}, previously reported to be capable of producing photoneutrons in Be and D, have been studied with a scintillation counter and were found to have an energy of 2.9 Mev.

(D. Alburger, E. der Mateosian, G. Friedlander, M. Goldhaber, J.W. Mihelich G. Scharff-Goldhaber, A.W. Sunyar)

Detection of Gamma Radiation Resulting from Neutron Capture

An investigation has been made of the possibility of detecting neutrons captured in a material such as boron by the scintillations produced in a crystal or a liquid by the emitted gamma radiation. For example, B^{10} emits a 480-kev gamma ray in 92% of the captures, and these can be detected with high efficiency in a crystal of NaI activated with thallium. This type of detector has the advantage over a BF_3 counter in that a large effective mass of absorbing material for the neutrons can be used without stopping the gamma rays from escaping into the scintillator; its efficiency is mainly limited by the solid angle the scintillator subtends at the absorber. There is special need for an increase in detector efficiency such as this device may offer in the region of neutron energies above 100 ev, and below the energy where proton recoils can be observed, since within these limits the BF_3 counters suffer from a very low efficiency. The fast rise time of the scintillation detector may also prove advantageous in time-of-flight experiments where, too, its relatively small spatial extension will reduce the errors usually resulting from poor localization of the captured neutron. Another advantage results from the fact that the pulse produced in the scintillator is proportional to the energy of the gamma ray and the pulse height distribution reveals the spectrum of gamma rays emitted. Background intensity may thus be reduced by selecting the pulse height.

Although no systematic experiments were done to determine the efficiency of a scintillation detector of the type described, the results obtained in the following experiment allow one to estimate that efficiencies of 20% can be achieved with crystals of readily available sizes.

Using a Po-Be neutron source, yielding 100 neutrons per sec on an absorber of cadmium, and recording coincidences between selected pulse heights (at poor resolution because of the low intensity), evidence has been obtained which indicates that neutron capture in cadmium is followed in some cases by a cascade of at least 4 gamma rays having energies of approximately 0.8 Mev, 1.3 Mev, 2.8 Mev, and 3.5 Mev. Each value is subject to an error of about

0.2 Mev. The sum of the energies in this cascade (8.4 Mev) is in fair agreement with the value reported by Hamermesh (ANL report 4447, 1950) for the most energetic gamma ray from neutron capture.

(E. Church, L. Madansky)

Reflection of Neutrons from Magnetic Mirrors

The index of refraction for neutrons in ferromagnetic materials has been studied by total reflection from mirrors. It is shown that Bloch's constant, C, is unity, i.e., the effective field for neutrons in a ferromagnet is B . For the case of total reflection, it is found that the magnetic part of the index is given by the field averaged over a region that is large compared to the size of the magnetic domains. Completely polarized thermal neutrons have been produced, without the necessity of monochromatization, by reflection from magnetized cobalt. Measurement of the polarization, performed by reflection at a second cobalt mirror, requires careful elimination of reorientation effects in the region between the mirrors. An extensive report on this work has been submitted for publication in Physical Review.

(D.J. Hughes; M.T. Burgy, Argonne National Laboratory)

Scattering and Polarization of Neutrons in an Iron Single Crystal

In 1947, Halpern (Phys.Rev. 72, 260 (1947)), stimulated by work of Shull and Wollan (Phys.Rev. 72, 168 (1947)) which indicated excessive incoherent neutron scattering, suggested the use of iron single crystals to reveal the source of the incoherent scattering. When slow neutrons are transmitted through a single crystal (oriented so that no Bragg scattering occurs), only incoherent scattering is observed. Halpern pointed out that of the three main sources of incoherent scattering (isotope disorder, spin-dependent scattering, and inelastic lattice scattering), only the last would be affected by a magnetic field and hence would be capable of producing neutron polarization. By measuring the neutron polarization as well as the transmission with an iron crystal, it would then be possible to isolate the inelastic scattering. Although most of the diffuse scattering observed by Shull and Wollan (Phys.Rev. 73, 830 (1948)) later proved to be instrumental (multiple scattering in the samples), it was important to investigate the iron single crystal because of the large polarization effects that had been observed in polycrystals by Bloch et al. (Phys.Rev. 70, 972 (1946)) and by Hughes et al. (Phys.Rev. 73, 1277 (1948)) as compared with theoretical estimates by Halpern, Hamermesh, and Johnson (Phys.Rev. 59, 986 (1941)). The latter authors had subtracted 2.5 barns of isotope disorder scattering from the cross section of iron in their calculation of neutron polarization and it seemed likely that the isotope effect was actually much smaller.

A single crystal of iron, 2 x 2 x 3 cm, containing 10% (by weight) of silicon was obtained from M.I.T. The total cross section of the single crystal, measured with monoenergetic neutrons obtained with the Argonne "chopper," is shown in Figure 1, together with earlier results for a polycrystalline sample. The single crystal cross section is much smaller than that of the polycrystal, especially in the region just above the "cut off" velocity (980 m/sec, below

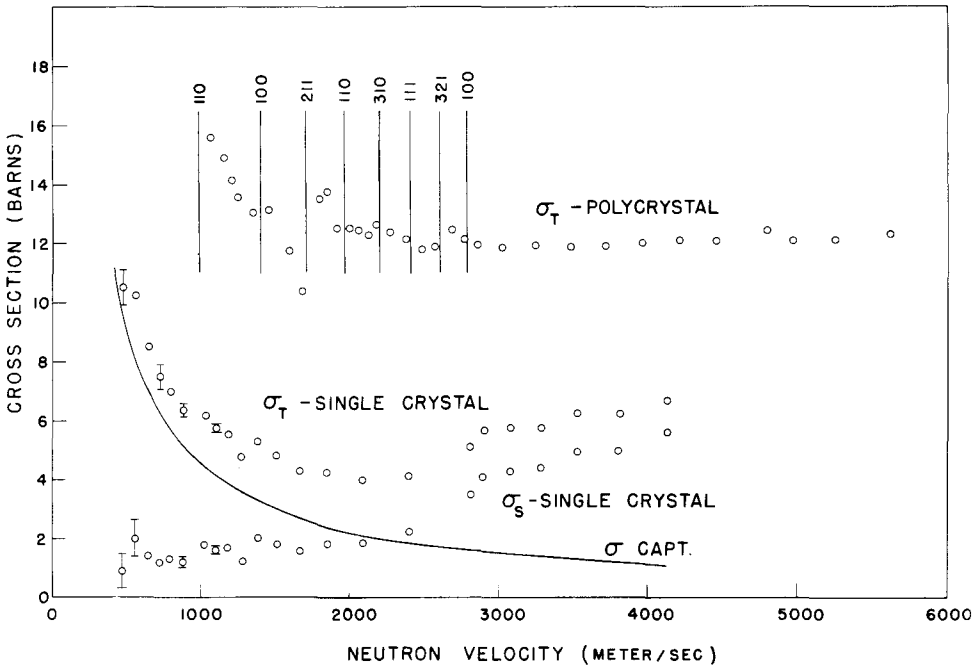

Figure 1. Measured total cross sections of an iron polycrystal and a single crystal of iron-silicon. The scattering cross section of the single crystal, σ_S, obtained by subtraction of capture, is also shown. The vertical lines are the limiting velocities for reflection by lattice planes, marked with the appropriate Miller indices.

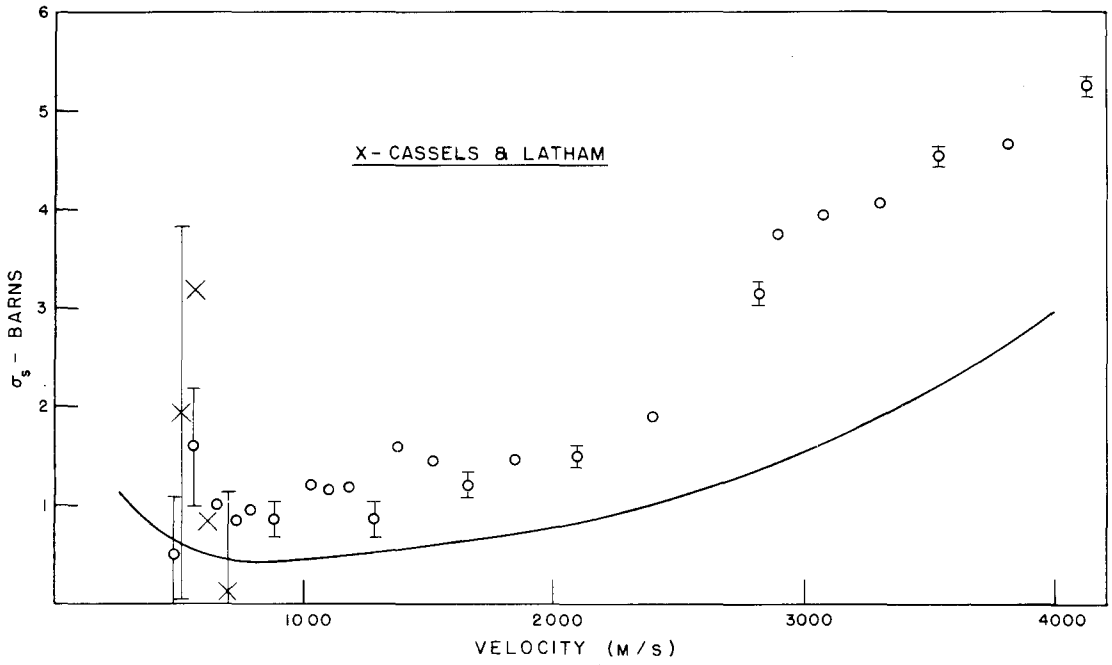

Figure 2. The incoherent scattering of the iron-silicon single crystal after subtraction of the calculated scattering resulting from the assumed random location of the silicon atoms. Results of Cassells and Latham and the calculated inelastic scattering (Weinstock) are shown for comparison.

which velocity the polycrystal exhibits no coherent scattering). The points marked σ_s are those for the single crystal after subtraction of the capture cross section, taken as 1/v and equal to 2.45 b at 2200 m/s for iron. (The single crystal cross sectionsin Figure 1 all refer to the "average atom" in the crystal, containing 18% silicon atoms.)

After an additional 0.40 b is subtracted from the single crystal points, to take account of the incoherent scattering caused by the assumed random location of the silicon atoms, the remaining scattering, shown in Figure 2, represents the incoherent scattering of the crystal. Some points obtained by Cassels and Latham (Phys.Rev. 74, 103 (1948)) are also shown (their data have been reanalyzed, using 2.45 b for capture instead of their 2.2 b), as well as the inelastic scattering calculated by them from the theory developed by Weinstock (Phys.Rev. 65, 1 (1944)). The variation of the incoherent scattering with velocity suggests that the scattering is mainly inelastic and about twice the calculated value. Both spin-dependent and isotope disorder scattering, in contrast to the inelastic scattering, would show no change with neutron velocity.

The polarization, which would result from inelastic scattering but not from other incoherent scattering, was next sought and found by magnetizing the crystal in a field of 11,000 oersteds and measuring the single transmission effect, E_s (the fractional increase in transmitted neutron intensity resulting from magnetization to saturation). The measured points for an iron thickness of 2.97 cm are compared in Figure 3 with the effect calculated from the observed incoherent scattering, assuming it to be entirely inelastic and isotropic. The form factor for the magnetic scattering used in the calculation is that given by Steinberger and Wick (Phys.Rev. 76, 994 (1949)). The silicon atoms constitute irregularities in the magnetic scattering of the magnetic single crystal. There will be corresponding production of neutron polarization from the resulting incoherence, in addition to that arising from inelastic scattering. The calculation of the polarization caused by silicon atoms is complicated by the unknown amount of order in the silicon location. The silicon effect in Figure 3 is based on the assumption of random location; if order were present, the silicon effect would be smaller but the inelastic effect would be larger by a comparable amount, leaving the total almost unchanged.

It is seen from the results, mainly those above 1200 m/s where the silicon effect is small, that the observed E_s is consistent with the assumption that the incoherent scattering in iron is largely inelastic. In fact, as the calculated E_s varies with the square of the inelastic scattering cross section, the presence of only 0.25 b of spin-dependent or isotope disorder scattering would change E_s by about 50% at 1500 m/s and destroy the agreement exhibited by Figure 3. The present results support the recent calculation of polarization in polycrystalline iron by Steinberger and Wick (Phys.Rev. 76, 994 (1949)), in which it was assumed that most of the total scattering (coherent plus incoherent) produces polarization. Acknowledgement is made to M. Hamermesh for his generous help in the analysis of these measurements. This work has been reported for publication in Physical Review.

(D.J. Hughes; M.T. Burgy, W.E. Wolf, Argonne National Laboratory)

Small Angle Scattering of Neutrons

The problem of small angle scattering of neutrons in finely divided powder grains, reported in the last quarterly progress report (BNL 64 (S-6)), has been treated by a more rigorous theory. The total cross section for scattering into small angles for each grain of radius R can be represented by

$$\sigma = 2\pi R^2 \left[1 - \frac{2 \sin \rho}{\rho} + \frac{2}{\rho^2}(1 - \cos \rho)\right] ,$$

where $\rho = 2\delta kR$, $1 - \delta$ is the index of refraction, and k is the wave number.

For $\rho \ll 1$ $\sigma = \pi R^2 \rho^2/2$ and for $\rho \gg 1$ $\sigma = 2\pi R^2$. In the latter case, the formula for multiple scattering has been shown to be non-Gaussian, since the individual scatterings, though independent, fall off more slowly than do Gaussian. However, the experimental data fit a Gaussian to within 10% at the half-width.

By measuring the breadth of the beams scattered from dry powder and from powders immersed in CS_2, the scattering cross sections of Cr and Si have been determined relative to that of CS_2. Using the known value of the latter, the following values have been obtained:

$$\sigma_{Cr} = 4.0 \pm .4 \text{ barns}$$

$$\sigma_{Si} = 2.0 \pm .2 \text{ barns}$$

Although Te in its natural mixture of isotopes scatters with positive phase, there was indication of pronounced incoherent scattering, suggesting a possible negative phase from one of the isotopes. This question was, therefore, investigated further with the Columbia cyclotron (see next item). A report of this and of the work described under this heading in the last quarterly progress report is being submitted for publication in Physical Review.

(S. Pasternack, R.J. Weiss)

Coherent Scattering Cross Section and Nuclear Resonances of Tellurium

The small angle neutron scattering measurements, described above, show that the coherent scattering cross section of tellurium is much smaller than the free scattering cross section. This can be explained by assuming that one of the tellurium isotopes has a strong resonance and a negative scattering length. Transmission measurements on normal isotopic tellurium with the Columbia neutron velocity spectrometer have confirmed the presence of a strong resonance at 2.2 ev; a number of smaller resonances at higher neutron energies has been found. Further transmission data on an enriched sample of tellurium containing 76.5% of Te^{124} are being obtained to determine if the resonance at 2.2 ev is to be attributed to this isotope. The incoherent, and from this, the coherent, cross sections of tellurium are also being determined by a method described by Bendt and Ruderman (Phys. Rev. 77, 575 (1950)). This experiment

utilizes an annular bank of BF_3 counters placed at an angle of 18° with respect to the neutron beam. Since inelastic scattering is small, only incoherently scattered neutrons are counted when the incident neutron energy is greater than 2.5 Å.

(R.J. Weiss; C.J. Heindl, I.W. Ruderman, Columbia University)

Total Cross Sections of Carbon and Hydrogen for 14-Mev Neutrons

The total cross sections of carbon and hydrogen have been measured for the absorption and scattering of 14-Mev neutrons. For this purpose, neutrons were obtained from the reaction of deuterons from the Laboratory's electrostatic generator with a tritium-zirconium target. After passing through carbon and polyethylene absorbers of several different thicknesses, the neutrons were detected in a liquid scintillator (a solution of terphenyl in xylene) where they produced recoil protons. From the measured attenuation of the neutron beam, the intensity of which was monitored by a count of the alpha particles emitted from the tritium target, the neutron cross section for carbon was found to be 1.32 barns, in close agreement with the values of Salant and Ramsey (Phys. Rev. 57, 1075 (1940)), of Ageno et al. (Phys. Rev. 71, 20 (1947)), and of Sleator (Phys. Rev. 72, 207 (1947)). Combining the data from carbon absorbers with those from polyethylene, the neutron cross section for hydrogen was found to be 0.66 b, which may be compared with the values ranging from 0.60 b to 0.69 b, reported by the above authors. Statistical errors in all the measurements cause the values to overlap. In any case, the comparison is not too meaningful, as the "monoenergetic" 14-Mev neutrons of the published work covered a band of energies of uncertain extent -- anywhere from 1 to 5 Mev wide. The detector used in the present work is extremely efficient compared with those previously used in work of this nature, and the counting rate is no longer a factor which limits the accuracy. The present uncertainties are in the geometrical alignment of the apparatus; further improvements now being made, in this respect, are expected to result in more accurate values of these cross sections.

(E.M. Hafner, H.L. Poss, E.O. Salant, L. Yuan)

Photodisintegration of Rh

Measurements of the distribution in angle and energy of protons arising from the disintegration of Rh by X-rays from a 20-Mev betatron have been completed. A preliminary report appeared in BNL 39 (AS-3).

The measurements are summarized in Figure 4, where the intensity I (number of protons per unit solid angle) is shown as a function of the angle θ between the proton path and the X-ray beam, and is given for several different ranges of proton energy.

One may visualize the photo-proton emission in the simplest way by assuming it to be due to two factors: an ejection of the proton by the electric vector of the light wave which gives an emission proportional to $\sin^2 \theta$, and an evaporation process which is isotropic. For any particular energy, the sum of these processes may be written as

$$I = a + b \sin^2\theta ,$$

where the ratio b/a is a measure of the relative importance of the angle-dependent process. That this simple picture gives a fair account of the observed angular distributions is shown by the solid curves of Figure 4, which are calculated with this equation and with the values of b/a as listed in the table below. It is seen that the anisotropic term becomes more important at the higher energies. Only the low energy protons come predominantly from simple evaporation. This energy dependence is seen by the rapid increase of b/a with proton energy; it varies approximately as $E^{7/2}$. Observed values of this ratio and values calculated from the empirical equation $b/a = E^{7/2}/1800$ are:

Mean E (Mev)	4.5	6.5	8.5	10.5
(b/a) obs.	0.13	0.40	0.99	2.0
(b/a) calc.	0.11	0.39	0.99	2.1

(N. Curtis, J. Hornbostel, E.O. Salant)

Stationary Properties of the Nucleus

Mass Synchrometer and Measurement of the Mass of S^{32}

A new method has been developed for measuring accurately the rotation period (T) of ions in a uniform magnetic field from which the mass can be calculated. After passing through a slit 180° from the source, ions are subjected to an electric field of small extent in space and time. Thus is formed a short bunch of ions of reduced energy, free to execute a large number (n) of rotations in the same plane without striking the source. Re-establishment of the electric field at time nT later further reduces the energy of the bunch so that it strikes a detector. Electronic measurement of the interval between two applied voltage pulses for maximum current to the detector yields a value of the ionic mass. From measurement of the time difference for S^+ and O_2^+ bunches (n = 40, nT = 840 μsec) formed in SO_2, a mass value S = 32.9823 ± 0.0010 has been obtained, which agrees with that of Aston. This result indicates, but does not prove, that a more recent value of Okuda and Ogata (Phys. Rev. 60, 690 (1941)) is too high. Results to date have been obtained in a small preliminary instrument. A larger "synchrometer," employing higher fields and believed capable of a precision of 10^6 or better, is being designed. A description of the instrument has been submitted for publication in Review of Scientific Instruments.

(L.G. Smith)

Atomic Masses of the Neon Isotopes

The absolute mass of Ne^{20} has been determined from several mass doublets by Jordan and Bainbridge (Phys. Rev. 51, 585 (1937)) and Mattauch (Phys. Zeits.

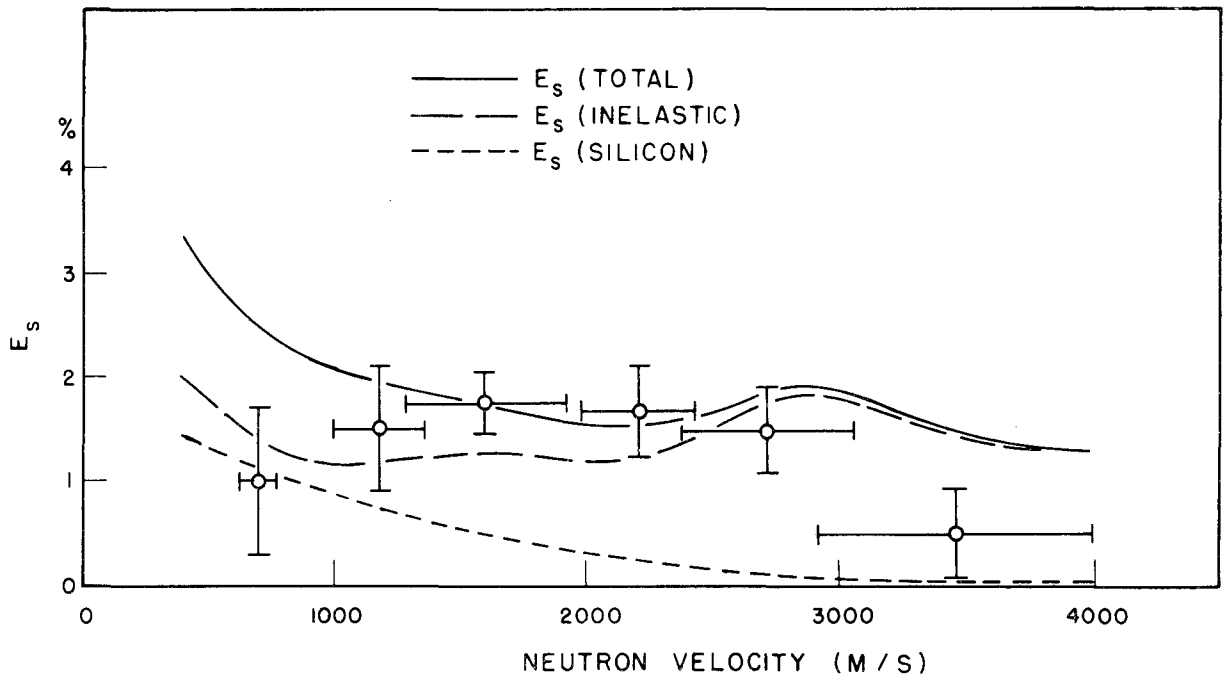

Figure 3. Observed single transmission effect, E_s, in a 2.97-cm single crystal of iron-silicon, compared with the calculated value.

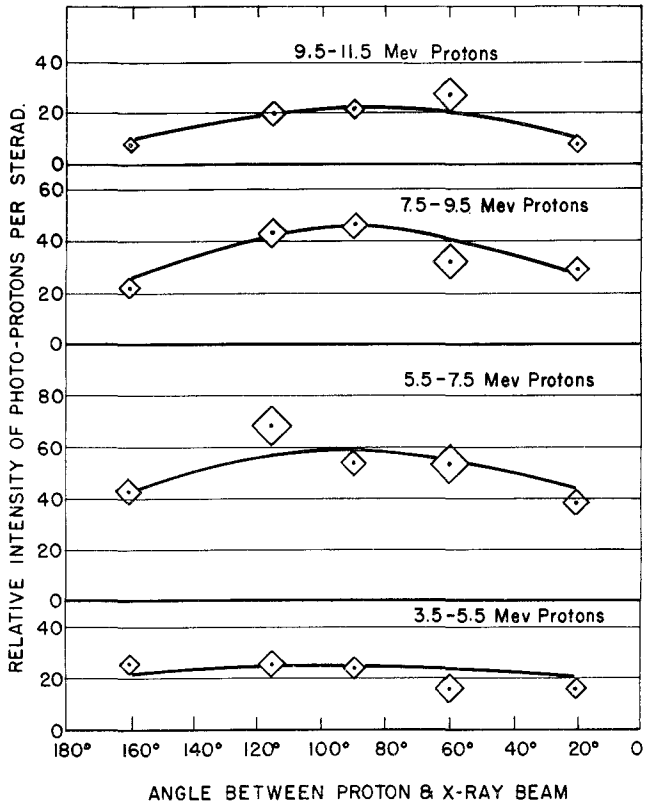

Figure 4.

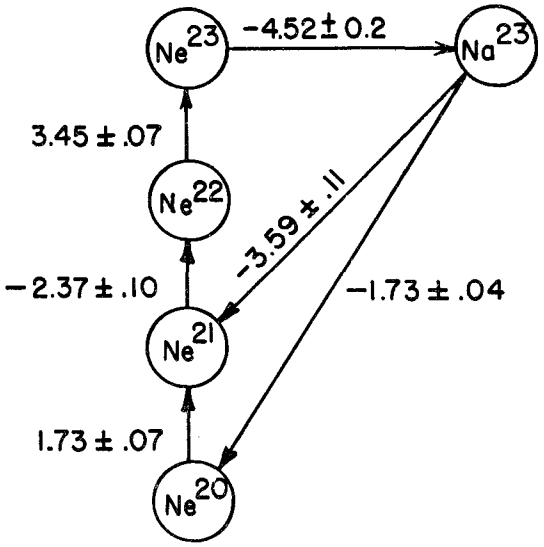

Figure 5. Observed mass differences from published reaction data given in milli-mass-units neglecting the whole number of mass units. Closed paths allow consistency checks on the observed values.

39, 892 (1938)). The mass spectrographic values for the Ne^{21} and Ne^{22} masses are given by Jordan and Bainbridge, but do not agree with the mass differences found from the (d,p) reactions on enriched neon. Recent reaction data allow a consistency check on the mass differences and a reliable calculation of the Ne^{21}, Ne^{22}, and Ne^{23} masses based on Ne^{20} as a standard. The consistency of the measured values is represented in Figure 5.

The reactions $Ne^{20}(d,p)Ne^{21}$ and $Ne^{22}(d,p)Ne^{23}$ have been studied by Elder, Motz, and Davison (Phys. Rev. 71, 917 (1947)), by Zucker and Watson (Phys. Rev. 78, 14 (1950)), and by Ambrosen and Bisgaard (Nature 165, 888 (1950)), all of whom report Q values that are in excellent agreement with each other. The largest observed Q value for each isotope is assumed to correspond to the ground state transition. For $Ne^{20}(d,p)Ne^{21}$, a weighted mean energy release of $4.52 \pm .07$ Mev is obtained. From this, the mass difference $\Delta(Ne^{21} - Ne^{20} = 1.73 \pm .07$ milli-mass-units (mmu), where the whole mass unit is omitted. For $Ne^{22}(d,p)Ne^{23}$, a weighted Q value of $2.92 \pm .06$ Mev results from the three observed values, giving $\Delta(Ne^{23} - Ne^{22}) = 3.45 \pm .07$ mmu. The reaction $Ne^{21}(d,p)Ne^{22}$ has been reported by Ambrosen and Bisgaard (Nature 165, 888 (1950)) as having a Q value of $8.34 \pm .10$ Mev, giving $\Delta(Ne^{22} - Ne^{21}) = -2.37 \pm .10$ mmu. Brown and Perez-Mendez (Phys. Rev. 78, 812 (1950)) have recently published results on the transition energy of the beta disintegration of Ne^{23}. Their value of $4.21 \pm .02$ Mev gives the mass difference $\Delta(Na^{23} - Ne^{23}) = -4.52 \pm .02$ mmu.

Combining the above four mass differences, $\Delta(Na^{23} - Ne^{20}) = 1.73 - 2.37 + 3.45 - 4.52 = -1.71 \pm .14$ mmu. Freemen (Proc. Roy. Soc. 63A, 668 (1950)) has reported that $Q = 2.35 \pm .04$ Mev for the $Na^{23}(p,\alpha)Ne^{20}$ reaction, which corresponds to $\Delta(Na^{23} - Ne^{20}) = -1.73 \pm 0.4$ mmu. The two values are in excellent agreement, thus confirming the assumption that it is the ground state transition, as well as the absolute value.

In addition to these reactions, $Na^{23}(d,\alpha)Ne^{21}$ has been found by Murrell and Smith (Proc. Roy. Soc. 173, 410 (1939)) to give an energy release of $6.75 \pm .1$ Mev. From this transition, $\Delta(Na^{23} - Ne^{21}) = -3.59 \pm .11$ mmu, but from the (d,p) reactions and $Ne^{23}(\beta^-)Na^{23}$, $\Delta(Na^{23} - Ne^{21}) = 3.46 \pm .13$ mmu. The (d,α) reaction allows a second consistency check on the (d,p) Q values, though the discrepancy is about equal to the individual probable errors. The (d,p) and (p,α) reactions are to be regarded as more reliable and are used in calculating the masses given below. The weighted means of the observed mass differences and their approximate probable errors in mmu are as follows:

$$\begin{aligned}
\Delta(Ne^{21} - Ne^{20}) &= 1.73 \pm .06 \\
\Delta(Ne^{22} - Ne^{21}) &= -2.39 \pm .07 \\
\Delta(Ne^{22} - Ne^{20}) &= -0.66 \pm .09 \\
\Delta(Ne^{23} - Ne^{22}) &= 3.45 \pm .06 \\
\Delta(Na^{23} - Ne^{23}) &= -4.52 \pm .02 \\
\Delta(Na^{23} - Ne^{20}) &= -1.73 \pm .04
\end{aligned}$$

Jordon and Bainbridge (Phys. Rev. 51, 585 (1937)) report the value $\Delta(Ne^{22} - Ne^{20}) = -0.47 \pm .35$ mmu, which is in agreement with the above value. It does not alter the most probable value significantly due to the large probable errror. These authors give $\Delta(Ne^{21} - Ne^{20}) = 0.96 \pm 0.2$, which does not agree with the difference from nuclear reactions.

The mass of Na^{22} can be linked to that of Ne^{22} from the measured transition energy of the $Na^{22}(\beta^+,\gamma)Ne^{22}$ disintegration through measurement by Alburger (Phys. Rev. 76, 435 (1949)), by Good, Peaslee, and Deutsch (Phys. Rev. 69, 313 (1946)), and by Macklin, Lidofsky, and Wu (Phys. Rev. 78, 318 (1950)). A mass difference $\Delta(Na^{22} - Ne^{22}) = -3.065 \pm .018$ mmu results from the observed positron and gamma-ray energies. Using Mattauch and Flammersfeld's value (Zeits. fur Naturforschung, 1949) for Ne^{20} as a standard, the following masses are calculated from the weighted reaction data; the deviation from integral mass values is stated in mmu.

Ne^{20}(M-A)	= -1.101 ± .047	standard
Ne^{21}(M-A)	= 0.63 ± .08	
Ne^{22}(M-A)	= -1.76 ± .09	
Ne^{23}(M-A)	= 1.69 ± .06	
Na^{22}(M-A)	= 1.30 ± .09	
Na^{23}(M-A)	= -2.83 ± .06	

The mass of Na^{23} may be used to extend the mass determination to Na^{24}, Mg^{24}, and Al^{27}. However, a discrepancy of 0.3 mmu appears between the (Al^{27} - Ne^{20}) mass differences determined from reactions and mass spectrographic data. The discrepancy is probably due to the Q value of $Na^{23}(d,p)Na^{24}$ and makes the extension of the mass chain above Na^{23} somewhat doubtful. This type of mass analysis is being extended to Z = 20, in an article being prepared for Reviews of Modern Physics.

(H. Motz)

Mass of S^{35} from Microwave Spectroscopy

The $J = 1 \rightarrow 2$ rotational transition for the molecule OCS has been observed in the K band region for the isotopic molecules OCS^{34} and OCS^{35} for the purpose of determining the atomic mass of S^{35}. The spectroscope, used last year for the nuclear spin of S^{35}, was improved considerably in sensitivity. With the aid of a new microwave frequency standard, based on a General Radio 100-kc crystal controlled oscillator, it was possible to measure the frequency difference between OCS^{35} and OCS^{34} to an accuracy of approximately one part in 27,000.

As has been shown by Townes et al. (Phys. Rev. 72, 513 (1947)), one may evaluate the expression

$$\frac{m_3' - m_3''}{m_3'' - m_3'''} = \left(\frac{\nu'' - \nu'}{\nu''' - \nu'}\right) \frac{\nu'''}{\nu'} \frac{m_1 + m_2 + m_3''}{m_1 + m_2 + m_3'''} ,$$

where m_1, m_2, and m_3 are the masses of O, C, and S, respectively; m_3', m_3'', and m_3''' are three isotopic masses for S; and ν', ν'', and ν''' are the frequencies for $m_1m_2m_3'$, $m_1m_2m_3''$, and $m_1m_2m_3'''$, respectively.

This expression implies two approximations: 1) that the corresponding bond distances are equal in each isotopic molecule, and 2) that the small vibration-rotation interactions, which have not been completely evaluated,

are proportional to mass. The errors thus introduced have been shown to be of the order of one part in 10^4 in the mass difference ratio.

Our value for the frequency difference $\nu^{34} - \nu^{35}$ is 273.896 ± .010. S. Geschwind and R. Gunther-Mohr, at Columbia, have just measured the frequencies of the OCS^{32}, OCS^{33}, and OCS^{34} lines with precision of nearly 10^{-7}. Taking their frequencies and the published mass values, we get:

$$\frac{m_{35} - m_{32}}{m_{34} - m_{32}} = 1.50154 \pm .00015$$

and

$$\frac{m_{35} - m_{32}}{m_{33} - m_{32}} = 2.99881 \pm .00030$$

The principal contribution to the stated error is the error estimated as arising from the neglect of the vibration-rotation terms.

In order to evaluate the $(m_{35} - m_{32})$ mass difference or the m_{35} value, one must assume values for the stable S masses. There is some question about the values given in the literature. Choosing the mass differences given by Davison, $m_{34} - m_{32} = 1.99691 \pm .00037$ and $m_{33} - m_{32} = .99963 \pm .00012$, we get 2 partially independent values for the difference, $(m_{35} - m_{32}) = 2.99846 \pm .00042$ and $2.99770 \pm .00048$, respectively. Taking the value of S^{32} mass recently published by Penfold (Phys. Rev. 80, 116 (1950)), which is $31.98199 \pm .00021$, we get $m_{35} = 34.98007 \pm 35$.

We have also calculated the OC-CS bond distances, using all available combinations of masses with the values given in Table 1. Here again, we have assumed the molecule to be a rigid rotor.

Table 1

Internuclear Distances

Isotopic Combination Used	C-O	C-S
32,-33	1.1634×10^{-8} cm	1.5584×10^{-8} cm
32,-35	1.1636	1.5583
33, 35	1.1638	1.5582
32, 34	1.1641	1.5579
33, 34	1.1648	1.5573
34, 35	1.1626	1.5591
Average	1.1637	1.5582
	mean deviation, .0005	mean deviation, .0004

The variation is considered to be indicative of the error due to neglect of the vibration-rotation interaction, rather than experimental error. This work has been submitted for publication in Physical Review.

(V.W. Cohen, W. Koski, T. Wentink)

Magnetic Electron Multipliers for Detection of Positive Ions

For the mass synchrometer (described above), two designs of a 15-stage electron multiplier, wherein focussing from one beryllium copper dynode to the next occurs in crossed electric and magnetic fields, have been developed particularly for detection of weak beams or pulses of positive ions in magnetic fields. One design with dynodes 3/8" wide is usable in fields between about 250 and 460 oersteds, while the other, with dynodes 1/8" wide, may be used in fields between about 300 and 1100 oersteds. It appears likely that, by using still narrower dynodes, such multipliers can be constructed to operate in fields of several thousand oersteds. Advantages of these designs over those of previously described multipliers employing crossed fields lie in the use of about half the number of insulated plates and less tendency, because of uniformity of the electric field, for breakdown and noise due to ion feedback to occur. The uniformity of the electric field also allows quite reliable calculation of the spread in transit time. From this it is concluded that, with a modified collecting system, a multiplier could be built with a rise time between 10^{-11} and 10^{-10} sec, which is very probably less than could be obtained with a static multiplier. A detailed report on this work has been submitted for publication in Review of Scientific Instruments.

(L.G. Smith)

High Energy Particle Physics

Meson Production by Primary Protons of the Cosmic Radiation

The work described under this heading in the previous quarterly progress report (BNL 64 (S-6)) has been continued, and the principal conclusions stated in that report have been strengthened by additional data. (See also papers by Salant et al. (Phys. Rev. 79, 184-5 (1950)). The analyses of nuclear emulsions exposed near the top of the atmosphere at two latitudes have also revealed the following facts which were not previously stated:

A census of the proton-produced stars in the light elements (those which show an incoming track of a relativistic particle and less than 8 heavy prongs) indicates that about half of the nuclear disruptions thus produced show no outgoing ionizing particles of high energy; about a quarter show one outgoing charged particle of high energy, and the other quarter of the stars are divided between events with more than one such particle. Although the events that show no outgoing high energy ionizing particles are often characterized by several heavy tracks of low energy particles, there is evidently a large discrepancy between the incoming energy and the total that can thus be accounted

for. It is necessary to assume that large amounts of energy are carried away by neutral particles of one form or another. Since one would expect proton and neutron emission to be equally probable, not more than half of the events in question can be readily explained by neutron emission, and it seems necessary to invoke assumptions implying the emission at high energy of other types of neutral particles.

A census has also been taken of stars produced by incoming ionizing rays of high energy in emulsions exposed under a carbon plate having a thickness of 30 gm cm^{-2}. The results have been compared with a similar census taken on emulsions exposed without such an absorber. The stars have been classified according to the number of heavy prongs (representing disrupted particles of low energy), for it is believed that the distribution of stars according to prong number may be characteristic of the energy distribution of the particles producing the disruptions. Table 2 shows the fraction of all stars produced under both conditions with various numbers of heavy prongs.

Table 2

Exposure	No. of Heavy Prongs			No. of Events
	1 - 5	6 - 8	9 or more	
Without absorber	0.41 ± .04	0.16 ± .03	0.43 ± .04	166
Under 30-gm carbon plate	0.50 ± .04	0.30 ± .04	0.20 ± .04	116

The results show a significant decrease produced by the absorber in the fraction of stars with 9 or more prongs and a corresponding increase in the fraction with smaller prong numbers. This shift in the distribution is thought to be indicative of the degradation in energy of the star-producing particles because of nuclear interactions in the carbon.

Attention has also been given to the effect of the carbon absorber on the average number of relativistic particles emitted from the stars. In order to distinguish between stars produced from light and heavy nuclei, the average numbers of relativistic tracks per star are listed in Table 3 according to the number of heavy prongs.

Table 3

Exposure	No. of Heavy Prongs			No. of Events
	1 - 5	6 - 8	9 or more	
Without absorber	1.4 ± 0.2	1.7 ± 0.3	2.0 ± 0.3	166
With 30-gm carbon plate	0.9 ± 0.1	2.1 ± 0.3	2.4 ± 0.3	116

Although the average number of relativistic particles produced in the many-pronged stars appears unaltered by the absorber, the absorber may have a significant effect on the average number produced in the small stars. If the incoming particles under the carbon plate are protons, the density of the track of the producing particle in those stars included in the census would indicate that their energies must have been in excess of a billion electron volts, and it is thought from previous work that the multiplicity of meson production in light nuclei (small prong numbers) is nearly independent of the energy of the incoming particle. The effect noted might be explained by invoking an assumption that an appreciable number of mesons from the carbon produces the smaller stars in the emulsion.

(E.O. Salant, J. Hornbostel, J.E. Smith)

Range-Momentum Measurements for Electrons in Gases

The high pressure cloud chamber described by Johnson, de Benedetti, and Shutt (Rev. Sci. Inst. 14, 265 (1943)) offers a convenient means for determining the range-momentum relations for slow electrons in gases. Gamma rays from Na^{24} were used to produce Compton electrons of momenta up to 1.1 Mev/c. The tracks were photographed in both hydrogen and helium at 136 atmospheres pressure and in a magnetic field of approximately 4000 gauss. The vapor was a water-alcohol mixture.

Because of the high energy loss in the dense gases, the particles were bent into spirals instead of the circles found at low pressure. Thus, each track that can be seen to its end could be used to give a range-momentum relation. A good fraction of the statistical fluctuation was eliminated by excluding tracks having high energy knock-ons, with accompanying sudden curvature changes. To obviate the necessity for corrections for drift in the line of sight, only regular spirals nearly in the plane of the cloud chamber were chosen. The curvatures were measured by fitting circles at approximately 1-cm intervals along the path. The results of measurements on 4 tracks in helium and 3 in hydrogen are given by the points in Figures 6 and 7. The large amount of useful data available from each track is evident.

An analysis of scattering-induced curvature in high pressure gases will be given in a later paper. It has been found that with the 4000-gauss magnetic field, about 1/10 of the curvature was due to scattering. In a heavier gas, such as argon, the scattering curvature is about equal to the magnetic curvature.

It is of interest to compare these experimental points with the usual energy loss theory. Radiation loss can be neglected; the only cases of importance would be the relatively rare emission of a large fraction of the energy in one photon, resulting in a detectable sudden change of curvature. No tracks with such curvature changes were included.

The collision loss was calculated from equation (76) of Møller (Ann. der Physik 14, 531 (1934)), with the use of Rossi and Greisen's formula (Rev. Mod. Phys. 13, 240 (1941)) for small energy losses. The value of the ionization potential I(Z) was taken from experiments of Mano (Ann. de Physique 1, 407

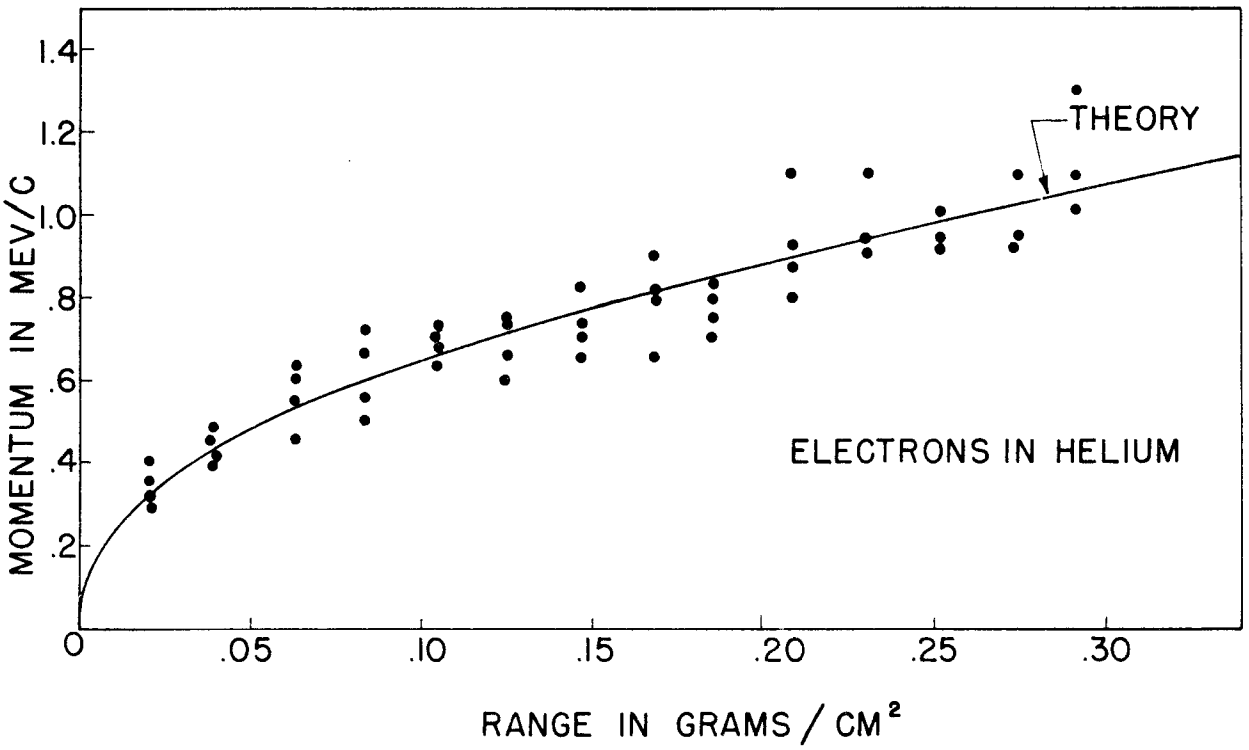

Figure 6. Experimental and theoretical range-momentum relation for electrons in helium.

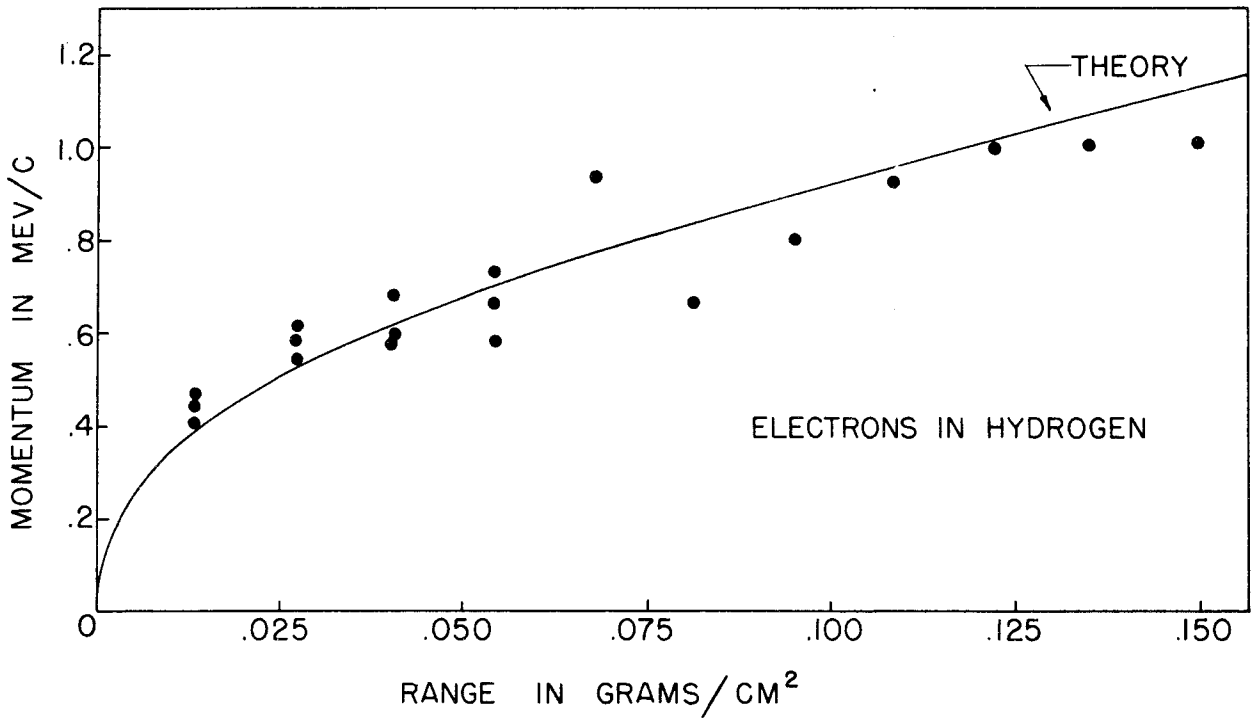

Figure 7. Experimental and theoretical range-momentum relation for electrons in hydrogen.

(1934)) on alpha particle ranges. A knock-on electron was considered as being certainly visible if its energy was 64 kev = $mc^2/8$, and this value was used as an upper limit in the integration of Møller's formula. Numerical integration was used above 375 kev/c momentum loss; below this value, a curve of the form $pc = AR^{.43}$ was used,* using the ordinate and slope of the integrated curve at $pc = 375$ kev to determine R at this point, and then to find A.

The resulting curves are given in Figures 5 and 6. It is evident that even a few tracks give a reasonable confirmation of the theory, and that this method is capable of yielding fairly accurate results. Present results are being published in Physical Review.

(G.F. O'Neill, W.T. Scott)

Continuously Sensitive Diffusion Cloud Chambers

Further experiments have been made on the operation and design of continuously sensitive diffusion cloud chambers of the type described by A. Langsdorf (Rev. Sci. Inst. 10, 91 (1939)). These chambers make use of strong gradients in temperature and vapor density. The basic arrangement of the chamber which thus far has given the best results is shown in Figure 8. Heat is supplied from a tray of water at room temperature which evaporates methanol carried in a sheet of sponge rubber on the ceiling of the chamber. The vapor diffuses downward and is recondensed on the floor of the chamber which is cooled by dry ice. The essential change from Langsdorf's arrangement is the addition of a metal collar which regulates the temperature gradient in the chamber and extends the depth of the region where tracks of ionizing rays can be seen forming. The greatest effective depth, amounting to about 2 1/2", has been realized with an aluminum collar. With a copper collar, tracks form in a shallow layer near the top of the collar, while with a lead collar, or with no collar, only a shallow layer at the floor of the chamber is sensitive. Under optimum conditions, thermocouple measurements have shown that the temperature gradient is about 7° C/cm. More careful control of the gradient might further extend the sensitive volume. Most of the observations have been made with air in the chamber at normal pressure.

When the chamber has reached equilibrium there is very little turbulence and cosmic ray tracks are straight, sharp, and of good contrast. They have been illuminated through a slot 4" wide in the collar. In the model shown, they are observed through the glass cylinder. Photographs have been made (Figure 9) through a transparent top plate made of two disks of lucite between which air was circulated at room temperature. In this case the vapor was supplied from a ring of felt on the ceiling of the chamber and the floor of the chamber was covered with a sheet of black glass. Since the chamber is continuously sensitive, photographs may be taken as frequently as the chamber can be illuminated with the available power supply.

*This formula was derived by fitting a power-law expression to the curves discussed in "Cosmic-Ray Physics," D.J.X. Montgomery, Princeton, 1949.

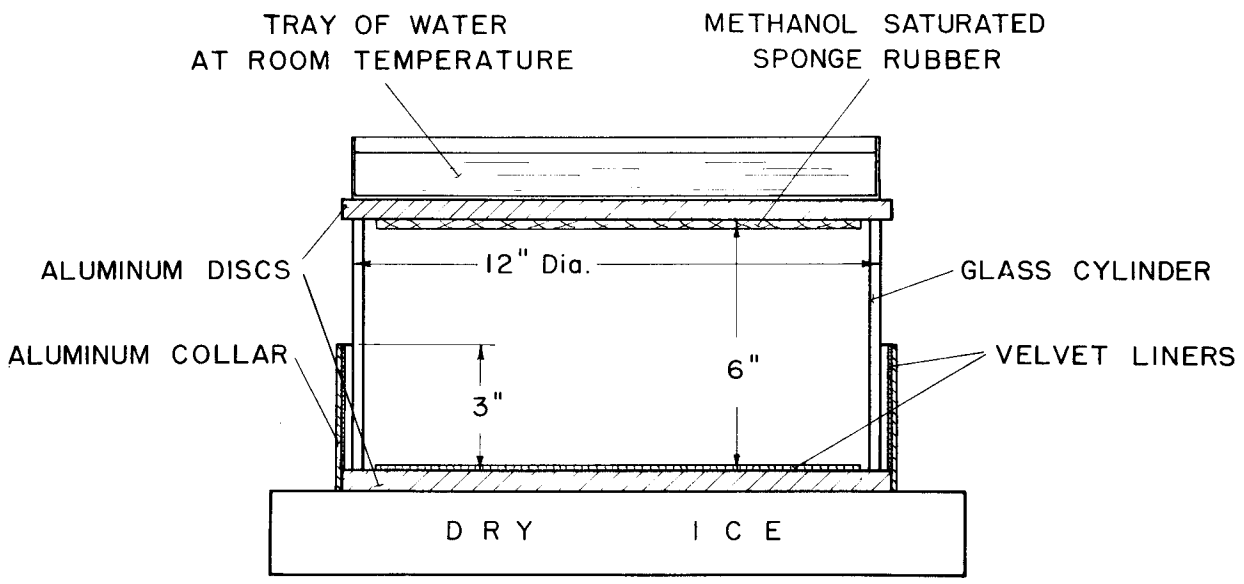

Figure 8.

Figure 9.

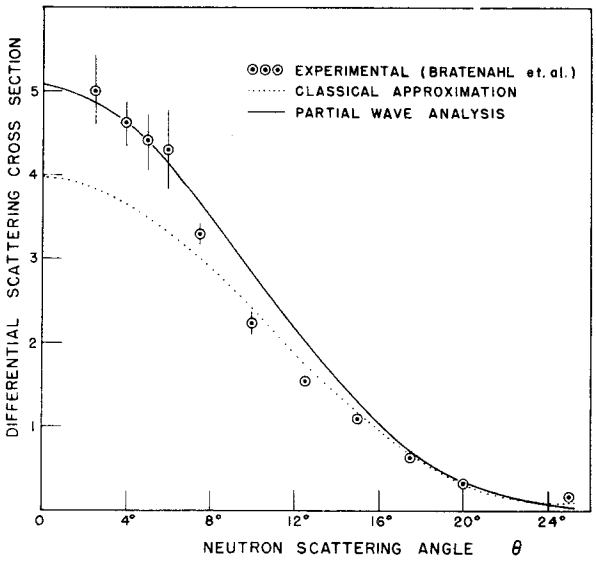

Figure 10.

After an intense irradiation of the chamber, it remains insensitive for about a minute. However, the sensitivity may be restored in a few seconds if the chamber is swept with an electrostatic field of 35 v/cm. Varying the height of the glass cylinder or the temperature at the ceiling has a very slight effect on the operation of the chamber. Ethanol and acetone are about as satisfactory as methanol. Argon in the chamber produces the same quality of tracks as air, but with helium and hydrogen at normal pressure, the chamber never reaches stable equilibrium. Presumably, the mixture at the ceiling, which is richer in vapor, attains a greater density than the cooler gas at the floor, and convection clouds can be seen at intervals of a second or two. At a pressure of 3 atmospheres of helium, conditions were stable and tracks could be observed. In argon at a pressure of 5 atmospheres, the tracks were of particularly good contrast. Unless special precautions are taken, vertical plates of absorbing materials placed in the diffusion chamber may disturb its equilibrium.

(E.C. Fowler, W.B. Fowler, G. John, D.H. Miller, R.P. Shutt, A.M. Thorndike)

General Physics

Oriented Overgrowth of Alkali Chlorides on Metals

The study of the oriented overgrowth of the alkali chlorides on metals, referred to in previous reports, has been completed. Metals representative of all groups, from the true metals (copper and silver) to those exhibiting homopolar binding (bismuth and antimony), were prepared in polycrystalline and single crystalline form. Oriented growth was readily produced on metals from all parts of the periodic table. It was concluded that, in most cases, such growth was not characteristic of the metal surface but rather was determined by the nature of thin oxide films.

For two metals, gold and silver, which do not combine with oxygen under ordinary circumstances, the oriented growth was determined by the nature of the metal-ionic crystal interface. It was found, contrary to previous work, that the limiting misfit between metals and ionic crystals is of the same magnitude ($\sim$10%) as that for purely ionic pairs. This result will require modification of existing theory to include large contributions to the attractive force terms between the metal and the ionic crystals other than simple electrostatic forces between ions.

The fact that silver is more effective than gold in promoting oriented growth, in spite of the fact that they are practically identical structurally, suggests that higher chemical activity favors epitaxy.

Under the conditions of the experiments, all other metals probably were covered by thin oxide films. Since oriented growth was observed for those metals (Cu, Zn, Pb, Sb, Bi, Fe), the oxide layers must have been oriented with respect to the metals. Such conclusions have been reached previously from electron diffraction measurements on Cu, Zn, Pb, and Fe for some orientations, but the generality of the effects for many orientations has not been reported.

Failure to observe oriented growth on Al, Mg, Cd, Sn, Ni, and In was attributed to the presence of amorphous or disoriented oxide films. Such films are known to be present on Al and Mg under usual atmospheric conditions from electron diffraction measurements. It cannot be assumed from those cases in which epitaxy was not found that the oxide films in the early stages of growth were not oriented, since it is well known that the oriented characteristics of films is reduced as the film thickness increases. Thus, while the first few layers might be pseudomorphic or oriented with respect to the substrate, after sufficient growth has occurred the preferred alignment might be lost.

(G.W. Johnson)

Particle Localization by Means of a Scintillation Detector

A long tube with flat ends containing scintillation liquid of a type suggested by Kallmann and Furst (Phys. Rev. 79, 857 (1950)) is placed between two photomultipliers. Neglecting reflection from the side walls, the intensity of light received at a photomultiplier from a scintillation is proportional to the solid angle subtended by the photocathode at the scintillation point. The ratio of two coincident pulses will then determine the location of the scintillation along the tube independent of light intensity (particle energy).

The pulse ratio was obtained by feeding one pulse to the vertical deflection plates and the other to the horizontal ones of an oscilloscope and measuring the inclination angle of the trace. The trace amplitude is related to the particle energy dissipated in the liquid.

Preliminary results on the localization effect were obtained using cosmic rays. The coincidence pulse from a G-M counter telescope perpendicular to the scintillation detector was used to unblank the oscilloscope. Uncertainty resulting from statistical variations of the photomultipliers was measured by means of a light source placed at various distances between the photomultipliers to simulate scintillations.

The localizer has possible applications to angular correlation and cosmic ray measurements. This work will be presented before the American Physical Society.

(C.L. Yuan, H.L. Poss)

Effect of Fringing Field on the Focussing Properties of Magnetic Spectrometers

An analytic expression has been obtained for the magnetic field in the air path between rectangular semi-infinite pole pieces. In spite of the idealizations involved, the function evaluated on the median plane is found to represent the measured fields of several actual magnets. From the vector potential given by this function, a simple integral representation can be written for ion orbits in the median plane. A number of typical orbits

has been evaluated and plotted. The procedure is useful for estimating the shapes of ion beams entering and leaving such fields and, since the functions are readily differentiable, for calculating vertical focusing effects and the basic properties of certain magnetic spectrometers. A detailed report of this work is being submitted for publication in Review of Scientific Instruments.

(E.M. Hafner)

Radioactive Tracer for Wear Tests

A novel method, suggested by work of Segrè and Wiegand (Phys. Rev. 70, 810 (1946)), has been used to apply radioactive tracer material to a surface as a means of studying wear. Tracer activity is deposited on the surface to be studied in the form of fission fragments from a uranium foil that is placed near the surface during an exposure to neutrons. Without altering the composition or physical condition of the surface, a layer a few milligrams per cm^2 in thickness can be made sufficiently active so that counting techniques can be used to detect very slight losses of material from the surface. For satisfactory use of this technique, it is necessary that the activity resulting from neutron capture in the material itself should be less than that deposited on the surface from the uranium. This condition is satisfied with most materials if foils of enriched U^{235} are used. In some cases, ordinary uranium foil may be used.

In a practical test of the method, a stainless steel surface was exposed at short range to the fission fragments from a highly enriched U^{235} foil during a 16-hr irradiation with a 1-gm Ra-Be neutron source. After allowing the 3-hr activity of Mn to decay for a day, the remaining activity was almost entirely from fission fragments embedded in the surface and amounted to about 100 cts/min/sq in. The surface was then lapped with an abrasive and the wear was measured with standard gage blocks and a Sheffield reed comparator. The decrease of activity, after correcting for decay, was found to be linear with wear until it was completely erased by removal of 2×10^{-4}", a layer about equal to the theoretical maximum range of the fission fragments. The method may have a wide range of applications, and has been submitted for publication in the Bulletin of the A.S.T.M.

(D. Frisch)

Cathode-Follower Fallacies

The low output impedance of a cathode follower is weighed as the best solution to the problem of rapidly driving a large capacity or a low-impedance line. The relative merits of the cathode follower and amplifier circuits are listed in Table 4, where Y_L is the load admittance and other symbols have their conventional meanings. Note that the output capacities of

the tubes can safely be neglected because, in general, they either will be small compared to the large load capacity or, across a low impedance line, they will affect the rise time less than preceding or succeeding amplifiers.

Table 4

	Amplifier	Cathode Follower
Output impedance	r_p	$1/g_m$
Gain = A	$\frac{\mu}{1 + r_p Y_L}$	$\frac{\mu}{1 + \mu + r_p Y_L}$
Rise time	$\frac{C_L}{G_L + 1/r_p}$	$\frac{C_L}{G_L + (1 + \mu)/r_p}$
Mid-band gain rise time	g_m/C_L	g_m/C_L
Input capacity triode	$C_{gK} + C_{gp}(1+A)$	$C_{gp} + C_{gK}(1-A)$
pentode	$C_{gK} + C_{gSc}$	triode-connected $C_{gSc} + C_{gK}(1-A)$; pentode-connected $(C_{gSc} + C_{gK})(1-A)$

Considering first the problem of driving a low-impedance matched line, it is often stated that the low output impedance of the cathode follower is required to match the sending end of the line. If the line is terminated exactly, however, there can be no reflections, and, hence, no need to match the sending end. While practical terminations can never be exact, the discrepancy is seldom serious; thus, the problem usually reduces to obtaining maximum signal voltage across the low impedance without unduly loading earlier stages. With a given tube and given $Z_L = R_L = Z_o$ more gain is invariably obtained with the "amplifier" circuit (Table 4). This gain, of course, will be unity or less with presently available tubes and coaxial lines, but it will still be greater than that obtained from cathode connection. The low gains involved result in input capacities for the two circuits which differ, even for a triode, by less than might first be expected. Thus, unless input loading or reflections are unusually critical, the amplifier is the better circuit. (Note that a large coupling condenser can be avoided by feeding the plate voltage through the termination.)

With a largely capacitative load, it might appear that the low output impedance of the cathode follower is required to give a reasonably fast rise

time. However, if C_L is given and C_L may be varied, as is the usual case, the gain-bandwidth product is the same for the cathode follower as for the amplifier (Table 4). Physically, the greater "inherent" gain of the amplifier allows one to use a lower resistor across C_L, thereby compensating for the higher output impedance and resulting in the same final rise time for the same signal voltage. Again, the gains involved are low and the input capacities do not differ greatly even with a triode. Thus, unless input capacity is extremely critical, the only essential difference between the circuits is the output polarity.

The cathode follower has only a slight advantage as regards input capacity, while the amplifier will generally give about twice as much signal voltage across a matched line and, for the same rise time, fully as much signal across a large capacity. Signal polarity will often be the determining consideration.

This work has been submitted for publication in Review of Scientific Instruments.

(P.I. Richards)

Theoretical Topics

Scattering of Light by Light

In a paper submitted for publication in Physical Review, the cross sections for several processes involving electromagnetic fields in a nonlinear manner have been derived from the electrodynamic scattering matrix. These cross sections are expressed in terms of the fourth order nonlinear vacuum polarization tensor. The differential cross section for the scattering of light by light is calculated as a function of energy and angle. Numerical values are given for scattering at zero and at 90° in the center of mass system. Near 1.75 Mev, the forward scattering cross section has its largest value of $4.1 \times 10^{-31} cm^2$/sterradions, while the maximum right angle scattering takes place near .7 Mev with a cross section of $2.8 \times 10^{-31} cm^2$/sterradions, all for unpolarized radiation. Numerical results are also given for scattering at the above angles between circularly polarized states. The conclusions in this paper agree with all the results previously calculated for special cases.

(R. Karplus, M. Neuman)

Fluctuations and the General Distribution Problem in Electron Cascades

Recent developments of Bhabha, Friedman, and Janossy are applied to the general probability distribution problem of electron cascades (cosmic ray showers). In particular, it is shown that the master function giving the probability of any number of particles with any given energy distribution at a depth t in a shower is determined, in principle, by the average energy

spectrum. Certain theorems connecting the various functions are derived, and a discussion is given of the as yet unsolved problem of getting satisfactory analytic or numerical results from the formalism. Only the simplified model originated by Furry has been discussed, but the theorems embody many properties of the actual electron-photon multiplication process. This work is being prepared for submission to Physical Review.

(W.T. Scott)

High Energy Neutron Scattering by Nuclei

The transparent model of a nucleus proposed by Serber (Phys. Rev. 72, 1114 (1947)) appears to be useful in treating the scattering of 90-Mev neutrons by nuclei. Fernbach et al. (Phys. Rev. 75, 1352 (1949)) have shown that the nuclear radii fitted from experiment by this model agree well with an $A^{1/3}$ law. However, calculated differential scattering cross sections deviated somewhat from the experimental observations of Bratenahl et al. (Phys. Rev. 77, 597 (1950)), the latter being 10 to 20% higher than the calculated values at low scattering angles. The purpose of this note is to show that the apparent deviations from experiment of the calculations based upon this model are at least partly due to the approximate calculational method used by the above authors, rather than to the model itself.

The differential scattering cross section $\sigma(\theta)$ for the transparent nucleus was calculated by the above authors by assuming the nucleus could be represented by a square well with potential 30.8 Mev and absorption. This is equivalent to the assumption that the nucleus is a sphere with a constant complex index of refraction. For this model, the classical approximation leads to an angular distribution amplitude given by

$$f(\theta) = k \int_0^R \left[1 - e^{(-K + 2ik_1)\sqrt{R^2-\rho^2}} \right] J_0(k\rho\sin\theta)\rho \, d\rho \quad ,$$

where k is the neutron wave number, K is the absorption coefficient, and k_1/K is the real part of the index of refraction.

Since the complex constant index of refraction is equivalent to the assumption of a square well with a complex constant potential, it was considered desirable to check the validity of the classical approximation by making an exact partial wave analysis for the complex square well, using the corresponding values of the parameters. This was done for aluminum; the results are shown in Figure 10. The circles represent the experimental points of Bratenahl et al., the dotted line the values of $\sigma(\theta)$ calculated using the classical approximation, and the solid line the values of $\sigma(\theta)$ calculated by means of the exact partial wave analysis. It is seen that the apparent deviations of the classical approximation from experiment are at least partly due to the calculational method, rather than to the use of the complex square well model.

The calculated total scattering and absorption cross sections differ somewhat from those obtained with the classical approximation. The scattering

cross section becomes 0.83 instead of 0.75 barns, and the absorption cross section is 0.45 instead of 0.36 barns. To make a closer comparison of the calculated differential scattering cross section with the experimental results, it would be necessary first to adjust the complex potential parameters to fit the experimentally determined scattering and absorption cross sections.

The phase shifts calculated by the exact partial wave analysis deviate considerably from those obtained by the classical method. The latter gives, for aluminum,

$$\delta_l = (1.35 + 0.452\ i)\ \left\{1 - (l + \tfrac{1}{2})^2/73.1\right\}^{1/2} \qquad l \leqq 8$$
$$= 0 \qquad l > 8$$

The former method yields the following phase shifts for aluminum (for l = 0,1,2,....):

1.29 + 0.38 i, 1.44 + 0.56 i, 1.20 + 0.40 i, 1.36 + 0.40 i, 1.12 + 0.49 i, 1.01 + 0.29 i, 1.11 + 0.32 i, 0.85 + 0.47 i, 0.27 + 0.19 i, 0.065 + 0.025 i, 0.012 + 0.005 i, 0.002 + 0.001 i, etc.

This work has been submitted for publication in Physical Review.

(S. Pasternack, H.S. Snyder)

Inelastic Scattering of Thermal Neutrons

The one-phonon cross sections, often principally responsible for the inelastic scattering, were calculated for a number of materials as a function of the incident neutron energy E for several crystal temperatures T. To shorten the calculations, the integrals, equivalent to those given by Weinstock, were evaluated graphically on specially ruled paper. This method is still laborious, owing to the large number of integrals, so the method of integrating over reciprocal lattice points was developed following a suggestion by Pomeranchuk and Akhiezer. This leads to the formula

$$\sigma = \sigma_o \frac{m}{M} \frac{E}{\theta} \left[F(\frac{E}{\theta},\frac{T}{\theta}) - rf(r)G(\frac{E}{\theta},\frac{T}{\theta})\right],$$

where $r = (m/M)\ (E/\theta)\ \phi\ (T/\theta)$ is essentially the Debye-Waller temperature exponent. Tables have been prepared of $F(E/\theta,T/\theta)$ and $G(E/\theta,T/\theta)$, as well as $\phi(T/\theta)$ and $f(r)$, permitting rapid calculation of the one-phonon cross section. The validity of the reciprocal lattice integration requires sufficient incident energy to involve a large number of crystal planes in the scattering process, but fortunately the tables agree quite well with the more laborious calculation, even at the lowest energies.

(D.A. Kleinman)

Electronics Division

Timer for Time-of-Flight Mass Spectrometer

Construction and calibration of the timer were completed by the end of September. In its final form, the standard signal is obtained from a 10-Mc crystal oscillator. A tuned frequency divider takes the frequency down to 1 Mc, which drives the ring divider circuits previously described. 0.1-μsec steps are obtained from a tapped delay line which may be calibrated directly by means of the 10 Mc. Finer adjustment is given by a continuously variable delay line which interpolates between the 0.1-μsec steps. The timer is thus made direct reading down to 0.01 μsec or less. (The variable gain amplifier is in process of development, but will not be reported at this time.)

Pulse Height Analysis

A ten-channel pulse height analyzer, of Oak Ridge design, was completed last Spring. It was found necessary to design a new type of calibrating instrument in order to test and make use of the sensitivity and stability of the analyzer. The calibrating instrument consists of a highly stabilized d.c. voltage source and precision attenuator (Helipot). The d.c. voltage may be accurately calibrated and continuously adjusted. The d.c. potential is converted to pulses by means of a mercury contact switch and further networks are incorporated for adjusting the rise and decay times of the pulse. The pulse height is adjustable from 0 to 100 v. Step attenuators may be inserted to reduce the output to any desired level. The impedance level at the output of the pulser is 160 ohms. The pulse amplitude may be manually adjusted or may be caused to vary linearly with time by driving the Helipot with a constant speed motor.

With the new pulser, it is easy to calibrate the analyzer or an over-all system of analyzer-plus-amplifier. The analyzer channels are found to be stable to 1 to 2% of channel width over a period of 1 hr, and the position of the channels remains stable to better than 1% of full scale. (A Sola line voltage regulator was used.) Although this would seem to be reasonably good performance, the resolution obtained in use (with a proportional counter to measure X-rays) was disappointing. Extreme stability is demanded of the amplifier in this application. However, it was found that the resolution was improved as the gain of the amplifier was increased and the gain of the proportional counter was lowered correspondingly. Evidently the gain stability of a proportional counter is poorer at higher voltage (and gain). Normally, the noise due to the amplifier will be small, so the gain of the amplifier rather than the counter voltage should be increased when measuring soft X-rays.

A single channel analyzer of Oak Ridge design has been constructed, which has proved satisfactory; another is under construction.

Coincidence Circuits

Two coincidence circuits of previous design were built during the report period. Three circuits of different design are worth a brief description. The first is a multiple coincidence circuit for use with four scintillation counters. Coincidences are taken between pairs of counters, and then the signals from the first two coincidence circuits are fed to a third. A fast amplifier is provided for each photomultiplier with a gain of 100 and rise time of 0.02 μsec. The resolving time of the coincidence circuits is 0.1 μsec and a delay may be inserted where desired.

The second coincidence circuit is designed for use in the μsec range. The resolving time is adjustable from 0.1 to 0.5 μsec and the delay is adjustable from 0 to 15 μsec in two ranges. Each channel has an amplifier for use with scintillation or G-M counters and a pulse height discriminator.

The third coincidence circuit is combined with a pulse height analyzer to take coincidences between pulses from a scintillation counter and pulses of selected amplitude from a proportional counter. Due to the finite rise time of the proportional counter pulse, the pulse height determination is delayed by a variable amount relative to the start of the pulse. However, the start of the pulse must be used in the coincidence circuit to be able to use short resolving times. Therefore, the coincidence circuit precedes the pulse height analyzer. If a coincidence is registered and the proportional counter pulse falls in the selected amplitude range, a gate is opened which will pass the signal from the analyzer. A delay may be inserted into either signal line; the delay circuit is a sawtooth circuit of novel design. The resolving time is determined by line controlled blocking oscillators.

The fast coincidence circuit, described in the last progress report, was rebuilt and calibrated.

Civilian Defense Monitoring

Preliminary measurements and design are complete on the scintillation type of monitor instrument, and a prototype has been constructed. The instrument makes use of average 931A photomultiplier tubes, a vibrator power supply, and a Westinghouse discharge tube. Indication is provided by a meter and phones, and power is supplied by two flashlight cells. The gain of the photomultiplier can be preset easily. The energy response curve is being determined.

Airborne Dust Activity Measurements

Data taken on the natural activity of dust particles at the Laboratory's area monitoring stations have shown wide fluctuations in both the alpha and beta-gamma components. Over a period of time it has been possible to find some correlation between this activity and weather conditions; this study is continuing. Also, by studying the rate of decay of the dust samples deposited on filter paper, it is possible to separate the radium and the thorium decay products. As a further check, an inonization chamber has been set up to measure the alpha activity of various samples of Long Island dirt. After the

dirt is put into a clean chamber, the activity is recorded as the sample and the decay products come into equilibrium. Then the dirt source can be removed and the decay of the products followed. As the information is analyzed it will be reported.

Counter Tubes

A number of heavy walled, soft glass neutron counter tubes have been made for operation inside the high pressure cloud chamber.

A complicated metal G-M counter was built for low counting rate experiments, to shield a conventional thin window counter. The enclosure is bell-shaped to fit over an end window counter so that the latter has, in effect, a counter above and a ring of counters around it, which can be used in anticoincidence to eliminate counts due to penetrating background radiation. Actually, the counter volumes are connected and the counter filled as one unit. The plateaus of the different anode leads have sufficient overlaps so that they may be connected in parallel.

A large BF_3 neutron counter was constructed specifically for use in a neutron crystal spectrometer.

Miscellaneous

A 1500-v adaptation of the precision high voltage supply was made for scintillation counter use. The low and high voltage are both obtained from a single radio type of power transformer. The high voltage regulator tubes are type 6BG6-G. The stability is similar to that of previous models, being a maximum of a few hundredths percent variation per day.

A scaler and ratemeter circuit are under construction for use on the Laboratory disaster team truck.

Eleven MX-3 ionization chamber instruments have been installed in rooms of the hot laboratory, and have been fitted with remote meters which are located outside the rooms. Lights indicate which scale has been selected.

An interesting device was made for controlling the level of liquid nitrogen in a Dewar flask. The sensing elements are two half-watt resistors located so that, when the lower resistor is uncovered, liquid nitrogen flows into the flask; the flow is cut off when the level rises enough to cover the second resistor. The circuit supplies about one-tenth watt to the resistors. The resistance changes by approximately a factor of two as the resistor is submerged. The change in voltage drop triggers thyratrons which control the flow valves. The resistors can be easily inserted into a complex glassware system and the control circuit may be located wherever convenient.

One of the smoke detectors built for the Meteorology Department some time ago has been rebuilt to increase the sensitivity. The principal change was a modification of the optical system to reduce the stray light background. The circuit was simplified and the general layout much improved from the point of view of servicing. The most sensitive scale of the new instrument is completely

overloaded by the dust in ordinary indoor or outdoor air. This high sensitivity is useful in testing dust filters.

A foot-operated tally was built for the Biology Department for cell counting and for similar operations where the eye must be kept on the microscope while both hands are occupied.

A G-M tube-ratemeter safety circuit was supplied for use in a hot cell to warn when the aluminum is stripped off a uranium slug by solution.

Health Physics Division

Building Survey

Fifteen days of "round-the-clock" health physics shift coverage was provided during the initial period of reactor start-up. Frequent surveys were made of the reactor shield and plenum chambers. Remote recording monitors and automatic alarms were provided for the plenum chambers that could still be entered between periods of low level operation. Exposure to personnel was negligible; the maximum dosage rate inside the plenum chambers with the reactor not operating was 4 mr/hr.

There has been a marked increase in health physics work at the hot laboratory in connection with a number of experiments, including the setting up of a 72-curie Co^{60} irradiation source. Detailed health physics procedures have been established by the Hot Laboratory Operations Group. There has also been an increase in survey responsibility at the "hot" machine shop, where machining of uranium and activated metals has been going on.

A collar has been designed and constructed for holding seeds directly next to the 16-curie Co^{60} source at the Biology Department field. The dosage rate in this collar was found to be of the order of 6000 r/hr. The use of this attachment resulted in about 8% reduction in dosage at other parts of the field. Measurements of dosage at various positions in the field have been made for the Biology Department.

The radiation intensity resulting from the 16-curie Co^{60} source was determined at various distances out to 500 m, using the dynamic condenser electrometer on the area monitoring mobile unit. The purpose was to determine air absorption characteristics for use in forecasting levels to be expected at the edge of the site due to a proposed 200-curie field source. The effective absorption coefficient was found to increase gradually from 0.001 per m, close in, to a value of 0.007 per m, at a distance of 300 m and beyond. The sizeable increase in absorption coefficient is to be expected as a result of degradation of the gamma radiation by scattering. A rough measurement was also obtained of the absorption characteristics of the woods surrounding the new site. In this case, the effective absorption coefficient was approximately 0.012 per m. Computations based on these data show that only negligible intensities of radiation will exist at the boundary of the site, and that there should be no interference with the operation of the reactor in terms of total off-site radiation.

An agreement was reached in regard to safety measures at the Chemistry Department's 2-Mev electrostatic generator. A steel door is to be set up between the laboratory and the area outside the door to the vault. A survey of the Chemistry Department's X-ray diffraction unit was made and showed 300 to 700 mr/hr near the beam and 50 mr/hr near the control panels. There were a number of "spills" of radioactive material in various parts of the laboratory -- none of very serious proportions. For the Medical Department, various problems were handled concerning personnel monitoring, exposure control, and waste disposal connected with some large therapeutic doses of I^{131}.

Fast neutron calibrations were made of the "Neut" survey instruments, using a polonium-beryllium source. The full scale sensitivity of these instruments with the gas pressures now in use is 80 fast neutrons/cm^2/sec. Calibration data were also obtained for the BF_3 counters used by the Survey Group, for both fast and slow neutrons.

Area Monitoring

The Health Physics Division and the Meteorology Group have worked out plans for cooperation during the reactor start-up and testing period. Daily dosage contour maps and forecasts, prepared by the Meteorology Group, are to be furnished to the health physicists. Up-to-the-minute dosage data from area monitoring stations at critical locations will be obtained by the Area Monitoring Group and made available to the Meteorology Group. Data from the area monitoring stations, and particularly from the mobile station, will be utilized to standardize the meteorological dosage computations.

The period of accumulation of undisturbed background data by the area monitoring stations is drawing to a close, since, in a few weeks, the reactor power will be raised to a level where effects at the stations will be detectable. A summary report on the area monitoring program prior to reactor start-up is being prepared and will be issued during the Fall. Minor modifications and improvements in apparatus are still being made, but the stations are essentially complete and operating satisfactorily.

An analysis has been made of the cost of installing area monitoring stations similar to Brookhaven National Laboratory's, since the Laboratory is sometimes asked for such information. The table below includes the cost of production and some of the engineering involved in cleaning up the product and putting it into operation. It does not include any developmental engineering, technical supervision, or administrative overhead applicable to this project. Essentially, the costs given below are based upon the assumption that a complete set of plans and circuits is already available.

A technique has been developed for calibrating the ionization chambers in the field by means of a suitably located cobalt source. A data board has been set up at the Area Monitoring office. Current data from the chart recorders in the stations are posted as they are brought in or received by radio from the service truck. This system will be used to make data readily available for comparison with findings of the Meteorology Group.

Table 1

Equipment	Cost*
Ionization chamber and dynamic condenser electrometer	$ 895.00
G-M counters and scale-of-8 scalers	840.00
Battery-operated ratemeter	885.00
Continuous dust monitor	1,165.00
Photographic recording assembly	535.00
Station housing and general items	2,695.00
10% for installation and testing	700.00
Total	$ 7,715.00

*The operating and maintenance expense for one year for one station is estimated to be $1,900.00. The figures are for one out of 16 stations. The cost of a single station might be somewhat higher.

Personnel Monitoring

With the advent of regular personnel monitoring services at the reactor on August 18, there has been a marked increase in the volume of personnel monitoring equipment utilized. Approximately 3000 film badges and 4000 pairs of pocket chambers are being used per month. No whole body exposures of more than the 300 mrep weekly limit were recorded.

The calibration curve of the sensitive film used in the film badges has been extended to an exposure of 50 r. The film is well saturated at a density of 3.5 but no evidence of reversal is noted. The useful range is 0 to 10 r.

Miscellaneous

Five AEC Fellows in Health Physics have completed a ten-week stay at the Laboratory, during which they obtained practical experience in eleven phases of health physics operations. Plans have been formulated for a similar but larger program next Summer.

The concentration of radioactivity in the effluent from the Laboratory sewage treatment plant remained well below the prescribed limit of 3×10^{-12} c/cc. During August, values averaged about 5×10^{-13} c/cc. Most of this was radioactive iodine, discharged, presumably, by the Medical Department. Sewage activity has since dropped to about a tenth of the August value.

Installation of equipment and waste control facilities for a decontamination laundry is well under way. The laundry is located near the hospital area steam plant and should be ready for use later in the Fall. Protective clothing for work with radioactive materials is being put on a Laboratory-wide pool basis

Publications

W.C. Reinig, W.H. Bishop, Jr., and B.E. Keene, An aspirator type air sampler, Ra-Det 3, 17-20 (1950)

S.J. Harris, An improved technique for radioautographing of dusts, Ra-Det 3, 14-5 (1950)

F.P. Cowan and J.V. Nehemias, Sensitivity of liquid waste monitoring by evaporation method, Nucleonics, in press

Cosmotron

The most conspicuous achievements since the last quarterly progress report are the winding of the magnet coils, now nearly finished, and the completion of the Van de Graaff injector, which is now being installed after performing very well in preliminary tests at Cambridge, Mass. The radio-frequency system, power for the magnet, general wiring, and controls are also well in hand. Somewhat disappointing, however, has been the progress of the vacuum chamber and, indeed, it is probable that this component will be the last one to be completed. The main attention of the Group is now focussed on this problem, but its complexity and the need for careful design and testing have delayed the start of construction. As reported below, fabrication is almost ready to begin. An estimate of the completion date must await the start of construction.

Building

The Cosmotron building is essentially complete, and is now in the final inspection stage. Repairs of minor leaks, electrical adjustments, and checks on all utility equipment have been necessary. The refrigerating plants and the water cooling system have been subject to thorough testing.

(J.S. Medd, L.D. Stoughton)

Power

The motor-generator-flywheel set has had its initial shakedown after installation by undergoing, almost daily, starting test runs for periods ranging from 2 to 6 hours. Starting time for the set is 7 min 15 sec, and shutdown time is 2 hr 5 min.

In operation, the motor-generator set has been found to produce sound of frequency of about 1000 cps and at an intensity level of approximately 100 db. An effort is being made to locate the source of the noise in order to correct this almost dangerous condition.

Under the direction of the manufacturer's supervisor, one 12-tank set of ignitrons has been degassed; work is progressing on the second set.

Plans are proceeding to power one quadrant of the magnet coil, using the 1200-kw power supply formerly used on the magnet testing program. Displacement of the coil and the steel laminations resulting from the magnetic forces will be observed with strain gages.

(A. Wise)

Magnet Coil

Ninety percent of the copper turns are completely fabricated and three quadrants have all turns assembled. Copper is now being placed in the final quadrant. Preliminary water-tightness tests have been completed in the assembled quadrants. Two leaks have been found and repaired. Preliminary voltage tests have indicated that the turn-to-turn insulation at 2500 v is very satisfactory.

(J.A. Kosh)

Injection

Protons will be injected into the Cosmotron by means of a 3.5-4.0-Mev horizontal Van de Graaff electrostatic generator. This machine was constructed by High Voltage Engineering Corp., Cambridge, Mass., and is now in the process of being assembled at the Laboratory. It is expected to be ready for preliminary operation by December 15.

Extensive testing of this machine was carried out at HVEC under Laboratory supervision and partly by Laboratory personnel prior to its acceptance and shipment. Many minor defects were found and eliminated, and the improvements necessary for achieving the desired goal of high current injection became apparent. Basically, the machine is well engineered and has operated satisfactorily in the 3.5-4.0-Mev range, delivering a pulsed proton current of about 1 mamp. Although electron loading, reported elsewhere, is still a problem, this performance was obtained after the installation of better vapor baffling on the diffusion pump and after some conditioning by running.

Fabrication of injection equipment between the electrostatic generator and the Cosmotron is proceeding satisfactorily and should be ready for injection of some protons into the Cosmotron vacuum chamber by the time the Van de Graaff injector is ready.

(C.M. Turner, J.G. Cottingham, G.J. Hoey)

Radio-Frequency System

The low level radio-frequency generation and control system is virtually complete. The diode network computer has undergone preliminary tests and its various parameters have been set to give a frequency which is correct at all inputs to 0.01%. The integrator is built and will shortly be included in the control system, so that dynamic tests can be made simulating actual operation of the Cosmotron.

The high level power amplifier is complete, except for its control wiring which is about three-quarters finished. It has been tested through the third stage. The final stage will not be tested until the amplifier is moved into its final position. The accelerating core still lacks about 5% of its ferrite load which has not yet been delivered from the supplier. The shield for the core and the vacuum chamber section, on which the core is mounted, is still

in the design stage.

(J.P. Blewett, J. Logue, M. Plotkin, A. Pressman, L. Yuan)

Pole-Face Windings

To insure maximum magnetic aperture at all times during the proton acceleration, and to regulate the high value magnetic fields so that the top energy of the Cosmotron can be attained, corrective magnetizing coils (pole-face windings) distributed along the pole faces of the magnet gap are being designed. By means of these pole-face windings and their necessary return windings, it is planned: 1) to correct the magnetic field index, n; 2) to move the magnetic median plane into coincidence with the geometrical median plane, if necessary; 3) to provide additional radial aperture at injection time, if needed; 4) to vary the parameters influencing the magnetic aperture in order to study their effects; and 5) to give flexibility to injection and ejection.

A complete mathematical analysis of the high field current required for the pole-face windings and its variation with time was made before the completion of the design. This analysis showed the required maximum current to be about 800 amp per inch (top and bottom). These computations were corroborated by measurements made on the quarter-scale magnet model. Current requirements for the injection fields were determined from a series of measurements made on the full-scale 11-block magnet model. Further computations on the effect of eddy currents in the pole-face windings on the shape of the magnetic field at injection served to determine the final dimensions of the bars.

Final drawings of the general arrangements and some details of the securing members have been completed. There will be a total of 8 pole-face windings (2 in each quadrant) fastened to the upper and lower pole faces of the magnet. The windings are being made nearly mutually noninductive by returning part in the rear and part in front of the gap. Each pole-face winding will consist of 58 copper conductors, of cross section 3/8" x 7/32", imbedded in a polyester laminate setting at room temperature and reinforced with Fiberglas cloth tape. The rear return windings, one per quadrant, consist of 64 conductors each, and are secured to the main coil wedging bracket. The front return windings, two per quadrant, consist of 34 conductors each and are located above and below the gap, secured to the bars holding the main coil return winding. The windings will be interconnected at terminal boards located on the spreader bars in the straight sections.

Receipt of materials and completion of molds is expected about November 15, 1950. The fabrication and installation of the windings will be done by Laboratory personnel.

(W.H. Moore, J.P. Blewett, M.H. Blewett, J.M. Kelly, J.J. Mede, L.W. Smith)

Vacuum Systems

Assembly of the 20" diffusion pump stands is now 90% complete. The remaining tasks are to install the refrigerated baffles, to complete the requi-

site connections, and to leak-test the assemblies. The prototype pump station has run satisfactorily for the past three months and has reached an ultimate vacuum of 3×10^{-7} mm Hg during the course of the speed tests when charged with Myvane-20 oil. Serious consideration is being given to the use of Octoil-S.

Speed tests on the newly designed, optically dense baffle have shown that it can reduce the pumping speed per pump, at the expected operating pressure of 5×10^{-6} mm Hg, from 2800 l/sec for the original baffle, to 2200 l/sec for this new design. Calculations show that the net pumping speed at the manifold opening will be reduced to approximately 1000 l/sec, due to the impedance of the 16" valve and the transition chamber. This is still in excess of the expected gas load, based upon tests of representative vacuum chamber construction, properly scaled, by at least a factor of five. Eight of the new baffle assemblies have already been completed; the balance will be completed at the rate of three per week.

The design of the transition chambers, between the pumps and the vacuum chamber, has been completed. A contract for the fabrication was let to the Chicago Bridge and Iron Co., Greenville, Pa. Progress under this contract has been reassuring to date and present estimates call for completion of these components in the latter part of November, 1950. The supporting bridge structures for these chambers and the 16" valve have been designed and their fabrication by the Laboratory has been completed. They will be installed as soon as the magnet coils are completed. The prototype 16" valve has been completed and tests have proved it satisfactory.

The layout and design of the fourth (the last) straight section, embracing the installation and shielding of the radio-frequency core, has been initiated.

(C. Lasky)

Vacuum Chamber

The design of the vacuum chamber is almost complete; negotiations with fabricators have been started.

The handling equipment for the vacuum chamber is in the design stage. This will consist of a trussed structure to support the sectors of the chamber at the ends and at each of the three pumping manifolds. This supporting structure will be handled at its center of gravity, and, with the vacuum chamber sector attached, can be turned over so that either side of the chamber can be worked on from above. After assembly on the truss, the sectors will be tested individually for leaks and for ultimate vacuum. The sector will then be inserted in the gap, the supporting structure will be detached, and the final pumping system will be connected.

The outer skin for the chamber will probably be extruded Kel-F, 0.010" thick. This material will be joined together with radial seams, made by dielectric heating, to form a complete sheet. Since the gasket around the edges of the vacuum chamber is perpendicular to these radial seams, this sec-

tion of seam must be smooth and without sharp bumps. Development of a technique to obtain this characteristic is proceeding.

(I. Polk, D. Jacobus)

Control and Wiring

The design of the master timing system is complete. This will provide time-marker pulses for oscilloscopes, fixed and variable delayed pulses, all phased with respect to the starter pulse which can be automatically clocked or operated manually. The complete system can be purchased in individual units by modification, to be undertaken by the manufacturer, of commercially available chassis. A circuit has been designed for the control of the ignitron bias supply for the motor generator timing.

Precise timing pulses, with respect to the magnetic field in the magnet gap, for the initiation of the Van de Graaff injection pulse and the radio-frequency cycle, for the provision of check points for the diode network (i.e., the frequency versus field relation), and for turning off the magnet, will be provided by means of "peaking strips." Each peaking strip consists of a 2" length of 2-mil Mo-Permalloy wire sealed inside a quartz tube (He atmosphere) of the same length with an O.D. of 0.05". The peaking strip is placed inside two coaxial coils and the whole assembly is set in the fringing field of the magnet. One of the coils, the back-bias coil, provides a very uniform magnetic field of 100 gauss. The other is a search coil which detects the large change in flux when the field to be measured is equal and opposite to that in the back-bias coil, i.e., when the total field in the vicinity of the peaker passes through zero. Preliminary tests indicate that an accuracy of ± 2 μsec or ± 0.04 gauss at the injection field of 300 gauss can be obtained.

Schematics of the control circuits for the major components of the Cosmotron are either being roughed out or are in the process of being drawn up in final form. Final schematics and prototypes have been made for thermocouple and ion gage chassis, mechanical pump and diffusion pump junction boxes, chassis for the communication center, and the vacuum motor control center; final construction is under way. The electrical wiring of the 15 diffusion pump stands has been completed and tested. The steel multi-channel wiring raceway is virtually complete and installed. The total wire required has been estimated (about 100 miles), has been ordered, and partial shipments have been received.

The console, where all the important controls, adjustments, and meters required for the operation of the Cosmotron are centered, is in the design stage. A preliminary model of the special oscilloscopes to be used in the console is under construction.

(G.K. Green, E. Dexter, R.R. Kassner, J.M. Kelly, F.J. Seufert, J.L. Walsh)

Special Investigations

Electron loading in the Van de Graaff tubes. The electron loading phenomenon, mentioned in the last progress report, has been investigated in some detail. Discussions with other operators of high voltage machines have shown that the phenomenon is a universal one and has been an important factor in the limiting operation of high voltage vacuum tubes. The phenomenon consists of the appearance of a spurious electron current from a region at or near the tube cathode. The current rises very rapidly with voltage (in this case, with about the sixth power of voltage) and results in the generation of intense X radiation and in heavy loading of the high voltage power supply. Probe experiments and studies of the X radiation have proven that the effect is associated with insulating layers, probably of pump oil or other organic materials, which acquire surface charges and emit electrons in a manner analogous to that observed in the Malter effect.

The effect has been observed in a parallel plane diode operated at voltages in the tens of kilovolts, but with small spacings, so that the gradients are of the same order as those in Van de Graaff machines. A clean vacuum system and vacuum diode are under construction so that the effect can be observed under carefully controlled conditions and the offending surface layers can be identified. Also, a theoretical attack on the Malter effect is under way and gives promise of yielding an explanation of this rather sketchily understood phenomenon.

(J.P. Blewett, C.M. Turner)

Vacuum testing. Since the successful operation of the Cosmotron depends critically on the vacuum obtainable, a careful study has been made of the factors affecting the ultimate vacuum. The tests have been made using a fairly large steel chamber which may be covered with a steel plate or, alternatively, with a steel grid and plastic sheet simulating a section of the proposed vacuum chamber. The pumping speed of the test equipment has been scaled accordingly.

In brief, the tests show that the plastic selected, a 0.010" Kel-F sheet, is, for vacuum purposes, practically as good as a steel surface, and contributes negligibly to the ultimate pressure. The principal limitation has been traced to the gasket material, neoprene rubber. Pressures of about 5×10^{-6} mm Hg, as read on a nitrogen calibrated ion gage, can be obtained using a rubber surface scaled to twice that estimated to be present in the final design of the vacuum chamber.

This is a satisfactory pressure and can be improved, by approximately a factor of two, by use of liquid nitrogen to increase the pumping speed for condensible vapors. On the other hand, several days pumping time is required to reach this condition; at temperatures (of the rubber) above 30°C, a satisfactory pressure is difficult to obtain. It is hoped that a better type of rubber can be secured in order to have a somewhat greater factor of safety. Tests have shown that pre-pumping of the gasket material will reduce the necessary pumping time on the chamber to one or two days.

(J.C. Street)

Magnet model measurements. In order to determine the magnetic forces that will exist in the Cosmotron magnet when it is pulsed to full power, some dynamic measurements, utilizing strain-gage techniques, have been made on the quarter-scale magnet model. The results are in agreement with previous calculations and show that the "spreader bars," now installed between the magnet quadrants, will be adequate to prevent excessive lateral motion of the magnet blocks during the magnet cycle.

Other measurements on this model indicate that the spreader bars have no deleterious effect, magnetically speaking, up to fields of about 10,000 gauss. Beyond this, the increase of leakage flux due to the onset of saturation of the iron is concentrated by the spreader bars to such an extent that some partial de-gaussing will be necessary in the accelerating section to avoid saturation of the ferrite.

(L.W. Smith)

60" Cyclotron

During the report period, much oscillator testing and running for vacuum chamber outgassing took place. The oscillator grid plane, mica-filled, insulation sheets broke down twice and were replaced once. They were then redesigned so as to be self supporting and air insulated. Burned up seran water hoses in the oscillator were replaced many times, and finally replaced with garden rubber hose which has been holding up well. High frequency parasitics, 70 Mc and above, in the original grounded grid oscillator caused transients, hot spots, and standing waves, with low output on the desired 11-Mc frequency. A period of trial of various types of self-excited oscillators, with several different output coupling arrangements, was followed by a promising period of using first a 1-kw, and then a hastily constructed 3-kw separate oscillator to "tickle" the main oscillator into operation. Dee voltages up to 120-kv dee to dee were obtained by this method.

After much unsuccessful beam searching, during which time three ion sources were designed and tried, many vacuum and water vapor leaks were repaired, and the 200-kc R-F arc filament supply was replaced by a d.c. generator, it was decided to install a high power (two 880-type tubes) driver oscillator. This was completed and installed on top of the original Collins oscillator cabinet. Early operation of the new master oscillator, driving the six 880 unit as an amplifier, included a period of debugging parasitics, component over-heating, and excitation and output coupling changes, until dee voltages of over 200-kv peak dee to dee were finally obtained.

On the evening of September 29, a sharp beam on a beryllium probe target at the 20" radius was obtained, and the neutron count rate meter was driven off scale. This was the first beam from the machine.

A current measuring probe was installed later, and first readings indicated a deuteron beam of about 0.1 μamp. Shimming runs were made, boosting this to about 0.7 μamp at about 10-Mev energy. More recently, an asymmetric

shim arrangement suddenly brought the beam up to 30 μamp and the foil target shield was burned up. Several more foils were disintegrated. Then, a water cooled probe target was constructed and the thermopile current indicator hooked up for use. A beam of more than 1.5-kw power was found. This indicates that more than 150 μamp on the probe at somewhat higher than 12.3 Mev is now being obtained. Further shimming experiments are to be made and plans are under way for deflector insertion in the chamber to give, ultimately, an outside beam.

(W.W. Merkle, C.P. Baker)

Electrostatic Accelerator

Further improvement work on the General Electric electrostatic accelerator has been suspended, pending conclusion of negotiations with the General Electric Company relative to contract settlement. Meanwhile, the instrument is being used for research in the energy range up to 2 Mev, where operation is reasonably reliable, by members of the Physics and Chemistry Departments. Protons or deuterons can be accelerated with beam currents of a few μamp.

CHEMISTRY DEPARTMENT

During the review period, investigations have been carried out in: a) general chemistry of various substances, b) radiation chemistry, c) chemical studies with isotopes, and d) nuclear problems. Considerable progress has been made with the design and construction of a neutron spectrometer. Service work in both analytical chemistry and radiochemistry has continued at a somewhat higher level than previously.

Individual reports, covering various phases of the Department's research, are given in the following sections. As in earlier progress reports, the detail in which the various studies are discussed varies considerably, depending on the nature of the problem and the degree of completeness of the work.

The magnetic susceptibility of cerous fluoride and its temperature dependence have been redetermined; similar measurements have been made on mixtures of cerous and lanthanum fluorides. The results indicate that the Heisenberg exchange does not occur between Ce^{+++} ions in CeF_3 and that the interaction energy represented by the Weiss constant is due to the crystalline field. The magnetic moment of the trivalent praseodymium ion has been determined by susceptibility measurements on a PrF_3 sample of high purity. Magnetic measurements on uranium tetrachloride have failed to confirm the unusual dependence of susceptibility on temperature reported in the literature; the present results are compatible with the supposition that the U^{++++} ion belongs to an "actinide series." In collaborative experiments with Los Alamos, the magnetic susceptibilities of some trivalent and tetravalent plutonium salts have been measured. The results deviate considerably from the free ion theory for a rare-earth-like series.

In radiation chemistry, three lines of investigation have been initiated with the aid of the 2-Mev electrostatic generator. The problem of dosimetry of 2-Mev X-rays is being studied. The standard methods of measurement with ionization chambers or with radiation-induced chemical change are found to be less precise than desired; improvements are necessary. The decomposition of aqueous solutions of bromide by X-rays is being studied. The yields of oxygen and hydrogen peroxide are less than expected from earlier work. Some observations have also been made on the decomposition of solid nitrates caused by exposure to high energy electrons.

New results on the kinetics of the electron transfer exchange reaction between ferrous and ferric ions are reported. As in the thallous-thallic and cerous-ceric systems, the rate increases with decrease in acidity. This effect suggests that hydrolyzed species participate in the reaction more effectively than do the unhydrolyzed ions.

Measurements on the reaction between charcoal and water vapor have shown similarities between this reaction and that of charcoal with CO_2. The reaction with H_2O permits the conversion of H_2O^{18} to CO^{18} without isotopic dilution of the oxygen. The carbon monoxide can be converted catalytically to carbon dioxide with a two-fold isotopic dilution. In connection with the

problem of assaying the deuterium content of hydrocarbons, measurements have been made on the absolute intensities of C-H and C-D bands in infrared spectra. Under certain conditions, the number of C-H and C-D bonds per molecule can be estimated from the infrared intensities.

In organic chemistry, the mechanism of the Faworskii reaction has been studied with C^{14} tracer. The data give support to a previous conclusion that the reaction proceeds through a symmetrical ring intermediate. Additional evidence for such intermediates in other reactions is presented. In connection with other work a simple synthesis of optically active secondary alcohols has been developed and is described.

An investigation has been started on the determination of the thermodynamic activity of hydrogen bromide at high dilution in acetic acid by vapor pressure measurement with the aid of radioactive bromine. Preliminary measurements made without tracer are reported.

The fractionation of carbon isotopes in decarboxylation reactions has been studied with two other compounds -- mesitoic acid and trichloracetate ion. The results are discussed in terms of the theory of the effect of isotopic substitution on reaction rates developed at the Laboratory. Good accord between experiment and theory is found; the results lend additional support to earlier work on malonic acid. A discussion of the errors in such experiments is included.

A double crystal neutron spectrometer, designed for structure determinations by neutron diffraction, has been designed and is nearing completion. Its features are described.

In nuclear chemistry, the proportional X-ray counter and pulse height analyzer have been used to measure the internal conversion coefficient of the 35-kev gamma ray of Te^{125}. The result suggests that the process is a mixture of magnetic dipole and electric quadrupole transitions. The decay scheme of I^{126}, which undergoes negative beta decay, electron capture, and positron emission is being studied. The data permit a re-evaluation of the γ,n yield of this isotope with 100-Mev X-rays and serve to clarify previous work on the trend of γ,n yields with atomic number. New results are also reported on the energy distribution of the Li^7 ions which recoil following electron capture in Be^7. The spectra show a peak near the maximum energy, and definitely favor the conclusion that only a single neutrino is emitted in the decay process.

A NOTE ON THE MAGNETIC SUSCEPTIBILITY OF CEROUS FLUORIDE

N. Elliott

The magnetic susceptibility of CeF_3 has been carefully measured over the temperature range 14°K to 293°K by de Haas and Gorter.[1] They found that above

[1] W.J. de Haas and C.J. Gorter, Proc. Acad. Sci. Amsterdam 33, 949 (1930).

the liquid nitrogen temperature, the Weiss-Curie law was followed. The susceptibility is given by the equation:

$$\chi_{mol} = \frac{0.79}{T + 62^\circ}$$

The calculated magnetic moment is 2.54 Bohr magnetons, in good agreement with theory.[2]

The measurements have been repeated at the Laboratory, and were extended to include the magnetic susceptibilities of isomorphous mixtures of cerous and lanthanum fluorides.

The temperature dependence of the susceptibility of CeF_3 indicates an appreciable ionic interaction, with $\Delta = 62^\circ$. This might be caused by the action of the crystal field on the Ce^{+++} ion, or the Heisenberg spin - spin exchange, or a combination of the two.

Recently, it has been shown experimentally that Heisenberg exchange interaction depends upon the number of interacting ions, and that the exchange can be decreased by diluting a paramagnetic salt with an isomorphous diamagnetic salt.[3] A preliminary experiment of this kind has been done, using mixtures of CeF_3 and LaF_3.

CeF_3 and two mixtures of CeF_3 and LaF_3, one containing 60 mol % CeF_3 and the other 20 mol % CeF_3, were prepared by precipitation from solutions of the nitrates with KF. The cerous nitrate was G. Frederick Smith Chemical Company's "reagent grade" material, and the lanthanum nitrate was obtained from Eimer and Amend.

The results of the measurements at room temperature (296°K) are shown in Table 1. Also included is the Leyden measurement.

Table 1

	CeF_3 (Leyden)	100% CeF_3	60% CeF_3	20% CeF_3
$\chi_{mol} \times 10^6$	2210	2210	2186	2215

All the measured susceptibilities are the same within the acccuracy of the experiment, generally considered to be ±2%.

Although CeF_3 and LaF_3 have identical crystal structures and lattice parameters that differ by less than 1%, X-ray powder photographs will be taken to prove whether or not the mixed crystals are really solid solutions.

---

[2] J.H. Van Vleck, The Theory of Electric and Magnetic Susceptibilities, Oxford Press, p. 243.

[3] L. Corliss, Y. Delabarre, and N. Elliott, J. Chem. Phys. 18, 1256 (1950).

At the present state of this experiment, it seems very likely that Heisenberg exchange does not occur between Ce^{+++} ions in CeF_3 and that the interaction energy, $\Delta = 62°$, is entirely due to the crystalline field. Since the crystal structure of CeF_3 is well known, it should now be possible to make a better comparison of the measured crystal field energy with that calculated from theory.

THE MAGNETIC SUSCEPTIBILITY OF PrF_3

M. Griffel* and N. Elliott

A very pure sample of PrF_3 was obtained from the Institute for Atomic Research, Iowa State College, Ames, Iowa. Its magnetic susceptibility was measured as a function of temperature by the Gouy method.

Three samples were measured over the temperature range 76°K to 295°K; the actual measurements were made at liquid nitrogen, dry ice, and room temperatures. The data for all samples agreed to better than 1%.

PrF_3 was found to obey the Weiss-Curie law over the temperature range of the investigation

$$\chi_{mol} = \frac{1.625}{T + 54°} ,$$

where χ_{mol} is the mol susceptibility and T is the absolute temperature. The results are given in Figure 1.

The magnetic moment of the Pr^{+++} ion is calculated to be 3.62 Bohr magnetons, in agreement with the theoretical estimation of Van Vleck.[1]

It was of some interest to us that the Δ term in the Weiss-Curie law, which is a measure of the crystalline field and Heisenberg exchange forces, turned out to be the same for PrF_3 as for NdF_3.[2]

Fortuitously, the magnetic moments of the Pr^{+++} ion and the Nd^{+++} ion are nearly the same, 3.62β and 3.68β, respectively.

The only other rare earth fluoride that has been investigated is CeF_3.[3] De Haas and Gorter found the Weiss-Curie law followed above the liquid nitrogen temperature with

*Institute for Atomic Research, Iowa State College, Ames, Iowa.

[1] J.H. Van Vleck, The Theory of Electric and Magnetic Susceptibilities, Oxford Press, p. 243.

[2] P.W. Selwood, Magnetochemistry, Interscience Publishers, Inc., New York, p. 88.

[3] W.J. de Haas and C.J. Gorter, Proc. Acad. Sci. Amsterdam 33, 949 (1930).

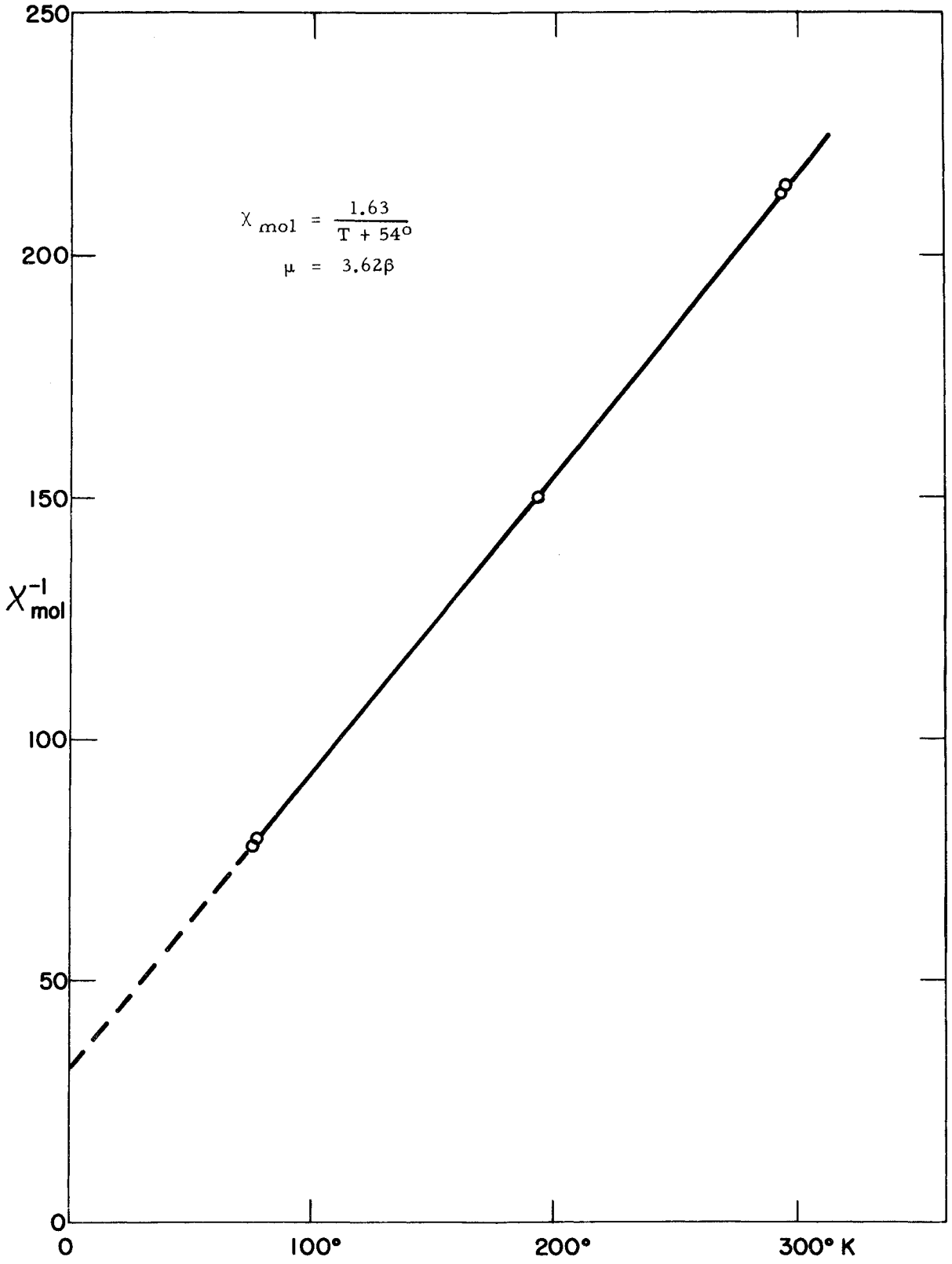

Figure 1. The magnetic susceptibility of PrF_3 as a function of temperature.

$$\chi_{mol} = \frac{0.79}{T + 62^\circ}$$

and $\mu = 2.54$ Bohr magnetons, also in good agreement with theory.[1]

It is planned to compare other cerium, praseodymium, and neodymium salts to obtain further data on the interatomic forces in rare earth compounds.

THE MAGNETIC SUSCEPTIBILITY OF URANIUM TETRACHLORIDE

R. Stoenner and N. Elliott

H. Bommer[1] has measured the magnetic susceptibility of anhydrous uranium tetrachloride, UCl_4, as a function of temperature. A Weiss-Curie law was reported for temperatures above 300°K with

$$\chi_{mol} = \frac{0.92}{T - 55^\circ}$$

The magnetic moment calculated for the U^{++++} ion from Bommer's data is 2.73 Bohr magnetons, in fair agreement with the value calculated for two spinning electrons, which is 2.83 Bohr magnetons. On the other hand, if the U^{++++} ion is a member of an "actinide series," its spectroscopic state is $^3H_4$, and one would expect a moment closer to 3.62 Bohr magnetons.

Examination of Bommer's data indicated the possibility of a crystal structure transformation in the neighborhood of room temperature with one value of the magnetic moment above room temperature and another value below. This is shown in Figure 1. Therefore, we prepared some UCl_4 and repeated the magnetic measurements.

Anhydrous uranium tetrachloride was prepared by a method reported by R. Mezey.[2] It was stored in a vacuum desiccator and all transfer operations were performed in a dry box.

Uranium analyses were done by dissolution of the samples in dilute H_2SO_4, addition of an appropriate quantity of ferric sulfate solution, and titration of the resulting ferrous iron with standard ceric sulfate. This method gave low and somewhat variable results unless precautions were taken to exclude air and keep the solutions cold while the samples were being dissolved. Good results were obtained if the dilute H_2SO_4 was cooled with an ice bath prior to solution of the UCl_4, and if the sample bottles were opened beneath the surface of the solution. Two analyses gave 62.12% and 62.16% U^{++++}. The theoretical value is 62.63%.

---

[1] H. Bommer, Zeit. Anorg. Allgem. Chem. 247-249, 249 (1941).
[2] R. Mezey, Manhattan Project Report C-1139.

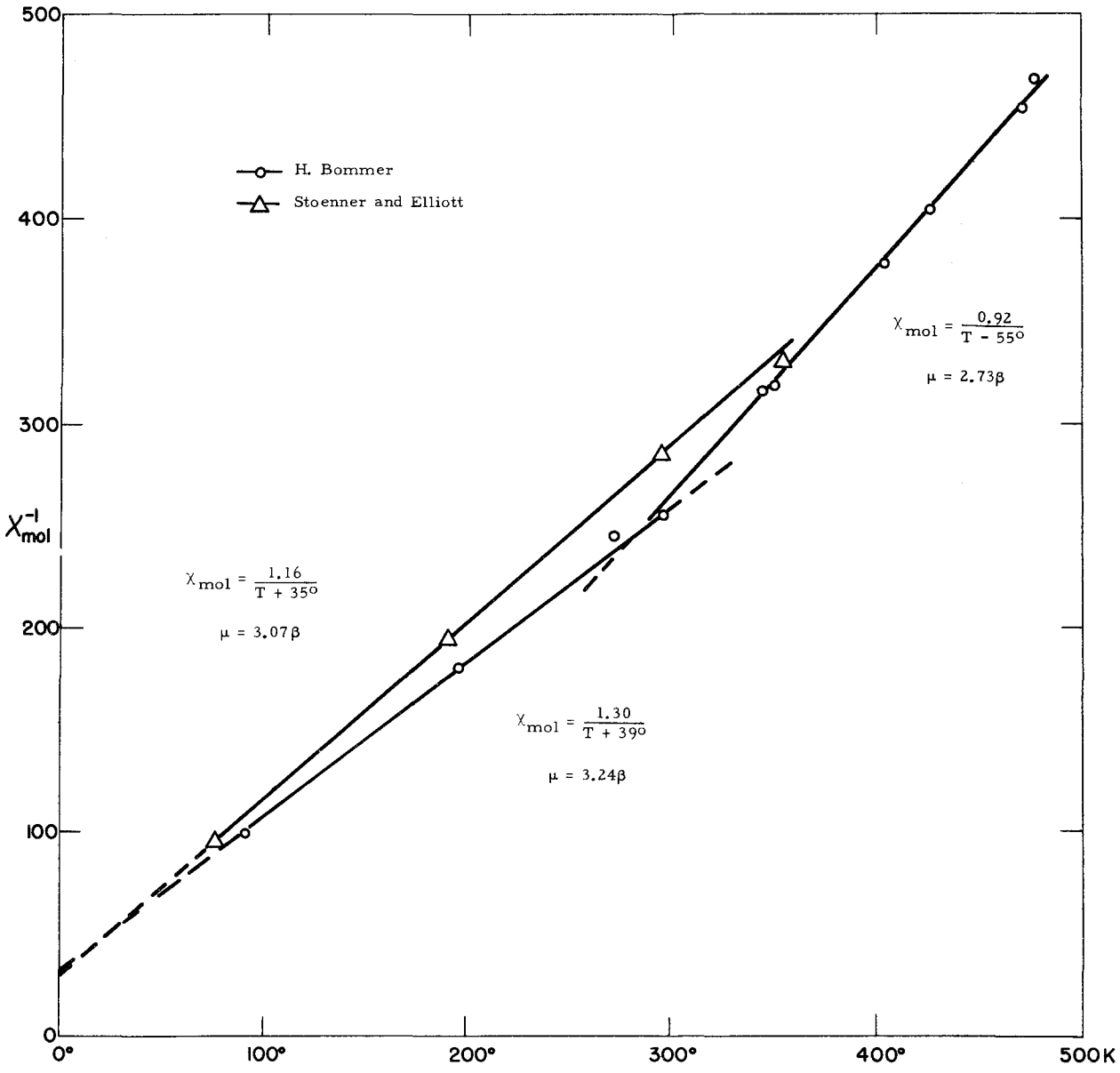

Figure 1. The magnetic susceptibility of UCl_4 as a function of temperature.

Magnetic susceptibility measurements were made on a Gouy balance over a considerable temperature range. No dependence of susceptibility on field strength was observed. The data are given in Table 1 and in Figure 1 for comparison with Bommer's results.

Table 1

Temp °K	76°	191°	295°	354°
$\chi_{mol}\ 10^6$	10340	5060	3490	3000

At present, we have no explanation for the discrepancies between our results and Bommer's, nor for the unusual temperature effect observed by Bommer.

A considerable number of salts of tetravalent uranium have been studied by now. The magnetic moments of the U^{++++} ion are found to lie in the range 2.73-3.75 Bohr magnetons. This is approximately the range of values to be expected if the U^{++++} ion were in a $^3H_4$ state with more or less quenching of the orbital moment by the crystalline fields, the predicted range being 2.83-3.62 Bohr magnetons. The situation is very different if one supposes tetravalent uranium to have two 6d electrons and the state $^3F_2$. By analogy with the corresponding ions of the iron group, the magnetic moment of U^{++++} should then be found in the range 1.63-2.83 Bohr magnetons.

THE MAGNETIC SUSCEPTIBILITIES OF SOME TRIVALENT AND TETRAVALENT PLUTONIUM SALTS*

W.B. Lewis** and N. Elliott

The magnetic moments of most tetravalent uranium compounds have been shown to correspond more closely to the $5f^2\ ^3H_4$ state than to any other.[1] The deviations from the free ion theory are considerable, however, and indicate that the electrons responsible for the magnetism of the U^{++++} ion are not as well shielded as are those of the rare earths. We have measured the susceptibilities of some plutonium salts and find even more striking deviations from theory for 5f configurations.

In order to avoid handling large quantities of exceedingly toxic plutonium in fragile apparatus, a technique based on the Curie-Cheneveau method was devised. A small sample, weighing a few milligrams, is placed in a lucite capsule and suspended from one arm of a microbalance in the magnetic field

*Work done at Los Alamos Scientific Laboratory.

**Los Alamos Scientific Laboratory, Los Alamos, New Mexico.

[1] C. Hutchison and N. Elliott, J. Chem. Phys. 16, 920 (1948); N. Elliott, Phys. Rev. 76, 431 (1949).

approximately at the position of maximum $H(\partial H/\partial X)$, where H is the magnetic field and $(\partial H/\partial X)$ is the field gradient. Since the force is proportional to $H(\partial H/\partial X)$, the susceptibility of any substance can be determined by comparison with an appropriate standard. For standardizing the apparatus, we used chrome alum, $KCr(SO_4)_2 \cdot 12H_2O$, and manganous sulfate, $MnSO_4 \cdot 4H_2O$. Both compounds are essentially magnetically isotropic, and exhibit moments and g values which correspond closely to pure spin values. The susceptibilities have also been determined with good agreement by more than one investigator.

The compounds were prepared according to methods described, for the most part, in Volume 14B, Part I, of the National Nuclear Energy Series. They were assayed for plutonium content by David P. Mariott and identified crystallographically by Eugene Staritsky.

Magnetic susceptibility measurements were made on PuF_3, PuF_4, and $Rb_4Pu(SO_4)_4 \cdot 2H_2O$.* Data were obtained at three temperatures only in this initial survey. They are presented in Table 1, and include a correction for the diamagnetism of plutonium, 40 x 10^{-6} c.g.s. units per mol, and for the anions.

Table 1

PuF_3		PuF_4		$Rb_4Pu(SO_4)_4 \cdot 2H_2O$	
Temperature	$\chi \cdot 10^6$ mol	Temperature	$\chi \cdot 10^6$ mol	Temperature	$\chi \cdot 10^6$ mol
76°K	2550	76°K	3020	76°K	1300
189.5°	1590	190°	2420	193°	1070
300°	1150	302°	1980	300°	920

The results are also shown graphically in Figures 1, 2, and 3, where the reciprocal mol susceptibility is plotted against the absolute temperature. It will be seen that the Weiss-Curie law is obeyed quite well down to the temperature of liquid nitrogen. The large values of the Δ terms, especially for the Pu^{++++} ion, show that it is impossible to draw conclusions about the spectroscopic states of the heavy elements from room temperature measurements of the susceptibilities alone.

Magnetic moment values were calculated for the Pu^{+++} and Pu^{++++} ions by means of the equation:

$$\mu = 2.83 \sqrt{\chi_{mol}(T + \Delta)}$$

If the Pu^{+++} and Pu^{++++} ions have unpaired 5f electrons giving rise to their paramagnetism, the corresponding electronic states would be $^6H_{5/2}$ and $^5I_4$,

*Lewis has since studied $Pu(SO_4)_2 \cdot 4H_2O$, $Pu(C_2O_4)_2 \cdot 6H_2O$, $Pu_2(C_2O_4)_3 \cdot 9H_2O$, and $NaPu(SO_4)_2 \cdot 4H_2O$. The results were reported at the September 1950 meeting of the American Chemical Society, Chicago, Illinois.

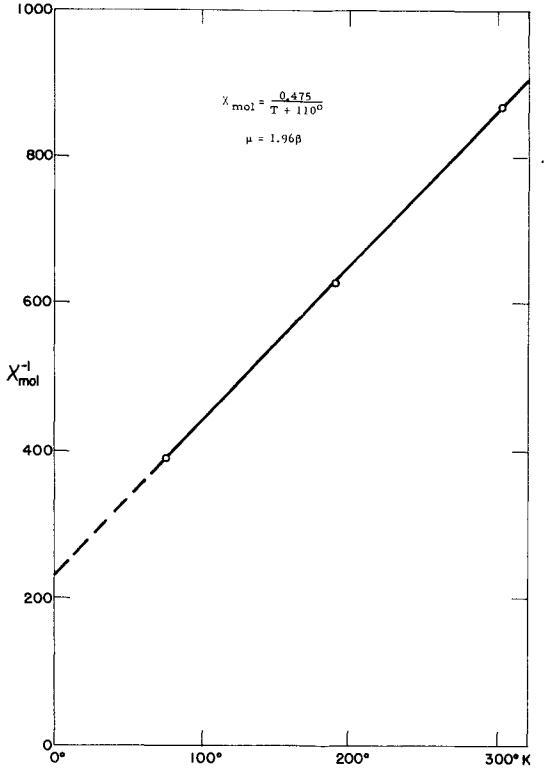

Figure 1. The magnetic susceptibility of PuF_3 as a function of temperature.

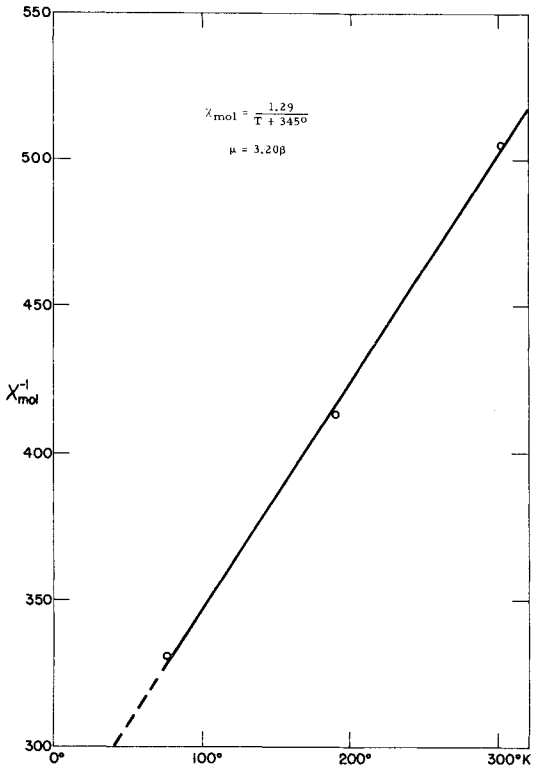

Figure 2. The magnetic susceptibility of PuF_4 as a function of temperature.

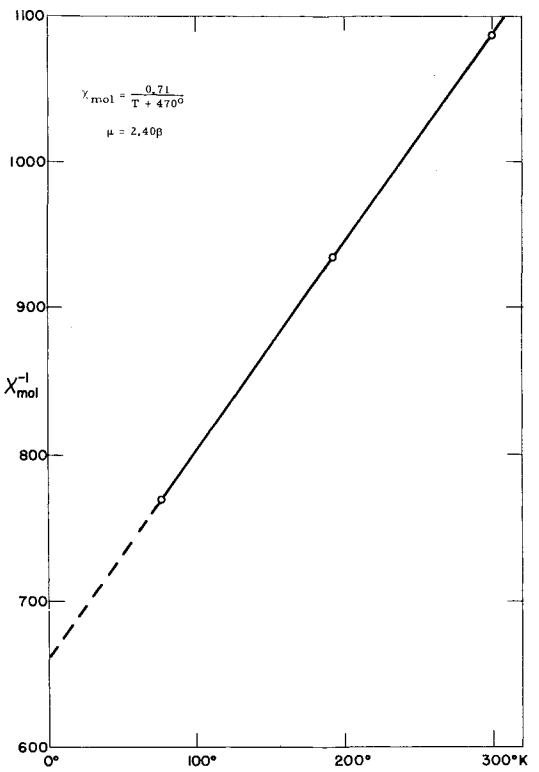

Figure 3. The magnetic susceptibility of $Rb_4Pu(SO_4)_4 \cdot 2H_2O$ as a function of temperature.

respectively. If these are 6d electrons, however, the states would be $^6S_{5/2}$ and $^5D_0$. The theoretical moments for free ions in these states are given in Table 2, together with the experimental values. Also included are the "spin-only" moments, for the case where the orbital moments are quenched. It is assumed that the multiplet splitting is large with respect to kT.

Table 2

Ion	Term	Moment in Bohr Magnetons		
		Spin + Orbital	Spin Only	Experiment
Pu^{+++}	$6d^5\ ^6S_{5/2}$ $5f^5\ ^6H_{5/2}$	5.92 0.84	5.92 5.92	1.96
Pu^{++++}	$6d^4\ ^5D_0$ $5f^4\ ^5I_4$	0.0 2.68	4.90 4.90	2.40; 3.20

In considering the ground states of these ions, the data for PuF_3 are perhaps the more interesting. If Pu^{+++} were in a $^6S_{5/2}$ state, the magnetic moment would be 5.92β, regardless of orbital quenching. However, its observed value, 1.96β, is much closer to that expected of the rare earth state, 0.84β, suggesting a configuration term $^6H_{5/2}$ with partial orbital quenching, as found for tetravalent uranium.

Within experimental error, the moments observed for the Pu^{++++} ion lie in ranges to be expected for either 5f or 6d electrons. In view of the experimental difficulties, it does not seem to be significant at present that one of the observed values is lower than 2.68β, which is the calculated lower limit for a $^5I_4$ state.

RADIATION CHEMISTRY

A.O. Allen

Work which has been carried out with the Chemistry Department's electrostatic generator is described in the following sections. Attention has been given to the problem of measuring 2-Mev X-ray irradiation dosage, to the radiation chemistry of aqueous solutions containing bromide ion, and to the decomposition of crystalline nitrates by 2-Mev electrons.

In addition, a number of service irradiations have been made. The results of these experiments are to be reported elsewhere. Dried proteins were irradiated in vacuo with the electron beam for Professor E.C. Pollard, of Yale University. The results provide an interesting comparison with his similar experiments with deuteron beams. Suspensions of visual purple were irradiated with

X-rays and dry visual purple was irradiated with the electron beam for Dr. J. Peskin, a visitor in the Biology Department from the University of Michigan. The X-ray beam was used by G.S. Goldhaber, Physics Department of the Laboratory, to excite a number of nuclides to isomeric states.

Dosimetry of 2-Mev X-Rays

(with A. Levy)

For quantitative experiments, it is desirable to know precisely the radiation dose due to the X-rays per ampere-second at given voltages at any point in the target area. Measurements of the radiation field are being made with ionization chambers (Victoreen r-meters) and by following the oxidation of air-saturated acidic solutions of ferrous ammonium sulfate. Both methods have been frequently used by others.

The ionization chamber measurements are irreproducible to the extent of several percent, some individual meters behaving better than others. The ferrous sulfate results fluctuate by about $\pm 3\%$ on duplicate runs. Neither method is considered to be of satisfactory precision at present for either relative or absolute measurements. For this reason, an attempt will be made to develop a calorimetric method for determining absolute intensities.

According to ionization chamber readings, the X-ray intensity in the forward direction decreases with the square of the distance from a point about 1 cm behind the target. At constant current and distance, the intensity was found to vary with the 2.65 power of the voltage. The highest X-ray intensity available (in a small region near the target) is about 22,000 r/min.

Radiation Chemistry of Aqueous Solutions

(with E.R. Johnson)

It is generally believed that water, upon irradiation with X-rays, is decomposed into the radicals H and OH. Some of the radicals escape by diffusion from the site of their formation, wander through the solution, and react with dissolved substances. Others react with each other before diffusing away; when like pairs combine, H_2 and H_2O_2 are formed. In pure water these soon react with radicals to reform water so that little net decomposition occurs. If the free radicals are destroyed by reaction with other solutes, however, hydrogen and hydrogen peroxide accumulate. For example, it has been reported that these are found in equal amounts in neutral solutions of bromide ion after exposure to X-rays. Further study of this system seems to promise useful information on the rates of simple reactions of free radicals; hence, a study of irradiated KBr solutions has been undertaken.

Redistilled water was freed of dissolved gases by repeated freezing, pumping, and melting in vacuo; it was then distilled under vacuum into small glass

bulbs containing the powdered KBr to be dissolved. These were sealed off and irradiated. They were opened in vacuo by freezing, and the gaseous products were pumped off for analysis. The analytical methods were demonstrated on known mixtures to be accurate to ±2%. Peroxide in the solution was determined iodometrically.

In a large number of runs at different dosages, the yield of hydrogen was found to be reproducible and proportional to the dosage up to 10^5 r. However, contrary to previous work, the yield of oxygen (in equivalents) is less then that of hydrogen and this difference increases with dosage. This lack of material balance is being studied further. It seems unlikely that it is due to impurities, since the present purification methods are more stringent than those of earlier workers. Furthermore, runs in which extra precautions were taken to protect the solution from impurities did not cause any improvement. It is possible that an oxidized product is formed which does not respond to present analytical methods.

Radiation Chemistry of Crystalline Nitrates

(with T.W. Davis*)

It is known that solid nitrates are decomposed by radiation to oxygen gas and nitrite. With barium nitrate it has been found[1] that the energy yield is small, indicating that most of the electronic excitation caused by the radiation does not result in chemical change. It was also found that solutions of the bombarded salt are quite alkaline, suggesting that other chemical changes occur. The purpose of the present work was to make a more detailed study of the reaction products formed in the irradiation of nitrates and the factors which influenced their yields.

Thoroughly dried powdered salt was given massive cathode ray doses under a helium atmosphere in a small glass vessel. After irradiation, the helium was pumped off along with gaseous reaction products coming out of the salt. The gaseous products trapped in the salt were obtained by distilling in gas-free water and pumping on the solution. The solution was titrated for nitrite with permanganate. Hyponitrite was looked for but not found.

With potassium nitrate, the quantities of gaseous product (largely oxygen) were not equivalent to the nitrite found, but were sometimes too large, and sometimes too small. Lithium nitrate gave much less gas and nitrite than did potassium nitrate. Sodium nitrite also gave gas after irradiation, indicating that secondary reactions may occur in the irradiation of nitrates. The problem requires further experimentation, with improvement in the analytical techniques.

*New York University.

[1] A.O. Allen and J.A. Ghormley, J. Chem. Phys. 15, 208 (1947).

ACID AND SALT EFFECTS ON THE RATE OF THE FERROUS-FERRIC EXCHANGE REACTION

J. Silverman and R.W. Dodson

Abstract

The second order character of the ferrous-ferric electron transfer exchange reaction, previously established at $HClO_4$ 0.54 f, 0°C, has been confirmed at $HClO_4$ 0.050 f, 0°C. At constant ionic strength, the rate increases as the acid concentration is decreased in a way that suggests that unhydrolyzed and singly hydrolyzed species participate in the reaction. The rate increases as the ionic strength is increased over the range 0.32 to 1.00 f. At $\mu = 0.54$, the rate is the same whether $NaClO_4$ or $La(ClO_4)_3$ is used to establish the ionic strength.

In the preceding quarterly progress report[1] were described measurements of the second order rate constant of the ferrous-ferric electron transfer exchange reaction at 0°C in 0.54 f $HClO_4$. This investigation has been continued with determinations of the dependence of the rate on acid concentration, perchlorate ion concentration, and ionic strength. The experimental methods were as previously described,[1] except that, in the presence of lanthanum, ferric iron was separated by precipitation with 8-hydroxyquinoline.

The effect of acidity on the rate was determined by measurements of the half-time of the exchange reaction over a range of perchloric acid concentration 0.0375 f to 0.54 f. The ionic strength was maintained at 0.54 f by addition of sodium perchlorate. The results are given in Table 1. It is seen that the rate increases as the acid concentration is decreased, a trend also exhibited in the thallous-thallic and cerous-ceric systems.

In order to determine whether the reaction remains second order at the lower acid concentrations, the ferrous and ferric concentrations were separately varied at an acid concentration of 0.0501 f. The results are given in Table 2. Within the error of the measurements, the data in Table 2 show that the reaction remains first order in both ferrous and ferric iron at a perchloric acid concentration as low as 0.05 f.

The data in Table 1 show that the over-all rate constant of the reaction is very nearly a linear function of the reciprocal of the acid concentration. This is illustrated in Figure 1, which shows a plot of rate constant, k, against $1/(H^+)$. The data are represented by a rate law of the form

---

[1] J. Silverman and R.W. Dodson, Quarterly Progress Report,(BNL 64 (S-6)), April 1 - June 30, 1950, p. 31.

$$R = (\text{Fe II})(\text{Fe III}) \left\{ k' + \frac{k''}{(H^+)} \right\},$$

where the parentheses represent concentrations.

This rate law suggests that the exchange reaction proceeds through either of two parallel paths, one acid-independent, and the other involving a species whose concentration is inversely proportional to the acid concentration. Since the ferric ion is known to be hydrolyzed, even in quite acid solutions, and the ferrous much less so, it seems natural to assume that the acid-dependent term

Table 1

Acid Dependence of Ferrous-Ferric Exchange Reaction

(0.0°C, μ = 0.54)

Fe^{++} (formal x 10^4)	Fe^{+++} (formal x 10^4)	$HClO_4$ (formal)	Half-time (sec)	k ($mole^{-1}$-liter-sec^{-1})
-	-	0.540	-	1.34*
3.87	1.14	0.289	739	1.87
"	"	0.163	570	2.42
"	"	0.113	426	3.24
"	"	0.0878	370	3.73
"	"	0.0748	333	4.15
(see Table 2)	-	0.0501	(see Table 2)	5.99*
3.08	1.04	0.0375	237	7.10

*Mean of five runs at different iron concentrations.

Table 2

Check of Reaction Order at Low Acidity

(0.0°C, $HClO_4$ 0.0501 f; $NaClO_4$ 0.490 f)

Fe^{++} (formal x 10^4)	Fe^{+++} (formal x 10^4)	Half-time (sec)	k ($mole^{-1}$-liter-sec^{-1})
3.083	1.040	272	6.18
2.059	1.039	374	5.98
1.029	1.037	591	5.66
2.059	2.075	270	6.14
2.059	3.111	228	6.00
			mean 5.99 ± 0.14

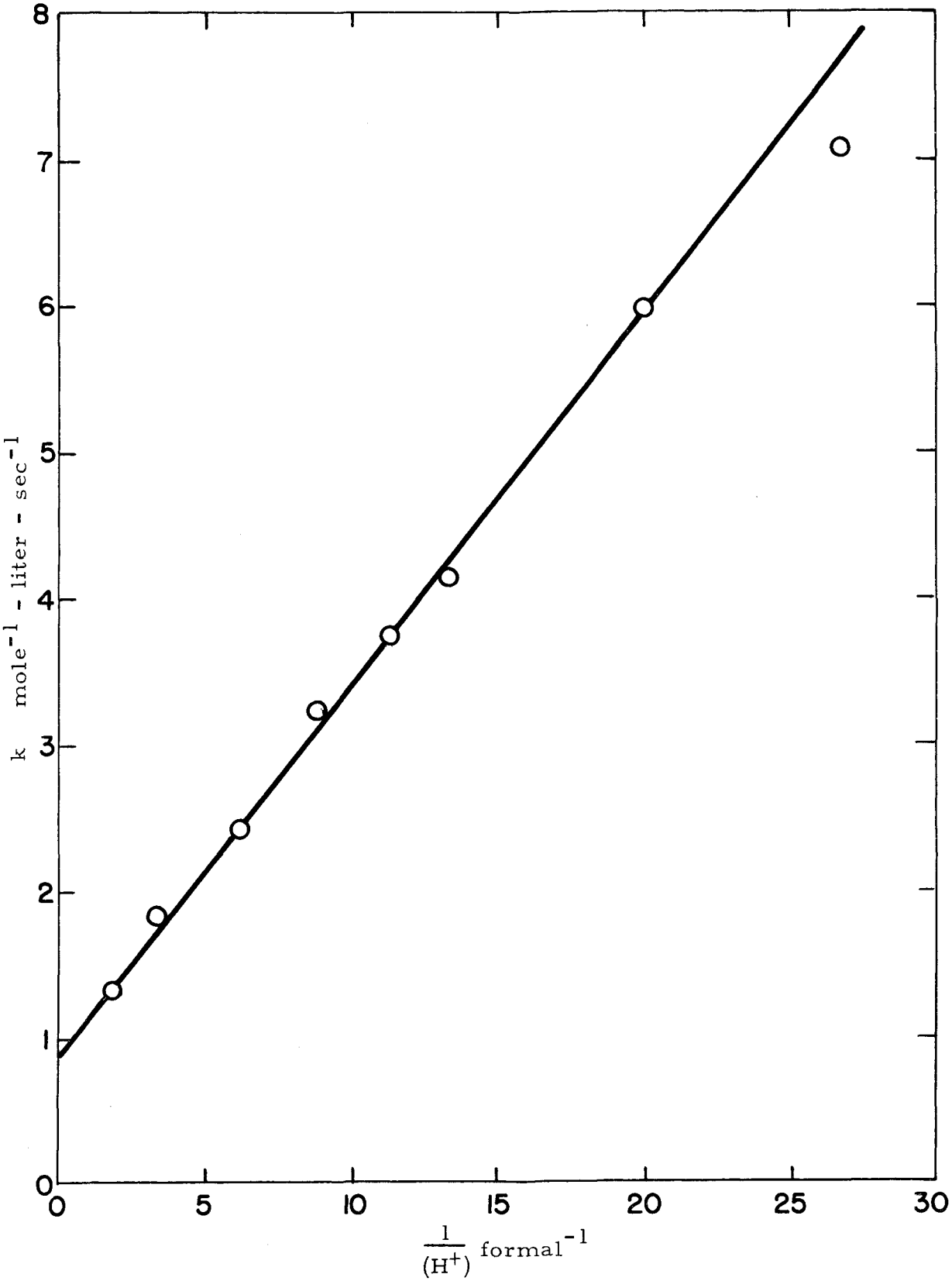

Figure 1. Over-all second order rate constant of the ferrous-ferric exchange reaction versus reciprocal of acid concentration, 0.0°C; ionic strength, 0.54 f.

represents the reaction between Fe^{++} and $FeOH^{++}$, the latter being formed in the quilibrium:

$$Fe^{+++} + H_2O = FeOH^{++} + H^+$$

$$K = \frac{(FeOH^{++})(H^+)}{(Fe^{+++})}$$

If the extent of hydrolysis of ferric ion is slight in the range of acidity covered, the rate of the parallel exchange between the unhydrolyzed ions will be inappreciably affected by changes in acidity.

When the possible bimolecular exchange reactions between Fe^{++}, $FeOH^+$, Fe^{+++}, and $FeOH^{++}$ are considered (with the exception of reaction between the two singly hydrolyzed species), the following expression is obtained for the total rate at which ferrous iron becomes ferric, and vice versa:

$$R = k_1ab \frac{(H^+)^2}{[(H^+)+K_1]\ [(H^+)+K_2]} + k_2ab \frac{(H^+)}{[(H^+)+K_1]\ [(H^+)+K_2]}$$

In this expression, a is the total concentration of ferric iron, b is that of ferrous iron, and (H^+) is that of perchloric acid. K_1 is the equilibrium constant for the hydrolysis of Fe^{+++} to $FeOH^{++}$, K_2 is the equilibrium constant for the hydrolysis of Fe^{++} to $FeOH^+$, and k_1 is the specific rate constant for the exchange reaction between the species Fe^{++} and Fe^{+++}. The quantity k_2 is a combination of hydrolysis equilibrium constants and true specific rate constants. The constant K_1 may be roughly estimated as 0.3×10^{-3} under our conditions from the results of Bray and Hershey[2]; K_2 is certainly smaller. Since the smallest value of (H^+) in the present experiments was 37.5×10^{-3} f, K_1 and K_2 may be neglected with respect to (H^+), and the above expression reduces to

$$R = ab \left[k_1 + \frac{k_2}{(H^+)} \right] ,$$

which is the observed rate law.

The effects on the rate of varying the ionic strength and of varying the charge type of the ions used to establish the ionic strength have also been studied. Table 3 gives data obtained with lanthanum and sodium perchlorates at constant perchloric acid concentration.

It is seen that the rate of the reaction increases as the ionic strength is increased, in qualitative accord with expectations for a reaction between ions of like sign according to Bronsted-Debye-Huckel theory. It is of further interest that the rate is constant within experimental error when Na^+ is replaced by La^{+++} at $\mu = 0.54$, which suggests that specific cation or anion effects are small under these conditions.

---

[2]W.C. Bray and A.V. Hershey, J. Am. Chem. Soc. 56, 1889 (1934).

Table 3

Effect of Salts on the Ferrous-Ferric Exchange Reaction

(0.0°C, $HClO_4$ 0.0878 f)

Na^+ (formal)	La^{+++} (formal)	ClO_4^- (formal)	Ionic Strength (formal)	k (over-all rate constant) ($mole^{-1}$-liter-sec^{-1})
0.452	--	0.541	0.54	3.73
--	0.0753	0.315	0.54	3.62
0.226	--	0.315	0.32	3.20
--	0.151	0.542	1.00	4.64

THE WATER GAS REACTION

James A. Amick and John Turkevich*

This investigation was carried out 1) to study the mechanism of the reaction by which water is decomposed by carbon to form H_2, CO, and CO_2; and 2) to find a procedure for the quantitative conversion, without isotopic dilution, of water enriched in O^{18} to CO_2.

The apparatus used was that employed by Bonner[1] in his investigation of a similar problem at the Laboratory. It consists of a silica reaction chamber (A) in which the charcoal is suspended, and a trap (B) which is used for the introduction of water. Water vapor is circulated over the charcoal by the thermal syphon consisting of the hot reaction chamber and the cold trap (Figure 1).

The reaction of water with charcoal to form CO and H_2 proceeds, at 850°C, in two steps: an initial collision of the water molecule with the charcoal resulting in the formation of H_2 and an oxygenated carbon surface, and a subsequent decomposition of this oxygenated surface into CO and CO_2. The latter step was found to be the slower of the two. The mechanism is thus similar to the one found by Bonner[1] in his investigation of the reaction of CO_2 and charcoal to produce CO.

The CO produced from water enriched seven-fold with O^{18} showed no isotopic dilution, which indicates that the degassing of the charcoal at 850°C removed all oxygen that was capable of exchanging with the oxygenated surface formed in the reaction with H_2O^{18}. It is thus possible to convert H_2O^{18} to CO^{18} and H_2 without isotopic dilution by continuous circulation of water vapor by the thermal syphon over the charcoal surface at 850°C.

*Department of Chemistry, Princeton University.

[1]F. Bonner and J. Turkevich, J. Am. Chem. Soc., in press.

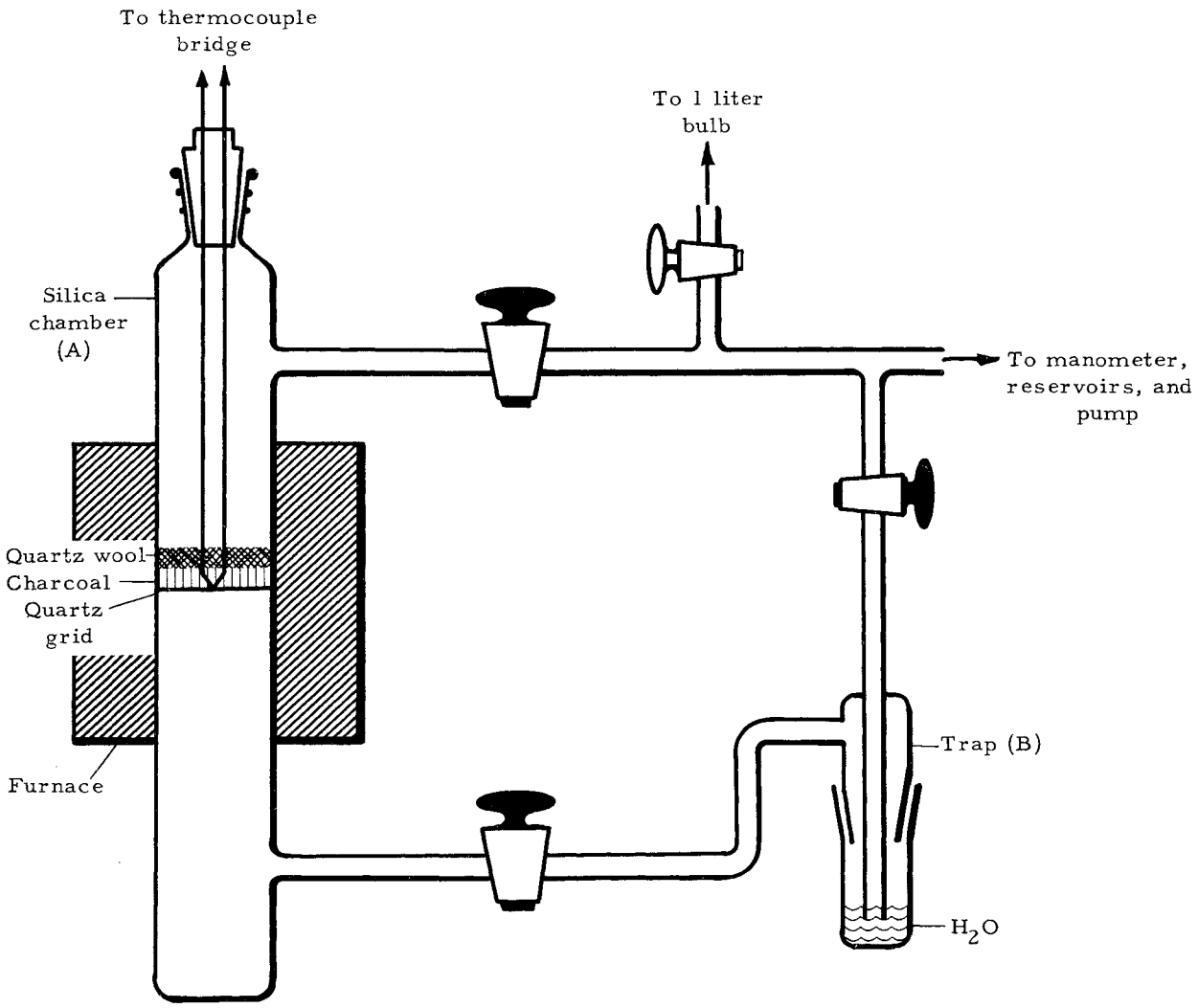

Figure 1. Reaction chamber and thermal syphon.

For the conversion of CO^{18} to $CO_2{}^{18}$, a water gas catalyst ($2Cr_2O_3 \cdot Fe_2O_3$) was prepared. The metal hydroxides were precipitated with ammonia from a solution of the nitrates, washed, centrifuged, and dried at 100°C. One-half gram of the catalyst so prepared was charged into a Pyrex tube. This was then incorporated into the apparatus in place of the silica tube (A) and the catalyst was evacuated by a mercury diffusion pump for 12 hr at 325°C to remove as much of the adsorbed water as possible. The pressure attained in the system after this pumping procedure was 10^{-5}mm Hg.

An amount of the H_2-CO mixture obtained from the charcoal experiments, sufficient to give 5 cm pressure in the system, was allowed to circulate for 30 min over the catalyst at 310°C and was then collected in an evacuated bulb. The isotopic composition was measured in the Consolidated-Nier isotope ratio mass spectrometer at the Laboratory.

The mass spectrometer results showed that about 50% of the original CO had been converted to CO_2. The remaining CO was isotopically identical to the starting material, which indicates that there was no exchange between the CO and the catalyst surface. The O^{18} concentration in the CO_2 produced was one-half that in the original CO. This dilution must be attributed either to oxygen associated with the oxide catalyst or to water still bound to the surface after the treatment described above. Further, the fact that there was no dilution of the CO remaining indicates that there was no exchange between the starting material and the CO_2 product under these conditions. Experiments will be done to determine whether the CO reacts with adsorbed water or with the oxygen of the catalyst itself.

ABSOLUTE INTENSITIES OF C-H AND C-D BANDS IN INFRARED SPECTRA

James A. Amick and John Turkevich*

Since the quantitative determination of the deuterium content of hydrocarbons by mass spectrometric analysis presents difficulties, the applicability of infrared analysis to this type of determination has been investigated. For a quantitative analysis of the deuterium in any hydrocarbon molecule, it is necessary to know: 1) the number of hydrogen atoms in the molecule, 2) whether the intensity of absorption in the infrared is directly proportional to this number, and 3) the ratio of the C-H to C-D intensities. In the present investigation, the C-H stretching band at 3000 cm^{-1} and the C-D stretching band at 2200 cm^{-1} were used.

With the Baird dual beam spectrophotometer, an instrument equipped with NaCl optics, the spectra of several hydrocarbons were obtained, and the data converted to "absolute intensities" by the method of Wilson and Wells.[1] The results obtained with ethane are given in Table 1.

*Department of Chemistry, Princeton University.

[1]E.B. Wilson and A.J. Wells, J. Chem. Phys. 14, 578 (1946).

Table 1

Absolute Intensity Values (A_i) for Ethane in the Gas Phase

A_i	Worker
367 x 10^{10} cy./cm	Thorndike[2]
377 x 10^{10} cy./cm	Schultz[3]
360 x 10^{10} cy./cm	present report

These data are useful as a check since the absolute intensities for the C-H bands in ethane have been calculated by Thorndike[2] and Schultz,[3] the latter using the same instrument that was used in this research.

The isomeric pentanes were studied next since the maximum differences due to isomerism should occur in these molecules. The curves from which the absolute intensities were calculated are shown in Figures 1 and 2, for the pentanes in the gas phase and in CCl_4 solution, respectively. It can be seen that within the limit of error, the position of a hydrogen on the molecule has no effect on the absorption at 3000 cm^{-1}. It will also be noted that the intensity per C-H bond in pentane in the gas phase is within 5% of the value for a C-H bond in ethane (Table 2).

Table 2

Absolute Intensity per C-H Bond in the Gas Phase

Gas	A_i
Ethane	360 x 10^{10} cy./cm
Isomeric pentanes	384 x 10^{10} cy./cm

Recently, it has been shown by Francis[4] that for solutions of the higher members of the saturated hydrocarbon series, the absolute intensities of the molecules can be represented as a function of the number of C-H's. Using his values for individual C-H intensities, and applying suitable conversion factors, one obtains results that check the saturated hydrocarbon values in Figure 3 within 5%. Figure 4 gives the results obtained when hydrocarbons belonging to different series are compared, the data being obtained from spectra taken on the gas phase, and normalized to "absolute intensity" per C-H bond. It is seen that the absorption per C-H bond is fairly constant from molecule to molecule, at least within a series, and that the number of C-H bonds can therefore be calculated from the total intensity.

[2] A.M. Thorndike, J. Chem. Phys. 15, 868 (1947).
[3] R.D. Schultz, Master's Thesis, New York University, May, 1949.
[4] S.A. Francis, J. Chem. Phys. 18, 861 (1950).

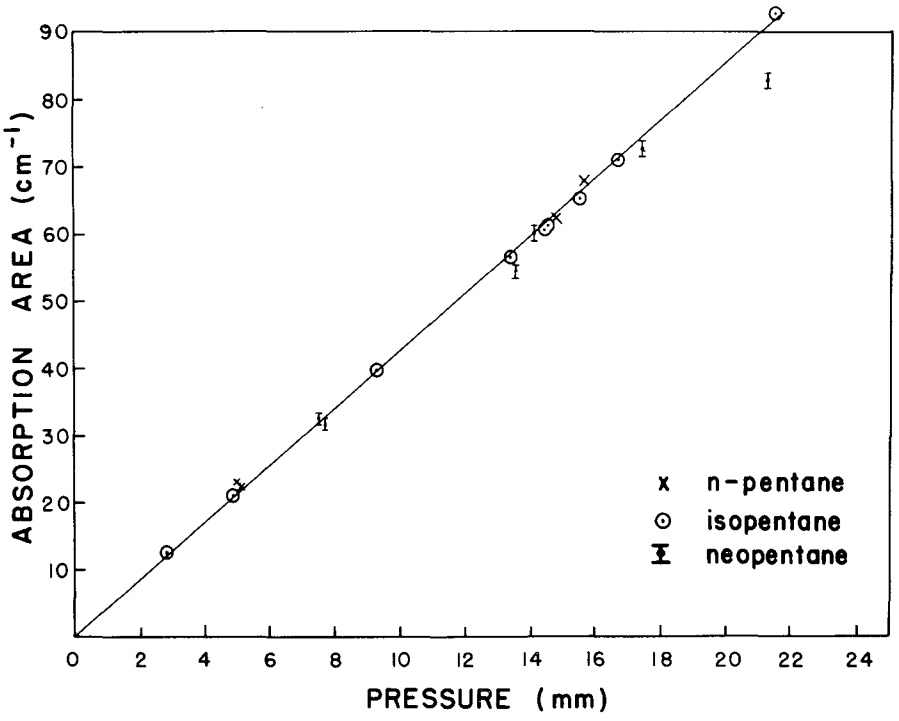

Figure 1. Absorption area in the C-H band at 3000 cm^{-1} as a function of pressure for the isomeric pentanes in the gas phase.

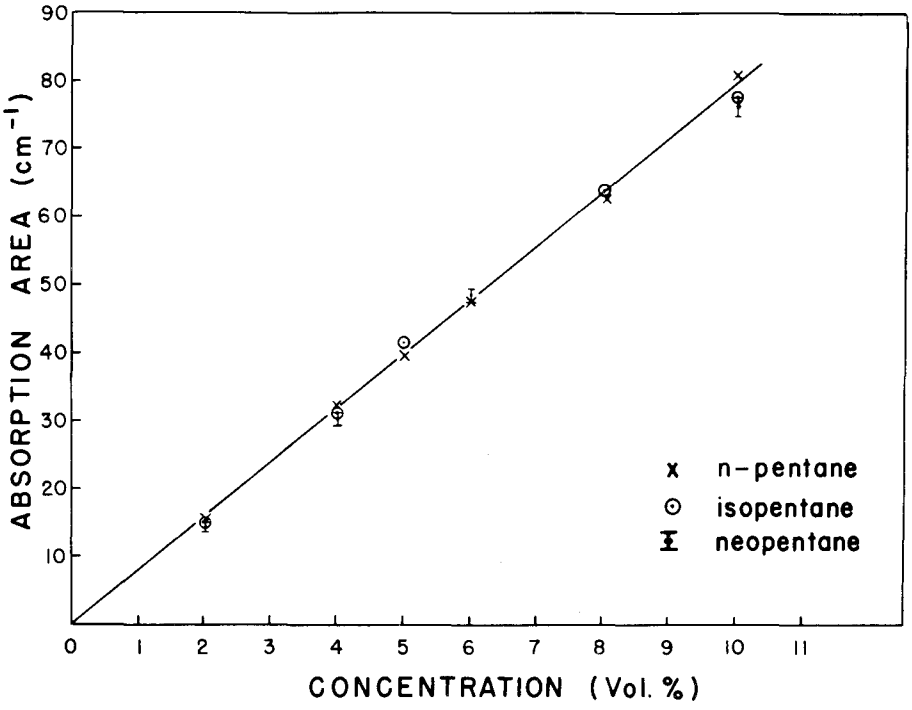

Figure 2. Absorption area in the C-H band at 3000 cm^{-1} as a function of concentration for the isomeric pentanes in CCl_4 solution.

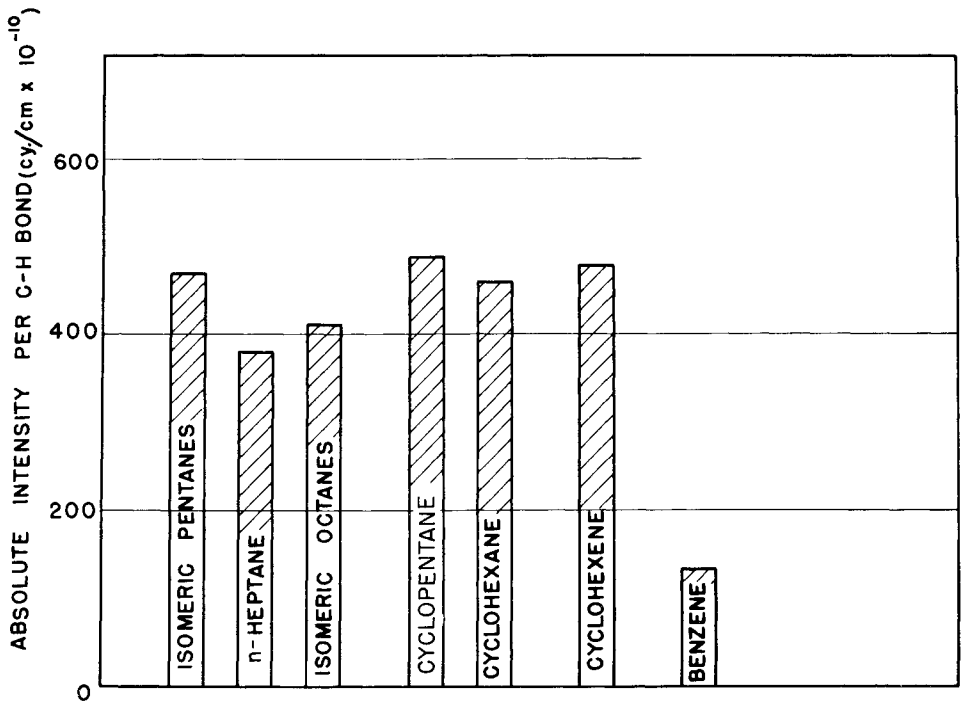

Figure 3. Absolute intensities of infrared absorption of C-H bonds in various hydrocarbons in CCl_4 solutions.

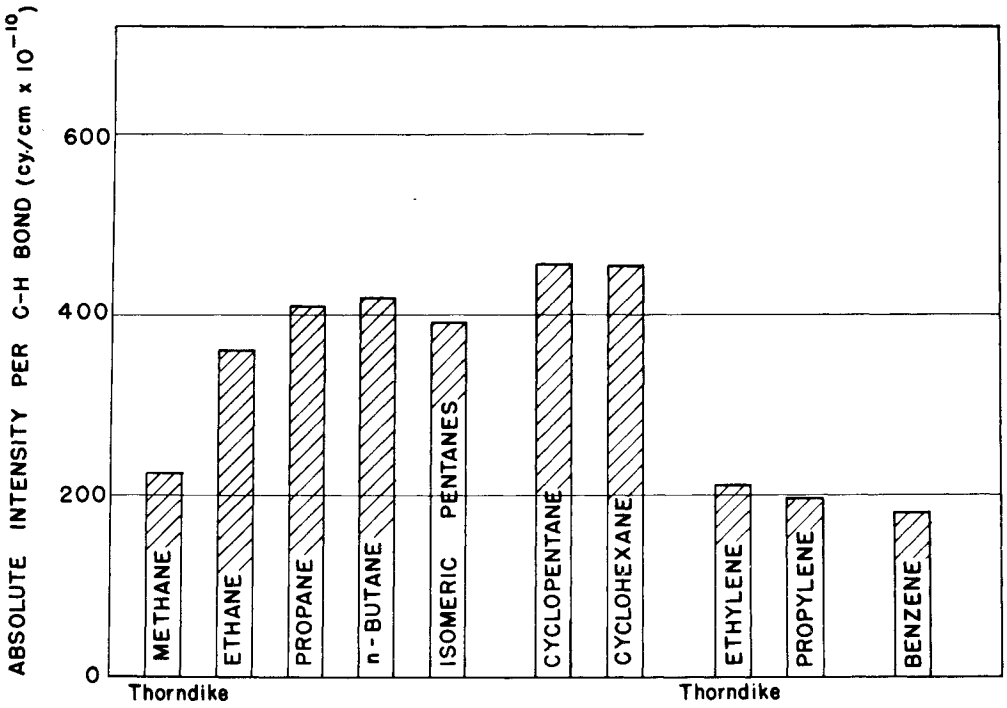

Figure 4. Absolute intensities of infrared absorption of C-H bonds in various hydrocarbons in the gas phase.

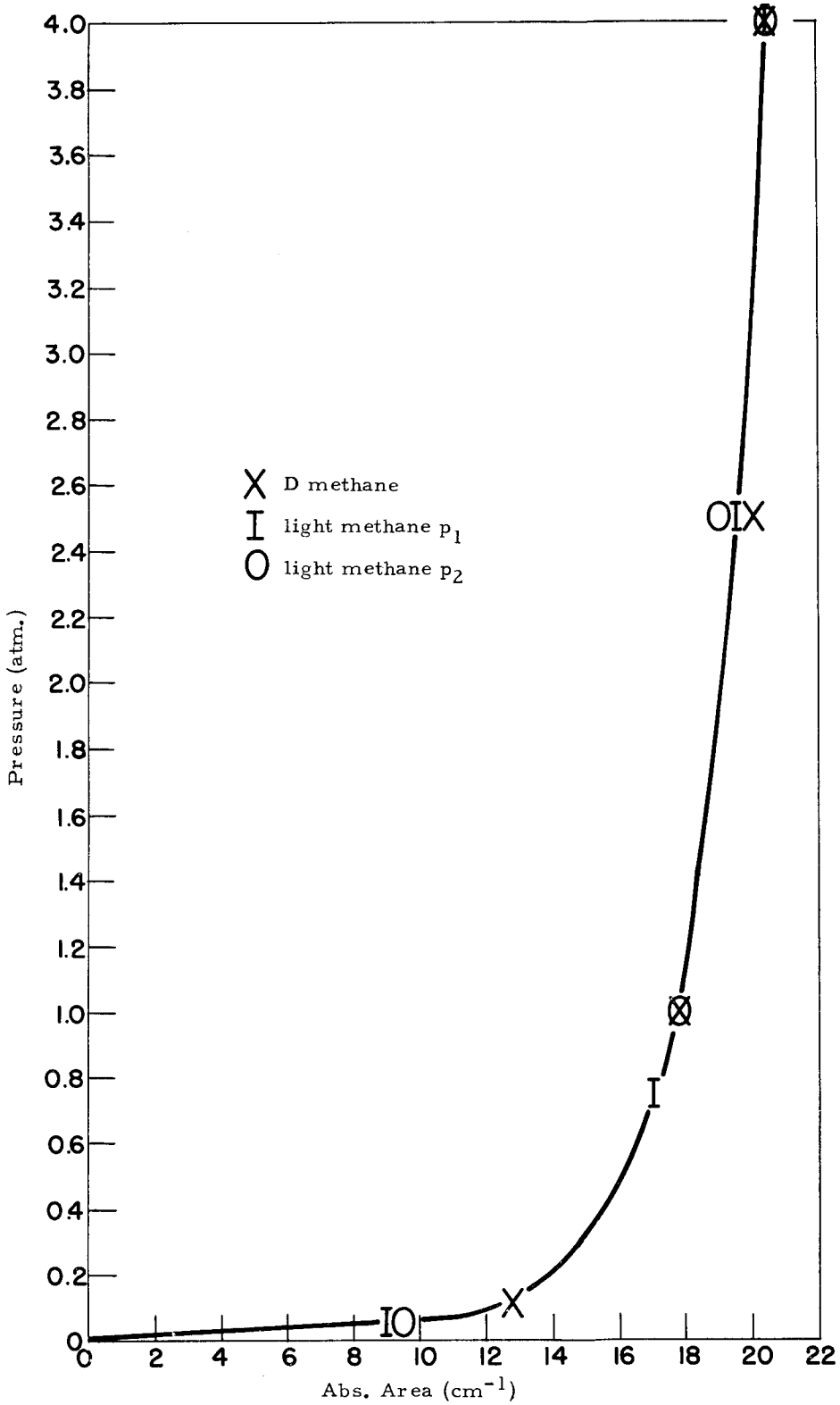

Figure 5. Plot of absorption area vs. total pressure for methane and deuteromethane (normalized at maximum pressure).

The spectra of methane, acetylene, deutero methane, and deutero acetylene have been obtained, in order to calculate the C-H/C-D intensity ratio. These compounds were employed in order that difficulties due to changes in symmetry could be eliminated. The pressure-broadening effect of Mathieson pre-purified N_2 on methane and deutero methane has been investigated, since it is known that methane is not sufficiently pressure-broadened at 1 atmosphere to give an accurate intensity measurement.[3] The curves in Figure 5 result from spectra taken with a particular amount of material at increasing total pressures; a spectrum was obtained after each increase in total pressure. The pressure-broadening effect on acetylene above 1 atmosphere is negligible and the data were obtained at a total pressure of 1 atm. instead of the 4 atm. used in the case of the methanes. The ratios found for C-D to C-H intensities are given in Table 3.

Table 3

Comparison of Absolute Intensities for C-H and C-D Bonds in the Gas Phase

A_i (cy./cm)

Compound	Hydrogen-Containing Molecule	Deuterium-Containing Molecule	Ratio: C-D/C-H
Acetylene	226×10^{10}	184×10^{10}	0.81
Methane	228×10^{10}	138×10^{10}	0.62

MECHANISM OF THE FAWORSKII REACTION

R.B. Loftfield*

The study of the Faworskii reaction using C^{14}, described in detail in Chemistry Conference Report #4 (BNL 44(C-10)), has been extended to include data on several unsettled points. The conclusion that the mechanism proceeds through a cyclopropane intermediate was subject to two sources of error. In the present report, data are presented which clearly eliminate one source of error and cast some doubt on the reality of the other.

The general problem involves the classical Faworskii rearrangement, as shown in the following reaction sequence:

*Harvard University; Massachusetts General Hospital.

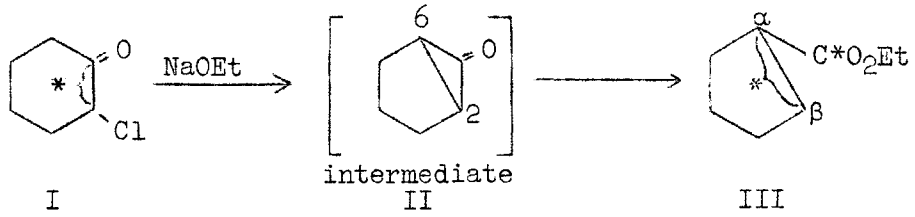

The cyclopentane carboxylic acid so obtained appeared to be labeled equally on the α and β carbon atoms when degraded; hence, it was concluded that the rearrangement proceeds through an intermediate (II) in which atoms 2 and 6 are equivalent.

Two sources of error might affect this conclusion. In the first place, although the chlorine atom is on the tagged carbon in the 2-chloro cyclohexanol-1,$2C_1^{14}$ (I), it seems possible that under alkaline conditions the chlorine migrates to position 6 (route 2) more rapidly than rearrangment occurs (route 1).

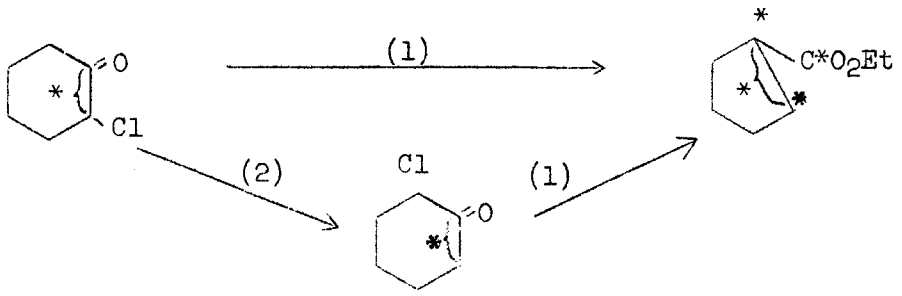

This would account for the observed results, whether the mechanism involved a three-membered ring intermediate or not. (An alternative mechanism would be a benzilic acid type of rearrangement.) In order to check this point, the reaction was carried out in isoamyl alcohol and stopped after 80% of completion. Unreacted I was isolated and degraded as shown. Since all the activity was in the CO_2

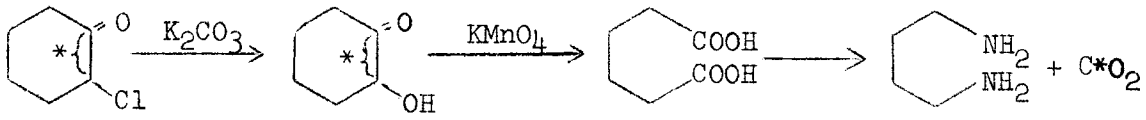

and none was in the putrescin, we conclude that no chlorine migration occurred.

A second uncertainty concerned the validity of the degradation method. That is, if α-labeled cyclopentane carboxylic acid (VIII) were degraded as shown below, would the activity show up in the putrescin, or would it appear in the CO_2, as it should?

The properly labeled acid was prepared as shown.

IV V VI VII VIII

This compound was then degraded by the same method as used in the previous work, i.e.,

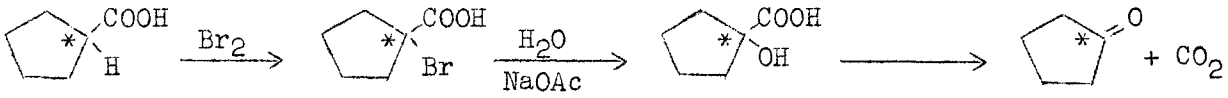

VII IX X XII XIII

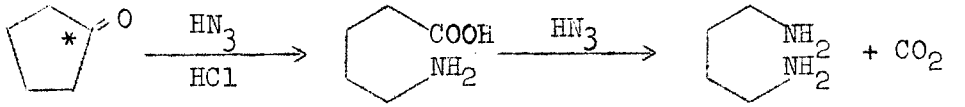

XIV XV XVI XVII

Eighty percent of the total activity appeared in the CO_2 (XVII) and 20% in the putrescin (XVI). Although this is conclusive evidence that the degradation does not account for the observed 50/50 distribution of activity in the α and β positions in III, it is disturbing that any activity is found in the putrescin. It is possible that some rearrangement of the ion (XVIII) accounts for the observed randomization.

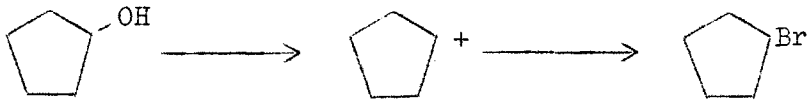

V XVIII VI

FURTHER EVIDENCE FOR THE CHLORONIUM ION AS A REACTION INTERMEDIATE

R.B. Loftfield*

A three-membered ring intermediate is suggested for the Faworskii reaction on 2-chloro cyclohexanol. (See above report.) It is also possible to postulate a three-membered ring intermediate (chloronium ion) for certain other cyclohexane derivative reactions. Evidence for this ion is reported.

*Harvard University; Massachusetts General Hospital

Two intermediates are postulated in the acetolysis of the trans chloro cyclohexanol derivative I shown below.

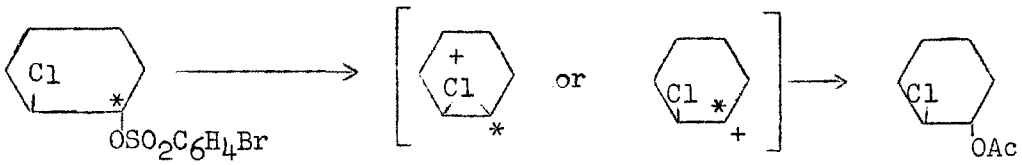

I II III IV

On the basis of kinetic studies, Winstein favors the carbonium ion III. There is some precedent for a chloronium ion II in the work of Lucas.[1] In order to make a decision between II and III as reaction intermediates, the trans chloro cyclohexanol derivative I was labeled as shown.

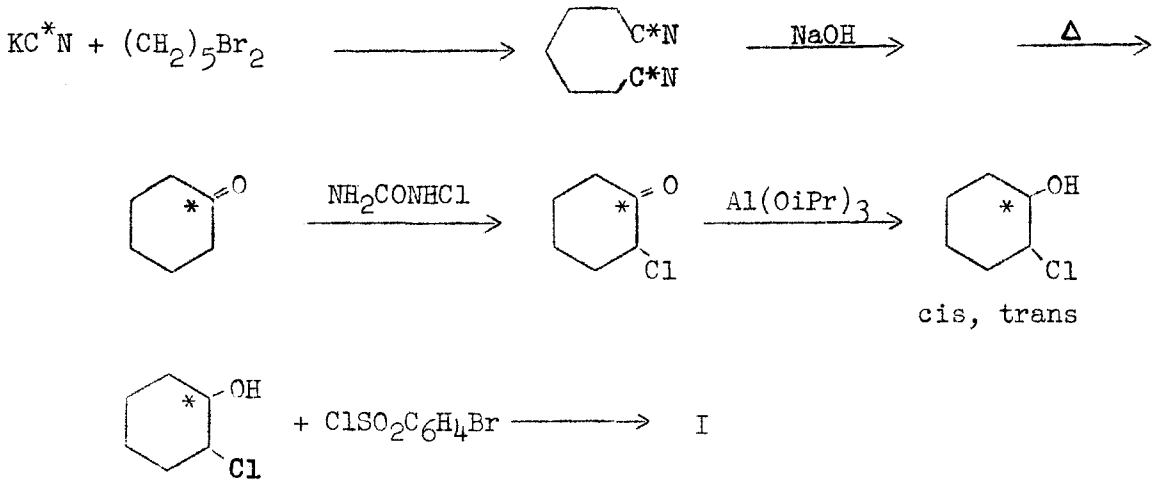

This product (I) was reacted with acetic acid and sodium acetate. Three products were isolated and the location of the C^{14} in these compounds was established to be as indicated.

trans-2-chloro acetyl cyclohexanol-1,2-C_1^{14} 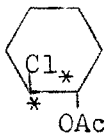 IV

cis-2-chloro acetyl cyclohexanol-1-C^{14} 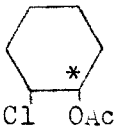 V

Δ^2-acetyl cyclohexenol-2-C^{14}(?) 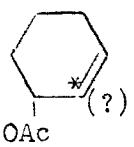 VI

[1] H.J. Lucas and C.W. Gould, Jr., J. Am. Chem. Soc. 63, 2541 (1941).

Product V presumably arises by Sn_2 displacement and inversion, and VI by trans-elimination of brombenzenesulfonic acid and solvolysis of the resultant 3-chlorocyclohexene. The fact that IV is equally tagged in two positions is a strong argument favoring intermediate II.

In cooperation with Dr. Ernest Grunwald, University of Florida, compounds I, VII, and VIII were prepared and the kinetics of acetolysis studied. VII and VIII react at the same rate, which is about one-third that of I. This, too, argues in favor of trans Cl driving force and, hence, intermediate II.

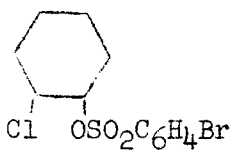

VII

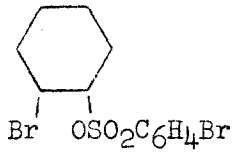

VIII

Further support may come from a study of the products of acetolysis of I and VII. If I yields intermediate III, VII should give the same ion; hence the same product. This is being investigated.

SIMPLE PREPARATION OF OPTICALLY ACTIVE SECONDARY ALCOHOLS

A.A. Bothner-By

It has been well established that reduction of some classes of organic compounds by lithium aluminum hydride is accomplished by transfer of a hydride ion to an electrophilic center of the molecule being reduced.[1] The nature of the ions or neutral molecules donating the hydride ion has not been determined, but a reasonable hypothesis is that in the reduction of a ketone, the forms $Al(OR)_m H_n$ are present, where OR represents the alkoxyl group derived from the ketone, and m and n are small integers. If this is the case, partial reaction of lithium aluminum hydride with d-camphor would give a species capable of asymmetric reduction of ketones. Similar asymmetric reductions have been reported by Vavon and co-workers,[2] Mosher and LaCombe,[3] and Doering.[4] Reductions of methyl ethyl ketone and pinacolone with lithium aluminum hydride-d-camphor have been performed. Table 1 shows, for three runs, the ketone reduced, the number of moles of lithium aluminum hydride, d-camphor and ketone used, and the boiling point and optical activity of the alcohol obtained.

---

[1] L.W. Trevoy and W.G. Brown, J. Am. Chem. Soc. 71, 1675 (1949).
[2] G. Vavon and B. Angelo, Compt. Rend. 224, 1435 (1947); G. Vavon, C. Riviere, and B. Angelo, ibid 222, 959 (1946).
[3] H.S. Mosher and E. LaCombe, J. Am. Chem. Soc. 72, 3994 (1950).
[4] W. von E. Doering, J. Am. Chem. Soc. 72, 631 (1950).

Table 1					
				Alcohol	
Ketone Reduced	$LiAlH_4$ (M)	d-camphor (M)	ketone (M)	B.P.	$(\alpha)_D^{25}$
Methyl ethyl	0.100	0.200	0.200	99.5-100°	+2.50°
Pinacolone	0.118	0.118	0.354	118-120°	+0.04°
Pinacolone	0.111	0.222	0.222	118-120°	+0.82°

Experimental

The reductions in each case were similar to the following:

Optically active sec. butyl alcohol. To a stirred solution of 3.80 g of lithium aluminum hydride in 300 ml of ether under nitrogen was added dropwise a solution of 30.0 g of d-camphor in 50 ml of ether. Addition required 1/2 hr. A mixture of 15.0 ml of methyl ethyl ketone and 50 ml of ether was then dropped in over 1/2 hr, followed immediately by 100 ml of 17% HCl. Stirring was continued until two clear layers were present. The layers were separated, and the ether layer, after drying with calcium chloride pellets, was fractionated through a small Vigreux column. The d-isoborneol solidified in the pot. The distillate was refractionated twice to obtain 10.0 g sec. butyl alcohol.

$$n_D^{25} = 1.3975, \text{ B.P. } 97\text{-}100°, \; d_4^{20} = 0.8084$$

A subsequent fractionation through a 40-plate column packed with glass helices gave alcohol having $n_D^{25} = 1.3974$, B.P. 99.5-100.0°, $d_4^{20} = 0.8081$, $(\alpha)_D^{25} = +2.50°$.

VAPOR PRESSURE AND DISSOCIATION CONSTANT OF HYDROGEN BROMIDE IN GLACIAL ACETIC ACID AT 25.0°C

E. Grunwald*

There is considerable evidence that the Arrhenius-Bronsted model of acid and base dissociation, proton transfer, and related phenomena fails in weakly basic aprotic solvents such as benzene and nitromethane.[1] For example, the acidity of "buffered" solutions of sulfuric acid and pyridinium acid

*University of Florida.

[1] e.g., L.C. Smith and L.H. Hammett, J. Am. Chem. Soc. 67, 23 (1945).

sulfate (measured by Hammett's acidity function[2]) varies greatly with the buffer concentration.[1]

The reasons for the deviations from the Arrhenius-Bronsted model may in a formal way be ascribed to abnormal values of the activity coefficients of the species involved, but they are not well understood.

Certain amphiprotic solvents, notably acetic acid, are intermediate in complexity between the aprotic ones and the well-studied aqueous systems. The acid-base equilibria involving the various forms of crystal violet are unexpectedly complicated.[3] Salt effects on reaction rates in acetic acid are highly specific and of unusual magnitude.[4] On the other hand, potentiometric titration curves of weak bases with strong acids are approximately as in water.[5]

Much information about acid-base behavior may be derived from the vapor pressure of volatile acids of moderate strength. For example, the vapor pressure of hydrogen bromide gives the same information as the e.m.f. of a cell having hydrogen and silver-silver bromide electrodes. Moreover, using Br^{82}, one can measure vapor pressures as low as 10^{-10} atm, at least in principle, and, therefore, can expect to obtain data at very high dilution. As a result, concentration ranges not usually accessible by other methods can be attained for study by this method.

This report contains preliminary values of the vapor pressure of hydrogen bromide in acetic acid measured by a modified dynamic method.[6,7] With inactive hydrogen bromide, concentrations as low as 1×10^{-3} M could be investigated. It is likely that radioactive hydrogen bromide will permit the study of dilutions greater by several orders of magnitude. This latter phase of the problem is to be investigated further.

The available data are summarized in Table 1. It is seen that the Henry's law constant, $H = p/c$, decreases with decreasing concentration, presumably due to the dissociation of the halogen acid. It is also seen that data obtained in two different solvent batches are not mutually consistent, and in this sense the results are unsatisfactory and tentative. The data lead to an estimate of 2×10^{-4} for the dissociation constant of hydrogen bromide and of 3.3×10^{-2} atm M^{-1} for the Henry's law constant of un-ionized hydrogen bromide. The magnitude of the dissociation constant here estimated is consistent with the rough value $pK_a = 3.5$ based on comparative conductance data for perchloric and hydrobromic acid in glacial acetic acid,[8] although the interpretation of the latter is highly uncertain.

---

[2] L.H. Hammett and A.J. Deyrup, ibid., 54, 2721 (1932).
[3] J.B. Conant and T.H. Werner, ibid. 52, 4436 (1930).
[4] J. Steigmann and L.H. Hammett, ibid. 59, 2536 (1937).
[5] N.F. Hall, ibid. 52, 5115 (1930).
[6] E.W. Washburn and E.O. Heuse, ibid. 37, 309 (1915).
[7] H.V. Tartar, W.W. Newschwander, and A.T. Ness, ibid. 63, 28 (1941).
[8] I.M. Kolthoff and A. Willman, ibid, 56, 1007 (1934).

Table 1

Vapor Pressure of Hydrogen Bromide Over Acetic Acid

(0.05N in acetic anhydride, 25.0°C)

Solvent Batch	Concn. of HBr x 10^3	p (mm Hg)	H (atm M^{-1})	K_a
A	25.71	0.560	2.87×10^{-2}	3×10^{-4}
A	20.94	0.462	2.90×10^{-2}	
A	12.22	0.246	2.65×10^{-2}	
A	6.00	0.118	2.58×10^{-2}	
B	3.10	0.0658	2.79×10^{-2}	1×10^{-4}
B	1.52	0.0296	2.56×10^{-2}	

Experimental Procedure

Materials

Hydrogen bromide was produced in 10 mM quantities by the action of five-fold excess of phosphoric acid on potassium bromide in the presence of a little red phosphorus at 150-180°C. The gas was carried by a slow stream of nitrogen over freshly reduced copper gauze and Drierite to remove bromine and water, respectively, and then into 35 ml of acetic acid. The 0.2N solution produced in this manner stayed colorless for 1 to 2 days. It was used immediately after preparation.

Acetic acid was obtained by distillation of commercial reagent grade acid in the presence of acetic anhydride and potassium acetate through an all-glass still with an efficiency of about 10 theoretical plates. Enough reagent grade acetic anhydride was added to the distillate to produce a solution 0.05N in acetic anhydride.

Vapor Pressure Measurements

All measurements were made at 25.00±0.05°C in a well-stirred water thermostat. The method of Washburn and Heuse was used.[6] Saturators of 50 ml size to hold 20 ml portions of solution were made in sections of two and connected by means of U-adapters with ball-and-socket joints. Spray traps between saturators and absorbers consisted of 20 cm glass spirals filled with 3/16" glass helices. The absorbers were identical in design with the saturators when the absorbing substance was liquid, and were Nesbitt absorption bulbs[9]

[9]Corning Glass Works, catalog No. 1900.

when the absorbing substance was solid. The apparatus consisted entirely of glass and the connections of the various parts were made with ball-and-socket joints. The joints were made water-tight by means of Apiezon grease, Type M. It was shown experimentally that the water from the thermostat did not enter the apparatus.

The entire apparatus was rocked through an angle of ±10° at the rate of 20 times per min. The air flow during the experiments was of the order of 1 liter/hr and produced a pressure drop of less than 0.3 mm Hg in the system.

The volume of air passing through the apparatus during an experiment was measured by the absorption of saturated water vapor on Anhydrone. The reproducibility of this measurement was better than 0.1%. Four to six saturators in series were used to obtain saturated vapor. Single saturators were 99.5% efficient in saturating dry air. Greater difficulty was encountered in obtaining highly reproducible saturation with acetic acid, probably due to the hygroscopic nature of this solvent. The average ratio of the weight of acetic acid absorbed by Askarite to that of water in 5 determinations was 3.990±0.014, in satisfactory agreement with the value 3.982±0.010 calculated from the data of McDougall[10].

The hydrogen bromide was absorbed in potassium acid phthalate in acetic acid and the absorber titrated argentometrically for bromide by the Volhard method. Although two absorbers were used in series, all but 0.5% of the bromide was found in the first. Usually 6-8 saturators were used in series and approximately 20 liter of air passed over the solutions at flow rates of 1 liter/hr. At the conclusion of the experiments the hydrogen bromide in the saturators was neutralized by addition of aliquot portions of potassium acid phthalate and determined argentometrically. The concentrations in the last saturator, and usually in the last few saturators, agreed to 2% or better with the original values. Also, the material balance was satisfactory, i.e., the hydrogen bromide lost in the saturators was equal to the hydrogen bromide in the absorbers within the experimental error.

[10] F.H. McDougall, J. Am. Chem. Soc. 58, 2585 (1936).

FRACTIONATION OF THE CARBON ISOTOPES IN DECARBOXYLATION REACTIONS. III. THE RELATIVE RATES OF DECOMPOSITION OF CARBOXYL-C^{12} and -C^{13} MESITOIC ACIDS

A.A. Bothner-By and J. Bigeleisen

Abstract

The relative reaction rates of decarboxylation of C^{12}- and C^{13}-carboxyl mesitoic acids have been studied at 61.2 and 92.0°C. The ratios of the rate constants at these temperatures are 1.037

± .003 and 1.032 ± .001, respectively. A comparison is made with similar ratios determined experimentally for other acids and with theoretical calculations of the ratios.

Introduction

In two previous communications from the Laboratory, the effect of the substitution of the isotopes C^{13} and C^{14} for C^{12} on the rate of decarboxylation of malonic acid has been discussed briefly from a theoretical[1] and an experimental[2] point of view. The theoretical calculations, which were based on a simplified model and neglected the vibrations within the carboxyl group itself,[2] indicated a much smaller isotope effect (on the decarboxylation rate resulting from C^{14} substitution in malonic acid) than had been reported in the literature.[3] The experimental results obtained at the Laboratory for the C^{13} fractionation in the decarboxylation of synthetic samples containing C^{13} of "natural" abundance cast considerable doubt on the validity of the C^{14} experiments of Yankwich and Calvin.[3] While the fractionation factors for C^{13} are but one-half those for C^{14}, one expects an over-all precision* of one order of magnitude greater for the mass spectrometric method with C^{13} than for beta counting with C^{14}. The fractionation factors for C^{13} in the decomposition of malonic acid were calculated with the plausible assumption that the C^{13} was distributed between different positions in malonic acid without any significant internal fractionation. This assumption was based on the fact that the $C^{13}O_2/C^{12}O_2$ ratio from the complete combustion of the malonic acid sample used was within 1°/₀₀ of that of ordinary CO_2.

Two lines of approach have been used at the Laboratory to check on the validity of the fractionation factors for malonic acid calculated with the above assumption of the distribution of C^{13} among the different positions. In a series of experiments, attempts were made to obtain quantitatively the carboxyl carbon atoms from both malonic acid and some substituted malonic acids in the form of CO_2. All of these experiments were subject to one or several objections and their results are, therefore, somewhat inconclusive. In no case was any evidence obtained which would have led us to reject the reported[2] fractionation factors for C^{13} in the decarboxylation of malonic acid.

The other attack we have made on this problem is a somewhat more inductive one. There are many monocarboxylic acids which decarboxylate readily in either acidic, neutral, or basic solutions. If a monocarboxylic acid is quantitatively decarboxylated, one can determine the C^{13} content of the carboxyl group without ambiguity. Measurement of the C^{13} content of cumulative CO_2 samples collected from reactions carried to known amounts of

---

[1] J. Bigeleisen, J. Chem. Phys. 17, 425 (1949).
[2] J. Bigeleisen and L. Friedman, J. Chem. Phys. 17, 998 (1949).
[3] P.E. Yankwich and M. Calvin, J. Chem. Phys. 17, 109 (1949).
*A more detailed discussion of the relative precision of the two methods is given in the next paper by J. Bigeleisen and T.L. Allen.

completion will permit the direct calculation of the ratio of the rate constants.

Subsequent to previous communications from this laboratory on this subject[1,2], Pitzer[4] proposed a model for the decarboxylation reaction. Calculations based on this model gave reasonably good agreement with the experimental results of Yankwich and Calvin on malonic acid but could not account for the large difference which they reported[3] between malonic acid and brom-malonic acid. An interesting aspect of Pitzer's model is that it leads to the prediction that the elimination of $C^{12}O_2$ from a singly carboxyl-labeled malonic acid would proceed at exactly one-half the rate of decarboxylation of an all-C^{12} malonic acid. The fractionation factor in the decarboxylation reaction should then be independent of the amount of decomposition. Irrespective of our method of calculation of the fractionation factor, our experimental determinations of the $C^{13}O_2/C^{12}O_2$ ratio of the gas formed in the decarboxylation of malonic acid showed a definite and significant change with the amount of reaction. In fact, the fractionation factor calculated from the experimental data for complete reaction[2] showed rather good agreement with previously published theoretical computations.[1] Pitzer also discussed the question of attainment of equilibrium in an activated complex which has two or more groups completely identical except for differences in isotopic constitution.

To obtain additional experimental data which might help to clarify some of the questions raised above, a study of the C^{13} isotope effect on the rates of decarboxylation of two rather different monocarboxylic acids has been carried out. In this paper, we report a study of the acid-catalyzed decarboxylation of mesitoic acid. In the next paper are reported the results of a study of the decarboxylation of trichloracetate ion in slightly alkaline solution. The acids also differ in that one is an aromatic acid with the possibility of some resonance (although probably considerably reduced from that in benzoic acid by steric effects), and the other is the ion of an aliphatic acid. An additional factor which suggested the choice of these acids is the fact that they both decarboxylate at rates that are first order with respect to the organic acid.[5,6,7]

Experimental

Materials

Mesitoic acid was prepared by the carbonation of the Grignard reagent of mesityl bromide.[8] The crude acid was recrystallized three times from normal heptane. The purified acid was ground to a fine powder and then dried *in vacuo*

---

[4] K.S. Pitzer, J. Chem. Phys. 17, 1341 (1949).
[5] W.M. Schubert, J. Am. Chem. Soc. 71, 2639 (1949).
[6] F.H. Verhoek, J. Am. Chem. Soc. 56, 571 (1934).
[7] R.A. Fairclough, J. Chem. Soc. 1938, 1186.
[8] "Organic Syntheses" (John Wiley and Sons, New York, 1941) Vol. 21, p. 77.

at 110°C for 24 hr. (M.P. 151.5-152.0°C corrected; previously reported 150-152°C.[8]) Sulfuric acid, 85.75% by weight, was prepared by dilution of "Baker's Analyzed" concentrated sulfuric acid. The composition was determined by acidimetric titration of a weighed sample.

Decarboxylation Apparatus and Procedure

In a typical experiment, a 0.35 g sample of purified mesitoic acid was weighed into the side arm A of the reaction vessel (Figure 1). A 50-ml sample of the sulfuric acid was delivered into side arm B from a pipette. The flask was attached to the manifold and carefully evacuated. Fifteen min were allowed for the contents of the flask to come to thermal equilibrium with the thermostat. Trap D was cooled by a solid CO_2 - acetone bath. The receiver vessel G was immersed in liquid nitrogen. The mesitoic acid was dissolved in the sulfuric acid by rotation of the vessel through 180° about the joint H. The mixing time was noted. The CO_2 evolved was continuously condensed in bulb G. After a predetermined time interval, stopcock I was closed, which isolated bulb G from the remainder of the system. To determine the amount of reaction up to this time, the CO_2 was allowed to come to room temperature and its pressure measured in the constant volume manometer J. The portion of the vacuum system which contained the CO_2 sample to be measured was previously calibrated for volume. The gas was then recondensed in bulb G.

A mass spectrometric examination of the CO_2 obtained in this way showed traces of mesitylene which would interfere with the determination of the $C^{13}O_2/C^{12}O_2$ ratio in the mass spectrometer. The CO_2 in bulb G was therefore purified further by three successive sublimations between vessels held at 165° and 77° K. The sublimation train is shown in Figure 2. The CO_2 was sublimed at a very slow rate to facilitate the adsorption and condensation of the mesitylene entrained in the CO_2. After this procedure, the sum of all the peaks in the mass spectrum of the gas in the range of m/e from 40 to 50, other than those resulting from the isotopic CO_2 molecules, was of the order of 0.01% of the peak at m/e = 44. They, therefore, contribute a negligible error in the determination of the $C^{13}O_2/C^{12}O_2$ ratio. All of the CO_2 introduced into the purification train (Figure 2) was quantitatively recovered to avoid any fractionation in this process.

Samples of mesitoic acid were decarboxylated at 61.2 ± 0.1° and 92.0 ± 0.1°C.

Isotopic Analyses

The C^{13} content of the CO_2 samples was determined by measurement of the 45/44 peak height ratios in a Consolidated-Nier isotope ratio mass spectrometer. Frequent intercomparisons of the individual samples were made with a reference sample of CO_2 to check on the stability and reproducibility of the instrument. Three or more analyses were made on each sample and the deviations shown are the average deviations from the mean. Small corrections were made to convert the results of the analyses of each sample to numbers corresponding to an average value for the reference gas. The deviations of the individual average values for the reference gas from an average of the averages was not more than the deviations in a series of determinations.

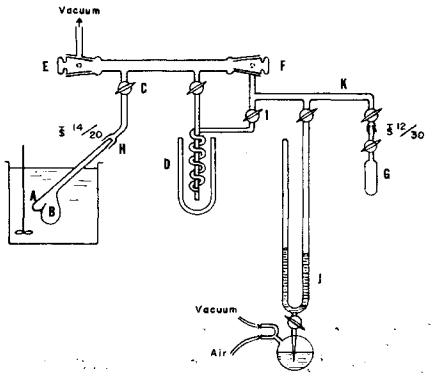

Figure 1. Decarboxylation apparatus.

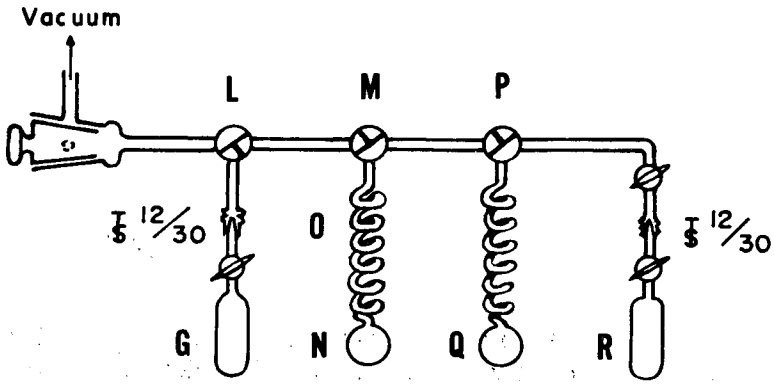

Figure 2. CO_2 purification train.

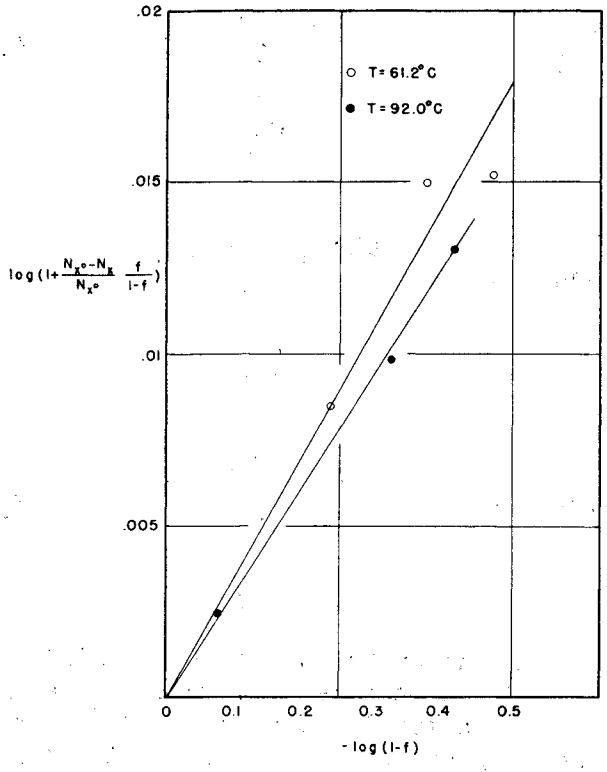

Figure 3. Isotope effect on the rate of decarboxylation of mesitoic acid.

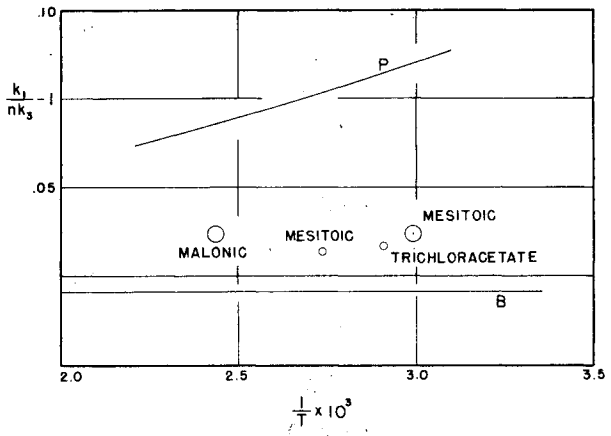

Figure 4. Comparison of theoretical computations and experimental data for the effect of C^{13} substitution on the rate of decarboxylation reactions. The curves marked P and B are calculated from the models proposed by Pitzer and Bigeleisen, respectively.

Results

The isotopic composition of the CO_2 collected up to any degree of completion of the reaction can be expressed in terms of the ratio of two rate constants. $C^{12}O_2$ and $C^{13}O_2$ are formed from the various isotopic species in accord with the following equations:

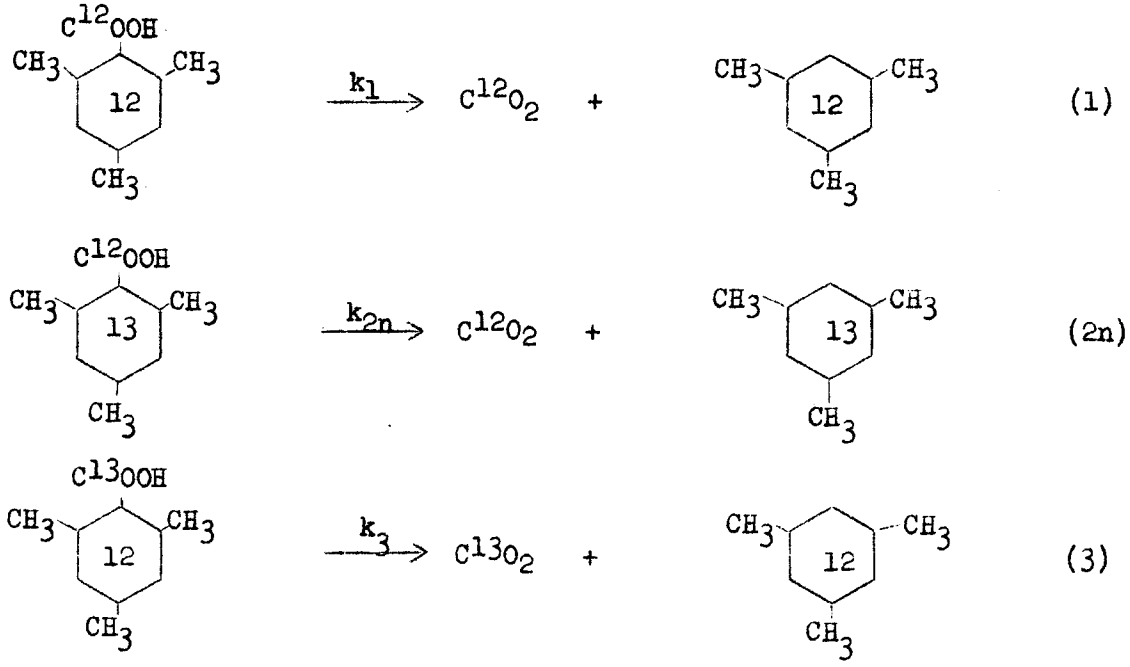

In equations (1)-(3), the symbol 12 means all the carbon atoms in the mesityl group are C^{12}. The symbol 13 refers to one C^{13} in the mesityl group. Inasmuch as the fractionation factors are small and the natural abundance of C^{13} is of the order of 1% of the total carbon, we may neglect reactions of species containing more than one C^{13} per molecule. Of all the equations (2N), the only one of any significance is the one with the C^{13} in the ring position attached to the carboxyl group. The rate constant of this reaction will be intermediate between k_1 and k_3. However, since this reaction produces $C^{12}O_2$ we can neglect it also.

The isotopic composition of the cumulative CO_2 sample collected up to any fraction, f, of complete reaction is, therefore, given by the following equation[9]:

$$\frac{N_x}{N_{x0}} = \frac{1 - (1-f)^{k_3/k_1}}{f}, \qquad (4)$$

where $N_x = C^{13}O_2/C^{12}O_2$ at $f = f$

$N_{x0} = C^{13}O_2/C^{12}O_2$ at $f = 1$

[9] J. Bigeleisen, Science 110, 14 (1949).

Equation (4) can be rewritten to give the deviation of the ratio of the rate constants k_3/k_1 from unity.[10] We get

$$\log\left(1 + \frac{N_{x0} - N_x}{N_{x0}} \frac{f}{1-f}\right) = \left(\frac{k_3}{k_1} - 1\right) \log (1-f) \qquad (5)$$

The results of the analyses of the CO_2 samples obtained from reactions carried to various degrees of completion are given in Table 1.

Table 1

Isotopic Composition of CO_2 Samples from the Decarboxylation of Mesitoic Acid

Sample No.	T°C	f	$N_x \times 10^4$	$(k_3/k_1) - 1$
Z - 95	61.2	0.420	122.22 ± 0.02	-0.0358
E - 95	61.2	0.579	122.41 ± 0.04	-0.0400
Y - 95	61.2	0.662	123.26 ± 0.04	-0.0324
2E - 95	61.2	0.920	124.93 ± 0.01	(-0.0172)
Average	61.2			-0.0361 ± .0026
2Y - 95	92.0	0.155	121.74 ± 0.03	-0.0341
H - 95	92.0	0.525	122.96 ± 0.05	-0.0306
A - 95	92.0	0.615	123.16 ± 0.05	-0.0315
2A - 95	92.0	0.990	125.18 ± 0.05	--
Average	92.0			-0.0321 ± .0014
Tank CO_2			129.60 ± 0.03	

To calculate the quantity $(k_3/k_1) - 1$ from the isotopic compositions given in Table 1, we must have a value of N_{x0}; the abundance ratios must be corrected for incomplete resolution of the mass spectrometer and the presence of O^{17} in CO_2. The resolution and O^{17} corrections can be expressed as an additive correction to the ratio and, therefore, need only be applied to N_{x0} as it appears in the denominator of equation (5). The resolution correction was determined experimentally and the O^{17} correction was made by suitable correction of Nier's data[11] to a value that would have been observed under the operating conditions of our spectrometer. In these experiments, the total correction is -9.22×10^{-4}. The value of N_{x0} was calculated from the analysis of sample 2A and an assumed value of $(k_3/k_1) - 1$ of -0.032. This gives $(125.38 \pm 0.05) \times 10^{-4}$ for the uncorrected value of N_{x0}. The values of the deviation of the ratio of the rate constants from unity in column V were

[10] This procedure was suggested to us by E. Grunwald.
[11] A.O.C. Nier, Phys. Rev. 77, 789 (1950).

calculated with this value of N_x0 and the above correction applied to it.

In the calculation of the average values of $(k_3/k_1) - 1$ the points at over 90% conversion were omitted. The expected precision of $(k_3/k_1) - 1$ calculated from these points is much lower because of the small fractionation factor and the magnification of errors in its determination by the quantity $f/(1-f)$. A plot of $\log (1+(N_x0-N_x)/N_x0)(f/(1-f))$ vs. $\log (1-f)$ is given in Figure 3. The best straight lines through the origin are drawn through the experimental points. The points at 61.2°C scatter somewhat more than would be expected from the reproducibility of the mass spectrometer analyses. However, equation (5) affords a very stringent test of the consistency of the experimental data. From the slopes of the lines in Figure 3 we obtain for the ratio k_1/k_3 the values of $1.037 \pm .003$ and $1.032 \pm .001$ at 61.2° and 92.0°C, respectively. In essence, the results obtained in this way constitute a different method of averaging the experimental data from that used in Table 1, which led to the values $1.037 \pm .003$ and $1.033 \pm .001$.

It is interesting to note that the carboxyl carbon of mesitoic acid prepared by reaction of Grignard reagent with excess dry ice is appreciably depleted in C^{13}. Most of this fractionation undoubtedly occurs during the reaction but is not readily interpretable. The process is complicated by diffusion effects as well as chemical rate phenomena.

The temperature coefficient of k_1/k_3 is so small that the difference in the results at the two temperatures is just outside the limit of the experimental errors. Figure 3 shows that the ratio at 61.2°C is clearly larger than that at 92.0°C, in accord with theoretical expectations.

Discussion

The results obtained for the ratios of the rate constants for the decarboxylation of C^{12} and C^{13} carboxyl carboxylic acids, k_1/k_3, may be compared to the results of similar investigations. In the following paper,[12] this ratio, for trichloracetate, is found to be 1.0338 ± 0.0007 at 70.4°C. For malonic acid, a value of $1.037 \pm .002$ at 137°C has been reported from the Laboratory. This value is subject to the assumptions discussed in detail in the introduction of this paper. In view of the small temperature coefficients that have been found and the fact that the ratio does not seem to be much affected by the acid studied nor by the medium, the present experiments add additional support to this value for malonic acid, and strengthen the plausibility of the assumption about the distribution of C^{13} in our sample of malonic acid. It follows, therefore, that the reported ratio of the probabilities of liberating $C^{12}O_2$ to $C^{13}O_2$ in a singly carboxyl-labeled malonic acid, k_4/k_3 of reference 2, will not have to be seriously altered because of this assumption in that calculation. The results obtained by Lindsay, McElcheran, and Thode[13] for the decarboxylation of oxalic acid are not strictly

[12] J. Bigeleisen and T.L. Allen, following paper.
[13] J.G. Lindsay, D.E. McElcheran, and H.G. Thode, J. Chem. Phys. 17, 589 (1949).

comparable to the other decarboxylation reactions. In the decarboxylation of oxalic acid, the products are CO_2, CO, and H_2O. This reaction involves the rupture of both carbon - carbon bonds and carbon - oxygen bonds. It is expected that such a reaction would be accompanied by larger isotope effects than the malonic acid reaction and this is indeed the case.

Yankwich and Calvin[3] reported quantities that are analogous to the k_4/k_3 ratio mentioned above. The results reported from the Laboratory for $(k_4/k_3)-1$ were $0.020 \pm .001$.[2] Yankwich and Calvin report values of $0.12 \pm .03$ and $0.41 \pm .08$ for C^{14}-labeled malonic acid and brom-malonic acids, respectively. These values can be compared directly with values obtained in C^{13} experiments by division of the C^{14} values by 2. It is clear that the values of Yankwich and Calvin would be too large even for the ratio k_1/k_3. Their results are difficult to understand, and no other work on the effect of isotopic substitution in decarboxylation reactions gives support for the large fractionation factors reported by them.

The experimental results for the ratio $(k_1/nk_3)-1$, where n is the number of carboxyl groups in the parent molecule, are compared, in Figure 4, with calculations based on Pitzer's model and on a model proposed previously by Bigeleisen.[1] It is clear that neither model is entirely satisfactory. The model proposed by Bigeleisen gives closer agreement with experiment and predicts a definite, but small, change in the fractionation factor for the decarboxylation of malonic acid as a function of the amount of reaction. Pitzer discusses this possibility in terms of the establishment of equilibrium between the activated complex and the substrate. Previous theoretical considerations of this general problem[14-16] seem to indicate that the question of equilibrium should not be a significant factor contributing to either the ratio k_1/k_3 or k_4/k_3. Neither the experiments using C^{13} in the oxalic acid decomposition,[13] nor those on the fractionation of O^{18} in the decomposition of ammonium nitrate[17] requires such assumptions.

The major shortcoming of the model proposed by Bigeleisen has been pointed out previously.[2] This model neglects the change in the vibrations within the carboxyl group on going from the normal molecule to the activated complex. Clearly some of these vibrations are weakened. Further discussion of this point will be postponed until the completion of some experiments now in progress.

We wish to thank A.P. Irsa for carrying out the mass spectrometer analyses.

[14] H.A. Kramers, Physica 7, 284 (1940).
[15] H. Eyring and B. Zwolinski, J. Am. Chem. Soc. 69, 2702 (1947).
[16] H.M. Hulburt and J.O. Hirschfelder, J. Chem. Phys. 17, 964 (1949).
[17] L. Friedman and J. Bigeleisen, J. Chem. Phys., in press.

FRACTIONATION OF THE CARBON ISOTOPES IN DECARBOXYLATION REACTIONS. IV. THE RELATIVE RATES OF DECOMPOSITION OF 1-C^{12} AND 1-C^{13} TRICHLORACETATE IONS

J. Bigeleisen and T.L. Allen*

Abstract

A precise determination of the relative rates of decomposition of 1-C^{12} and 1-C^{13} trichloracetate ions has been made. The 1-C^{12} ion has been found to decompose 1.0338 ± .0007 times as fast as the 1-C^{13} ion into chloroform and bicarbonate at 70.4°C.

Trichloracetate ion has been found to undergo a decomposition reaction that gives chloride ion but no CO_2, OH^-, nor H^+. The ratio of the rate constants for the production of Cl^- and bicarbonate is 0.078.

The errors in the determination of the effect of isotopic substitution on the rates of chemical reactions are discussed. In the study of the isotopes of carbon, experiments using mass spectrometric analyses of C^{13} are capable of a precision of one order of magnitude better than those in which the specific activity of C^{14} is determined by counting.

Introduction

In the preceding paper,[1] the need for precise experimental data on the fractionation of the isotopes of carbon accompanying decarboxylation reactions is discussed. This paper presents the results of such an investigation on trichloracetate ion. The kinetics of the decomposition of trichloracetate have been investigated and the reaction has been found to be first order in trichloracetate and dependent upon pH only through the ionization of trichloracetic acid.[2] In alkaline solutions, the rate of the reaction is independent of pH.

Verhoek[2] postulates the following mechanism for the reaction:

$$Cl_3C\text{-}CO_2^- \longrightarrow CCl_3^- + CO_2 \quad \text{(slow)} \qquad (1)$$

$$CCl_3^- + H_2O \longrightarrow CHCl_3 + OH^- \quad \text{(rapid)} \qquad (2)$$

*University of California, Davis, California.

[1] A.A. Bothner-By and J. Bigeleisen.

[2] F.H. Verhoek, J. Am. Chem. Soc. 56, 571 (1934).

Checks on the nature of the reaction which we have carried out simultaneously with the study of the fractionation of the carbon isotopes indicate that there is a side reaction of trichloracetate which occurs to a small but definite extent. The side reaction, which does not interfere with the fractionation study, is also described in this paper.

Experimental

The procedures and techniques used throughout the investigation were those customary in quantitative work, except in one respect. The thermostat used was a commercial glass jar thermostat filled with oil; the temperature of the reaction system was constant to within a few hundredths of a degree C. This temperature control is adequate for the present work because substitution of C^{13} for C^{12} produces little change in the activation energy of the reaction[1,3] and the ratio of the rate constants of the C^{12} and C^{13} ions is measured directly in one experiment.

Sodium trichloracetate was prepared and purified according to the method of Hall and Verhoek[4] from Baker and Adamson's U.S.P. trichloracetic acid and carbonate-free sodium hydroxide. Carbonate-free sodium hydroxide was used throughout the investigation to avoid the introduction of extraneous CO_2 into the CO_2 from the decomposition reaction. It was prepared according to the method suggested by Kolthoff and Sandell.[5] The distilled water used in this work was boiled before use and was carbonate-free.

The decomposition reactions were carried out in flasks similar to the one shown in Figure 1. The sodium trichloracetate solutions were prepared by the dilution of a 0.535 M stock solution. Prepurified nitrogen was passed through a trap at liquid nitrogen temperature and was bubbled through the trichloracetate solution to remove dissolved air. The test tube containing sodium hydroxide, which was inserted to prevent loss of CO_2, was then lowered into the reaction flask. The flask was then placed in a bath at 50°C and nitrogen was bubbled through the reaction solution for 15 min. The stopcocks on the flask were then closed and the flask was transferred to the thermostat. The reaction was allowed to proceed for a predetermined time, after which the flask was removed from the thermostat and the reaction was quenched by cooling the flask in ice water. The sodium hydroxide in the test tube was then added to the reaction mixture by shaking and tilting the reaction flask. The CO_2 was recovered from the solution in the apparatus shown in Figure 2.

The contents of the reaction flasks were quantitatively transferred to the acidification vessel shown in Figure 2. The contents of this vessel were successively frozen, pumped, and melted until all the air was removed. Excess

---

[3] J. Bigeleisen, J. Chem. Phys. 17, 425 (1949).
[4] G.A. Hall, Jr. and F.H. Verhoek, J. Am. Chem. Soc. 69, 613 (1947).
[5] I.M. Kolthoff and E.B. Sandell, Textbook of Quantitative Inorganic Analysis, New York, Macmillan Co., 1946, p. 551.

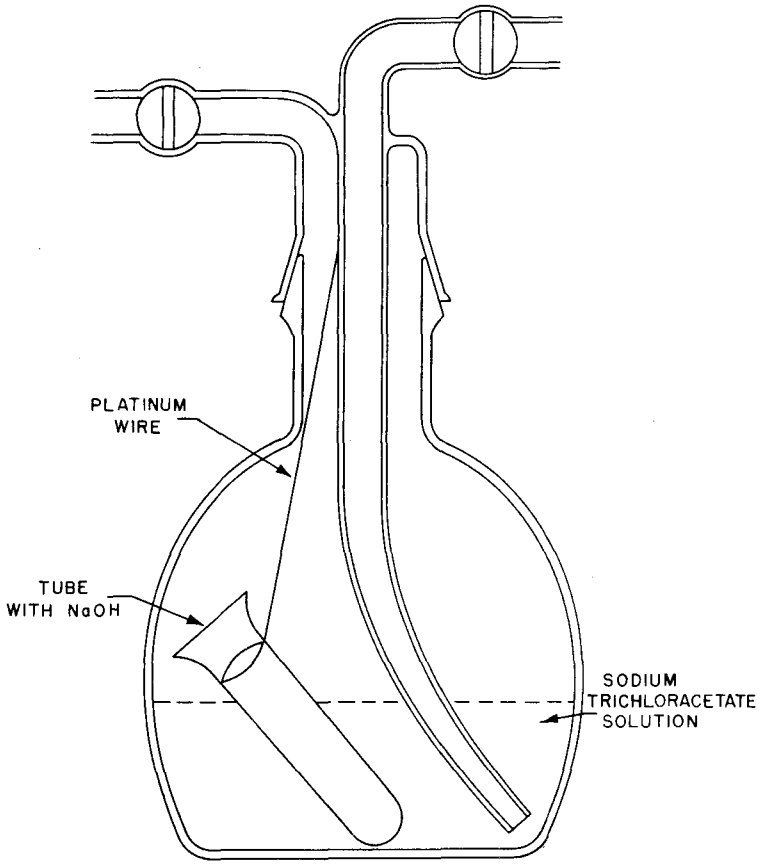

Figure 1. Reaction flask.

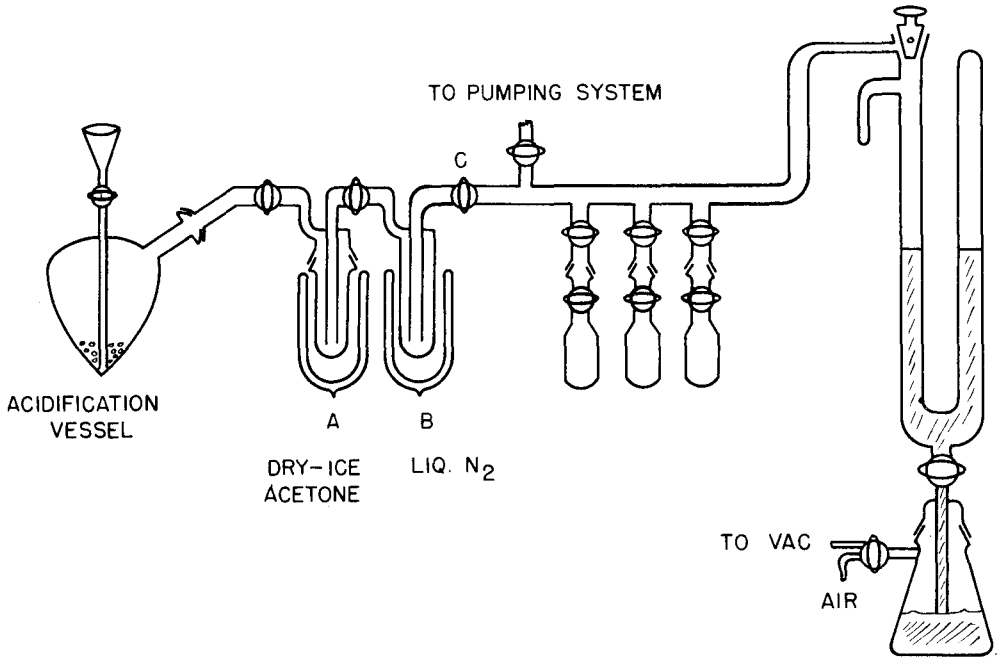

Figure 2. Apparatus for recovery and purification of CO_2 from bicarbonate solutions.

sulfuric acid was then introduced into the acidification vessel. CO_2 and some chloroform were collected in trap B; chloroform and water were collected in trap **A**. A mass spectrometric examination of the CO_2 fraction showed appreciable quantities of chloroform.

Final purification of the CO_2 from chloroform was effected in the following manner: A duplicate acidification vessel containing sodium hydroxide solution was placed on the line and evacuated. The CO_2 and some of the chloroform were sublimed from a vessel at -80°C into the sodium hydroxide vessel which had been cooled with liquid nitrogen. The solution was acidified and the CO_2 was collected again in trap B. Stopcock C was closed at all times while CO_2 was being collected. The CO_2 was then transferred to the gas burette and its volume was measured. The measured volumes were corrected for gas imperfection by means of Van der Waals' equation. The CO_2 sample was stored in a bulb for the mass spectrometer analysis. The method was checked for quantitative recovery of CO_2 by collecting the CO_2 from a known volume of a standardized $NaHCO_3$ solution. Recovery of CO_2 by this procedure was found to be quantitative.

Mass spectrometer analyses of the CO_2 separated from the reaction mixture after the above purification procedure showed that the samples were essentially pure CO_2. The only peaks in the mass spectrum of the gas in the mass range examined (28-70) were those from the isotopic CO_2 molecules and their ion fragments.

After the CO_2 had been removed from the reaction mixture, the samples were back-titrated with alkali and then titrated for chloride by the Mohr method. Blanks were run for the chloride titrations with $CaCO_3$ and Na_2SO_4 added to the distilled water. Reactions were carried out in individual vessels for different lengths of time. Mass spectrometer analyses of the CO_2 samples were made on a Consolidated-Nier isotope ratio mass spectrometer.

Results

Verhoek[2] and Hall and Verhoek[4] found that the decomposition of trichloracetate ion in aqueous solution was accompanied by the production of chloride ion, which they ascribed to oxidation of chloroform to phosgene and its hydrolysis, and to hydrolysis of chloroform in basic solution, respectively. We find that neither of these assumptions is adequate to establish a material balance in our experiments. In Table 1 are presented data on the production of HCO_3^-, H^+, and Cl^- at 70.4°C in solutions which were each initially 0.107 M in sodium trichloracetate.

In experiment 4-71 of Table 1, it is seen that after the reaction has been extended for 13 half-lives, the CO_2 produced is only 92.8% of the starting material. Obviously, some of the trichloracetate must react in a way which does not give CO_2 when the final solution is acidified. In addition, it is evident from experiments 3-56 and 5-62 that chloride is produced without either H^+ or OH^-. The ratio of chloride to CO_2 in these two experiments, as well as in other experiments in which there was less than 25% decomposition, is a constant. This means that up to 25% decomposition chloride ion is produced with

Table 1

Stoichiometry of the Aqueous Trichloracetate Decomposition Reaction

Exp. No.	Initial Amount of Trichloracetate (mM)	Elapsed Time (hr)	CO_2 Produced (mM)	OH^- Produced (mM)	Cl^- Produced (mM)	Cl^- (Calculated) (see text) (mM)
3-56	5.35	4.0	1.231	1.242	.081±.01	.089
4-71	2.68	1361	2.480	1.590	1.031±.01	.863
5-62	13.4	0.90	0.6719	0.6785	.046±.01	.048
6-66	2.68	12.0	1.428	1.325	.174±.01	.190
7-72	2.68	24.2	2.017	1.611	.462±.01	.463

the same half-life at HCO_3^-. This would not be the case if the chloride came exclusively from the chloroform, the hydrolysis of which is slow. Rather it shows that the chloride comes exclusively from the trichloracetate up to 25% reaction. It is noteworthy that the chloride that comes from the trichloracetate is accompanied neither by H^+ nor OH^-.

A possible reaction to explain the production of chloride ion from trichloracetate ion without change in pH is given by equation (3).

$$Cl_3C\text{-}CO_2^- \longrightarrow Cl_2C\overset{O}{\diagup\diagdown}C = O + Cl^- \qquad (3)$$

The lactone formed in equation (3) may react with trichloracetate ion to form a six-membered ring.

It is possible to account for all of the experimental results in Table 1, except the production of chloride ion in experiment 4-71, by the assumption that the decomposing trichloracetate which does not give CO_2 gives Cl^- and that Cl^- is also produced by hydrolysis of the chloroform. The respective amounts of chloride produced by each of these reactions can be calculated from the yield of CO_2 in experiment 4-71 and the difference between the amounts of CO_2 and OH^- produced in any experiment. The amount of chloride calculated in this way is in good agreement with experiments up to 80% decomposition. The discrepancy between the calculated and found amounts of chloride in experiment 4-71 may be due to a further change in pH of the solution by means of some hydrolysis of the lactone of equation (3) or a condensation product of it. There is also the possibility that the lactone loses chloride slowly by hydrolysis in basic solution.

We have carried out some additional exploratory experiments on the effect of oxygen and hydroxide ion on the rate of production of chloride in solutions of sodium trichloracetate. Air has no effect on this rate in solutions of sodium trichloracetate but doubles the rate in solutions of chloroform in water buffered by sodium bicarbonate. Alkali increases the rate of chloride production in sodium trichloracetate solutions. Just how much of this increase is due to an increase in the rate of hydrolysis of chloroform has not yet been established.

While our studies on the nature of the side reaction that produces chloride in the decomposition of sodium trichloracetate solutions are incomplete, they suffice for our measurement of the relative rates of decomposition of $1\text{-}C^{12}$ and $1\text{-}C^{13}$ trichloracetate ions. The side reaction occurs to a small extent and has little if any effect on the isotopic composition of the carboxyl group. The only complication it introduces lies in the calculation of the amount of reaction. Since the amounts of CO_2 produced as a function of time have been measured, the amount of reaction which has occurred up to the time t can be calculated from the ratio $(CO_2)_t/(CO_2)_\infty$.

The method of treatment of the experimental data on the isotopic composition of the CO_2 formed in the decomposition reaction is analogous to the one described in the preceding paper.[1] The resolution correction of the mass spectrometer was somewhat larger in these measurements than in the preceding ones.[1] The total correction to the $C^{13}O_2/C^{12}O_2$ ratio for resolution and O^{17} is -10.67×10^{-4} in these experiments. The results of the analyses and the deviation of the ratio of the rate constants from unity are given in Table 2.

Table 2

Isotopic Composition of CO_2 Samples from the Decomposition of Sodium Trichloracetate Solutions*

Sample No.	f	$N_x \times 10^4$	$k_3/k_1 - 1$	Expected error in $k_3/k_1 - 1$
3-56	0.2481	127.33±.05	-0.0327	2.1%
4-71	0.9999	130.63±.02	-	
5-62	0.05416	127.07±.02	-0.0305	1.1%
6-66	0.5755	128.12±.03	-0.0327	2.0%
7-72	0.8130	129.07±.03	-0.0328	4.2%
Accepted value			-0.0327±.0007	
Tank CO_2		130.13±.01		

*T = 70.4°C.

Since sample 4-71 is the one from which the reaction went 99.99% to completion, the analysis of this sample was used to determine the composition of the CO_2 at complete reaction. Each of the other samples was inter-compared directly with a sample of this gas.

k_1 and k_3 refer to the reactions in equations (4) and (5), respectively:

$$H_2O + Cl_3C^{12}\text{-}C^{12}O_2^- \longrightarrow C^{12}HCl_3 + HC^{12}O_3^- \qquad (4)$$

$$H_2O + Cl_3C^{12}\text{-}C^{13}O_2^- \longrightarrow C^{12}HCl_3 + HC^{13}O_3^- \qquad (5)$$

Plots of the data in Table 2 as well as of the amount of reaction as a function of time are given in Figure 3. The isotope fractionation data and the first order plot of the reaction rate data fall on good straight lines through the origin. The half-time for the disappearance of trichloracetate as determined from this plot is 10.0 hr and the corresponding rate constant is 1.93×10^{-5} sec^{-1}. The rate constants for the CO_2 reaction (equation (1)) and the chloride reaction (equation (3)) are 1.79×10^{-5} sec^{-1} and 0.14×10^{-5} sec^{-1}, respectively. Interpolation of Verhoek's data[2] gives 1.95×10^{-5} sec^{-1} for the over-all rate constant.

Discussion

In connection with the malonic acid work, it is significant to note that the ratio of C^{13}/C^{12} in the carboxyl group of trichloracetic acid is but 0.3% greater than the C^{13}/C^{12} ratio of ordinary CO_2. Malonic acid is usually synthesized from monochloracetic acid and cyanide. The conversion of monochloracetic acid to the trichloro acid should involve little fractionation of the carboxyl-carbon even if the reaction proceeds in low yield. Therefore, we may assume that mono- and trichloracetic acids derived from the same source of a C_2 carbon chain will have the same isotopic composition in the carboxyl group. If cyanide is formed from natural carbon sources in high yield and the subsequent malonic acid is also formed in high yield, one would expect synthetic malonic acid to have a C^{13}/C^{12} ratio in the carboxyl groups very close to that of ordinary CO_2. It is not surprising, therefore, that calculations of the fractionation data on the decomposition of malonic acid utilizing such an assumption give results for the ratio of the rate constants in good agreement with the ratios of rate constants for carboxyl $-C^{12}$ and $-C^{13}$ decomposition reactions in other acids.[1]

The significance of the ratio k_1/k_3 found in the present work is discussed, together with similar ratios in the decarboxylation of other acids, in the preceding paper.[1]

It is appropriate at this point to consider some of the errors that arise in the mass spectrometric determination of such ratios and to compare the precision of the mass spectrometric method with the one using C^{14} and beta counters. The significant quantity which is of interest is the deviation of the ratio of the rate constants from unity. If the isotopic substitution is for an atom whose position is unique in the molecule, as in the present case, and the effect of this substitution on the rate of a reaction is studied, then the deviation of the ratio of the rate constants from unity can be expressed in terms of the isotopic composition of the product accumulated up to any fraction of reaction by equation (5) of the preceding paper. The fractional error in the deviation of the ratio of the rate constant from unity is given to a good approximation by the relation

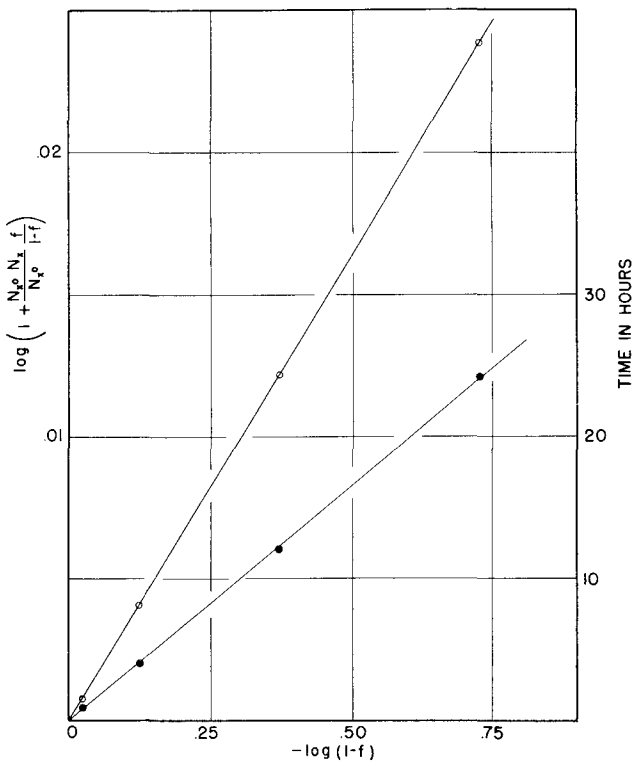

Figure 3. C^{13} isotope effect on the rate of the decomposition of trichloracetate ion, o ; time of the decomposition reaction, ● .

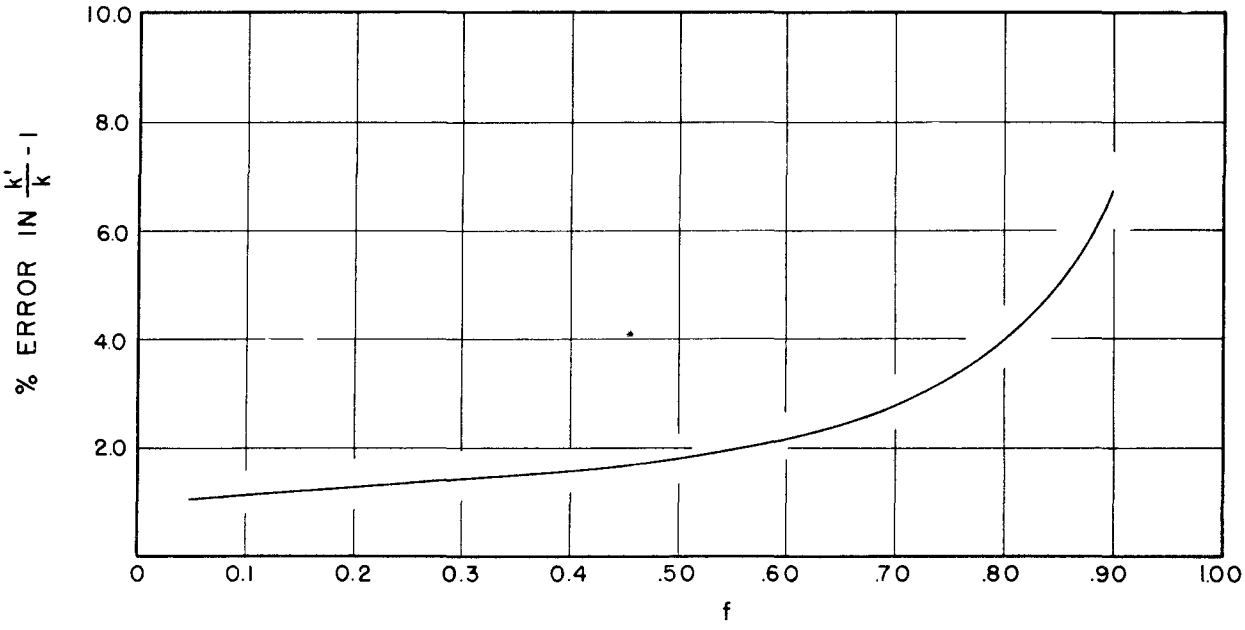

Figure 4. Expected errors in the determination of the effect of isotopic substitution on the rate of a chemical reaction. The curve is calculated for a value of k'/k - 1 of -0.10, a precision of 0.1% in ratio of the isotopic composition of two samples, and an error in the chemical determination of the amount of reaction of 0.5%.

$$\frac{\delta\left(\frac{k'}{k}-1\right)}{\left(\frac{k'}{k}-1\right)} \simeq \frac{\frac{f}{(1-f)}\,\delta\left(\frac{N_{x0}-N_x}{N_{x0}}\right)+\frac{N_{x0}-N_x}{N_{x0}}\,\frac{\delta f}{(1-f)^2}}{ln\left(1+\frac{N_{x0}-N_x}{N_{x0}}\,\frac{f}{1-f}\right)}+\frac{\delta f}{(1-f)\,ln(1-f)} \qquad (6)$$

where δ refers to an error, k' to the rate constant for a reaction of a molecule isotopically substituted, and the other symbols are those used in the preceding paper.

The error in the determination of the amount of reaction can usually be made sufficiently small so that most of the error in $(k'/k)-1$ arises from the isotopic analyses. In Figure 4 is plotted a curve of the expected error in $(k'/k)-1$ for the case where the ratio of the isotopic compositions of two samples can be determined to 0.1%, the error in the amount of reaction is 0.5% and $(k'/k)-1$ is -0.10. The curve rises so steeply above 90% reaction that it is impossible to include that portion of the curve on a graph of reasonable size.

In analyzing the results of this experiment, we have weighted the individual determinations in accord with the expected error. We find that the result of experiment 5-62 deviates from the weighted average of the other experiments by six times the expected error. Therefore, we feel that the best value for $(k_3/k_1)-1$ can be obtained by neglecting this experiment. The other experiments lead to an accepted value of $(k_3/k_1)-1$ of $-0.0327 \pm .0007$, or $k_1/k_3 = 1.0338 \pm .0007$.

If the present experiments had been carried out with trichloracetate-1-C^{14}, we would expect to find $(k'/k)-1$ equal to -0.065. We may estimate the error to be expected in this value from errors in the determination of the ratio of the specific activities of two nearly identical samples. Some of the most precise work on the determination of the specific activities of C^{14} samples has been done in connection with the determinations of the half-life[6] of C^{14}. Inspection of the reproducibility of the specific activity determinations in some of this work leads one to expect a precision of about 2% in the ratio of the specific activity of two samples. This would lead to an error of the order of 30% in $(k'/k)-1$, whereas in the present experiments the error in the similar quantity is of the order of 2%. In experiments of the type considered, it is evident that one can expect to obtain a precision of one order of magnitude better with the mass spectrometric method than with counting techniques with C^{14}. If the fractionation factor for C^{14} in some reaction drops much below the value expected for the decomposition of trichloracetate ion, the technique of using C^{14} and counting procedures for such an investigation can give a qualitative answer at best.

---

[6] A.G. Engelkemeier, W.H. Hamill, M.G. Inghram, and W.F. Libby, Phys. Rev. 75, 1825 (1949).

It is important also to consider the effects of impurities in both the mass spectrometric and counting methods. Impurities can play a serious role in both methods because the fractionation factors for the isotopes of all the elements except hydrogen are small.[7] In work with C^{13} of natural abundance, an impurity of mass 45 present to the extent of 1% in one sample of CO_2 can give a 100% error in the fractionation factor. Fortunately, the mass spectrometer itself provides a method of detecting impurities present to such a small extent and capable of producing such large errors. A mass spectrum of the gas to be analyzed will detect such impurities. Other checks are afforded by measurement of the O^{18} content of the same sample.

Kamen[8] has discussed some aspects of the effects of impurities in the use of radioactive isotopes. In addition to the points stressed by Kamen about decontamination of samples from other radioactive compounds, experiments which are designed to measure the specific activity of a sample of a certain compound are valid only if other inactive substances are absent. In many reactions of organic compounds the latter condition is not easily achieved.

For the reasons stated above, we have restricted ourselves at present to the mass spectrometric method in the investigations of the effect of isotopic substitution on the rates of chemical reactions.

We wish to thank A.P. Irsa for carrying out the mass spectrometer analyses.

[7] J. Bigeleisen, Science 110, 14 (1949).
[8] M.D. Kamen, U.S. Naval Medical Bulletin, Supplement (1948), p. 115.

NEUTRON SPECTROMETER

J. Hastings and L. Corliss

The construction of a double crystal neutron spectrometer is nearing completion. The instrument has been designed primarily for structure determinations on powders, single crystals, and liquids, but can also be used for the study of crystal imperfection, measurement of cross sections, etc.

The apparatus consists of three more or less separate parts: 1) a shutter and initial collimator inside the reactor shield, 2) a first crystal table which serves as monochromator and wave length selector, and 3) a sample, or second, crystal table and detector.

The shutter is a bar of stainless steel 20" long which can be moved laterally to intercept the beam coming from the reactor. It can be positioned mechanically from outside the reactor shield to expose a part or all of the first or "pile" collimator which is situated directly behind it. This collimator consists of 64 rectangular steel tubes, each 22" long and 1/8" x 1/2" in cross section, packed into a 2" x 2" housing. This parallel slit construction permits

the use of a wide beam without loss of geometrical resolution. The shutter and collimator are imbedded by means of concrete in a liner which fits into one of the experimental holes in the reactor shield. The construction is such as to permit easy removal of the collimator, thus making it possible to vary the geometry of the slit system.

The first spectrometer table, which holds a monochromating crystal of dimensions approximately 11" x 2-1/2" x 1/2", is located in a 2' square recess in the reactor shield. The entire spectrometer can be translated longitudinally with respect to the neutron beam. The rotating crystal mount is provided with additional tilting and translational motions which are useful in orienting selected crystallographic planes. A second, or "wave length" collimator, whose dimensions are identical with those of the "pile" collimator, is carried on an arm which rotates about the same axis as the crystal. In actual operation, a particular neutron wave length is selected by first fixing the angular setting of the collimator and then orienting the monochromator so that the Bragg condition is satisfied. All of these motions are performed by remotely controlled Selsyn motors. In the choice of monochromating crystal, it is desirable to have not only high peak reflectivity at the Bragg angle, but also a rocking curve width of the same order of magnitude as the angular divergence of the collimating system. A metallic crystal such as lead, which can be readily grown to the size required, appears to be satisfactory in these respects. The recess containing the first spectrometer table is surrounded by a removable paraffin-lead shield provided with a slot in which the "wave length" collimator moves.

The second spectrometer table, which is considerably more massive than the first, carries the sample and a 6' rotating arm. On this arm are mounted a "detector" collimator, whose dimensions are once again the same as those of the "pile" collimator, and a $B^{10}F_3$ neutron detector. The arm and sample table can be rotated automatically so that a 2:1 angular relationship is maintained. Several speeds in the range from 1/2 to 4 degrees per hr are available. In addition, the arm and sample table can be decoupled and each operated manually. Angular settings are indicated by graduated circles mounted on the main spindle shaft. The center of rotation of the second spectrometer can be positioned in the beam by means of a set of crossed tracks.

Provision has been made for automatically recording the incident, diffracted, and background neutron intensities. The incident flux is measured by a fission counter mounted on the exit end of the "wave length" collimator, and background readings are obtained by interposing a cadmium shutter in the main beam.

We should like to thank S.H. Bauer of Cornell University for much helpful assistance in the design of this instrument.

CONVERSION COEFFICIENT OF THE 35-KEV GAMMA RAY OF Te^{125}

G. Friedlander and M.L. Perlman

The 58-day isomer[1] of Te^{125} is known to decay by a two-step transition.[2] A 109.7-kev transition which is at least 99% converted[1] is followed by a partially converted 35.4-kev gamma ray. The K/L ratio for the 109.7-kev transition was measured by two groups[3,4] as 1.5 and 1.2; the L/M ratio has been reported[3] as 3.5. The L and M conversion electrons of the 35.4-kev transition were observed in a spectrograph.[5] The K conversion electrons have escaped detection because of their low energy. By a coincidence method, the fraction of the 35.4-kev transitions internally converted (c) was estimated[2] as 0.80 to 0.85, and the fraction of the transitions converted in the K shell (c_K) as 0.6 to 0.8. The unconverted 35.4-kev gamma ray was observed with Geiger counters by critical fluorescence and absorption measurements.[2]

With the use of a proportional counter and pulse height analyzer,[6] the 35.4-kev gamma rays have now been measured directly from a pure Te^{125} source prepared by separation from Sb^{125}. A 4"-diameter brass counter with a beryllium window and filled to 3 atm with 97% krypton and 3% ethane was used. The observed pulse height distribution with peaks representing the Kα and Kβ X-rays of tellurium and the 35-kev gamma ray is shown in Figure 1. An I^{126} source, which gave a Te K X-ray intensity due to K capture comparable with that from the Te^{126}, had a negligible counting rate in the 35-kev region (Figure 1).

The relative peak heights for the K X-rays and the gamma rays, after corrections for the X-ray fluorescence yield of tellurium, counter window transmission, counter efficiency, and peak position, give a ratio of K holes to 35-kev gamma rays of 17.2. From this ratio and from the previously measured[3,4] conversion fractions $c_{K109} = 0.51$, $c_{L109} = 0.38$, and $c_{M109} = 0.11$ of the 109-kev gamma ray, one may calculate the unconverted fraction $c_{\gamma 35}$ and the K conversion fraction c_{K35} of the 35.4-kev transition, provided an assumption is made about the ratio c_{K35} to the total c_{35}. It will be seen that the values of $c_{\gamma 35}$ is not sensitive to the value assumed for this ratio. If c_{35} is assumed to be 1.1 c_{K35}, then

$$1.1\, c_{K35} + c_{\gamma 35} = 1 = c_{109} = 1.95\, c_{K109} \qquad (1)$$

From the measurements above,

$$c_{K35} + c_{K109} = 17.2\, c_{\gamma 35} \qquad (2)$$

---

[1] G. Friedlander, M. Goldhaber, and G. Scharff-Goldhaber, Phys. Rev. 74, 981 (1948).
[2] J.C. Bowe and G. Scharff-Goldhaber, Phys. Rev. 76, 437 (1949).
[3] R.D. Hill, G. Scharff-Goldhaber, and G. Friedlander, Phys. Rev. 75, 324 (1949).
[4] B.D. Kern, A.C.G. Mitchell, and D.J. Zaffarano, Phys. Rev. 76, 94 (1949).
[5] R.D. Hill, Phys. Rev. 76, 333 (1949).
[6] W. Bernstein, H.G. Brewer, Jr., and W. Rubinson, Nucleonics 6, #2, 39 (1950).

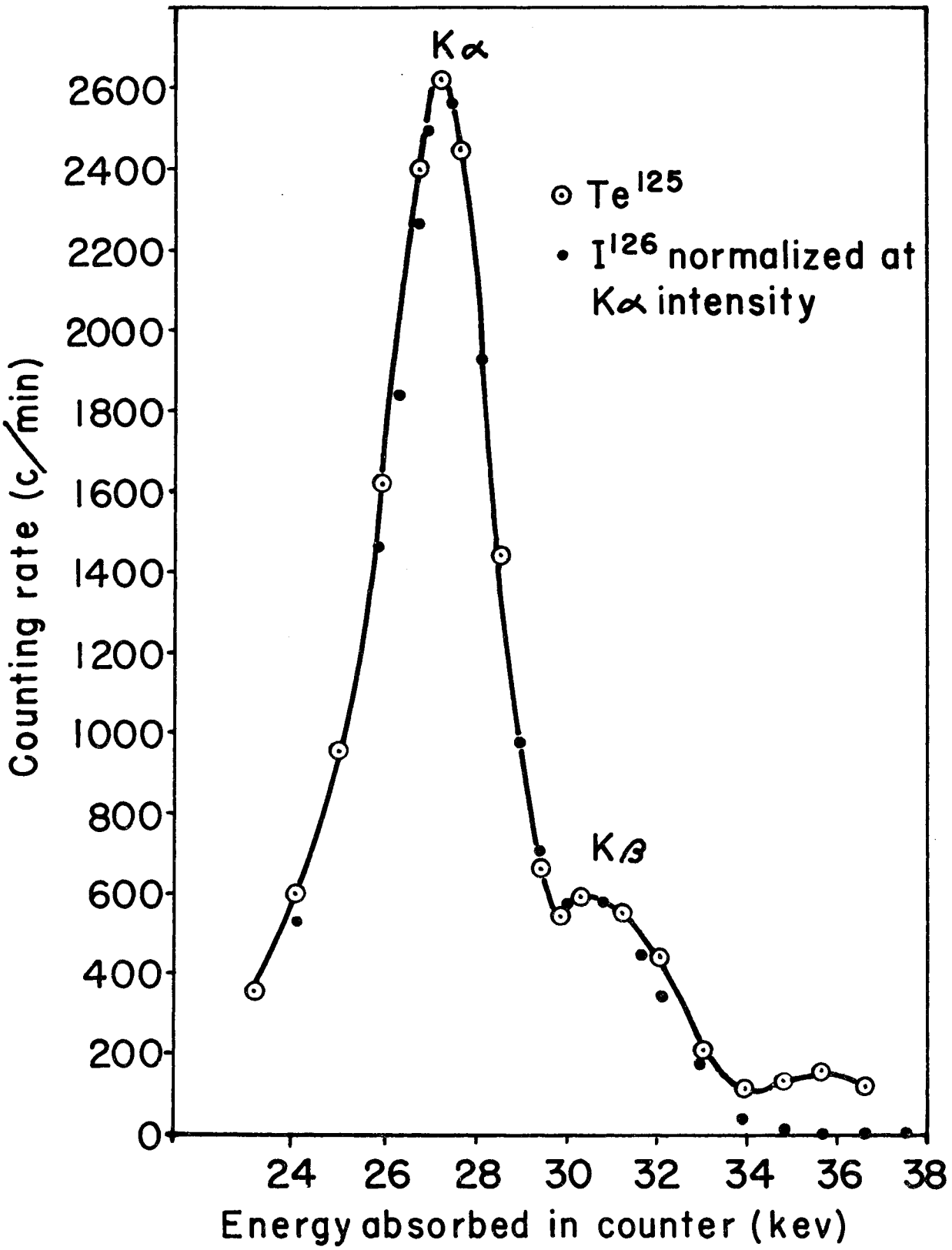

Figure 1. Proportional counter pulse height distribution for Te^{125} and I^{126} radiations.

Combining (1) and (2), one obtains:

$$c_{\gamma 35} = 0.153 \; c_{K109} = 0.078$$

and

$$c_{K35} = \frac{1-c_{\gamma 35}}{1.1} = 0.84.$$

If c_{35} is assumed to be 3 c_{K35}, then $c_{\gamma 35} = 0.048$ and $c_{K35} = 0.32$. These values and the theoretical values[7,8] for various types of transitions are listed in Table 1.

Table 1

Values	c_{35}/c_{K35}	$c_{\gamma 35}$	c_{K35}
Electric dipole	1.13[a]	0.23	0.68
Magnetic dipole	1.10[a]	0.12	0.80
Electric quadrupole	3.16[a]	0.018	0.31
Present work	(1.1)[b]	0.078	0.84
" "	(3)[b]	0.048	0.32

[a]For these calculations, conversion in shells higher than the L shell has been neglected.
[b]Assumed values.

The present experiments establish that the unconverted fraction of the 35.4-kev transitions cannot exceed 0.08 ± 0.01, even if there is no conversion outside of the K shell. According to the theory of internal conversion, the transition, therefore, is not electric dipole, but would appear to be a mixture of magnetic dipole and electric quadrupole. This is in agreement with the shell structure model of M.G. Mayer,[9] which predicts a spin charge of one unit without parity change.

We wish to thank Elizabeth Wilson for valuable assistance.

[7]M.H. Hebb and E. Nelson, Phys. Rev. 58, 486 (1940).
[8]S.D. Drell, Phys. Rev. 75, 132 (1949).
[9]M.G. Mayer, Phys. Rev. 75, 1969 (1949).

RADIATIONS FROM IODINE-126

G. Friedlander and M.L. Perlman

Abstract

The decay scheme of I^{126} produced by I^{127} (n,2n) reaction is being investigated by X-ray spectrometer, beta-ray spectrometer, scintillation spectrometer, absolute beta counting, and coincidence measurements. The ratio of electron capture probability to beta decay probability has been found to be 1.35 ± 0.2. Negative beta ray groups with end points at 1.24 and 0.85 Mev and conversion electrons of a 0.382-Mev gamma ray have been observed. Coincidence measurements have shown that the high energy beta rays go to the ground state of Xe^{126} while the low energy group is followed by a single gamma transition. On the electron capture side, a 640-kev gamma ray and some gamma-gamma coincidences have been observed. A small amount of positron decay, tentatively estimated as 2% of all transitions, has also been established. Further work on the decay scheme is in progress. In the light of the results, the yield of the reaction I^{127} $(\gamma,n)I^{126}$ as determined by beta counting and the trend of (γ,n) yields with atomic number are discussed.

Iodine-126 is known to decay with a half-life of 13 days, emitting negative beta particles and gamma rays.[1] However, the yields reported for the reactions I^{127} $(\gamma,n)I^{126}$,[2] $Sb^{123}(\alpha,n)I^{126}$,[3] and Bi^{209} (d,fission),[4] as determined from the I^{126} beta activity seem low, which suggests that I^{126} may decay by emission of radiations only inefficiently detected by Geiger counters. No very soft beta component has been observed, but the disposition of the stable isotopes of Xe and Te makes it seem likely that electron capture may occur. An investigation of the decay scheme of I^{126} has therefore been undertaken. In particular, a search has been made with a proportional counter X-ray spectrometer[5,6] for Te X-rays that would be emitted as a result of electron capture.

The I^{126} was produced by the reaction $I^{127}(n,2n)I^{126}$ and concentrated by a Szilard-Chalmers separation. One kg of solid potassium iodate was irradiated for several hours with fast neutrons generated by the deuteron bombardment of

---

[1] A.C.G. Mitchell, J.Y. Mei, F.C. Maienschein, and C.L. Peacock, Phys. Rev. 76, 1450 (1949).
[2] M.L. Perlman, Phys. Rev. 75, 988 (1949).
[3] L. Marquez and I. Perlman, Phys. Rev. 78, 189 (1950).
[4] R.H. Goeckermann and I. Perlman, Phys. Rev. 76, 628 (1949).
[5] G. Friedlander, M.L. Perlman, D. Alburger, and A.W. Sunyar, Quarterly Progress Report (BNL 51 (S-5)), (1950) pp.46-52; Phys. Rev. 80, 30 (1950).
[6] W. Bernstein, H.G. Brewer, Jr., and W. Rubinson, Nucleonics 6, #2, 39 (1950).

beryllium at the M.I.T. cyclotron. The salt was dissolved in slightly alkaline water to which milligram quantities of potassium iodide had been added. The solution was then acidified and shaken with several small portions of carbon tetrachloride. Approximately 20% of the I^{126} was found in the organic phase, which was washed with dilute acid and then shaken with dilute sulfurous acid in order to reduce the I_2 to I^- and transfer the activity to an aqueous phase of small volume. This solution was placed in a small glass cell over a cleaned copper foil and the iodide was oxidized to iodine by a slight excess of nitrous acid. The activity deposited itself onto the copper foil as a result of the reaction $2Cu + I_2 \longrightarrow 2CuI$.[7] A closed cell was used when it was desirable to minimize loss of iodine by volatilization; the deposition process was hastened by agitation. With this technique, uniform samples could be prepared of thickness certainly as small as 0.1 mg/cm^2.

Thus far, the following types of measurements have been made: absolute beta disintegration rate, beta absorption, beta spectrum, X-ray spectrum, absolute K X-ray emission rate, and gamma ray spectrum. Preliminary coincidence experiments have also been done.

The proportional counter used in the X-ray measurements is similar to one previously described,[5] except for the following modifications: The central wire is made of very smooth stainless steel, an electrostatic shield of fine wires is used so as to maintain the cylindrical symmetry of the field near the beryllium window (107 mg/cm^2), and the gas composition is 97% krypton and 3% ethane at a total pressure of 3 atm. The gas filling and counter dimensions are such as to give approximately 90% efficiency for counting tellurium K X-rays. The counter was operated at 4200 v. With a Te^{125} source of X-rays, the width of the Kα peak at half height was 12%.[5]

Samples of I^{126} were found to emit Te K X-rays. A typical pulse height spectrum is shown in Figure 1, curve A. The Kα (27.3 kev) and Kβ (31.1 kev) peaks were easily resolved; their relative intensities were the same as observed from the Te^{125} source, and agreed with values given by Compton and Allison.[8] An upper limit of about 2% of the Te X-ray intensity was established for Xe K rays (29.8-kev) which could arise from internal conversion of gamma rays following negative beta decay. The pulse height distribution curve was measured for an I^{126} sample covered by a 600 mg/cm^2 beryllium absorber for the beta particles and L X-rays. The K X-ray counting rate was determined from the curve by the method previously described.[5]

From this rate, in turn, the absolute K electron capture rate was calculated with the aid of corrections for geometrical efficiency, counter efficiency, and fluorescence yield (0.80)[9] and for the following losses: dead time, absorption in beryllium, air, and electrostatic screen, and in a small layer of counter gas between the window and electrostatic screen. The L capture rate may be estimated by the method of Rose and Jackson[10] to be 12% of the K rate.

---

[7] This method of preparing thin iodine samples was developed by W. Orr.
[8] A.H. Compton and S.K. Allison, X-rays in Theory and Experiment, 2nd ed. D. Van Nostrand Co., New York, 1935, p. 640.
[9] R.M. Steffen, O. Huber, and F. Humbel, Helv. Phys. Acta 22, 167 (1949).
[10] M.E. Rose and J.L. Jackson, Phys. Rev. 76, 437 (1949).

The absolute beta disintegration rate was measured for an I^{126} sample of known capture activity by correction of the measured Geiger activity for solid angle, absorption in air and counter window, back scattering, coincidence loss, and X and gamma activities.

The ratio of the electron capture probability to the beta decay probability for I^{126} was found to be 1.35 ± 0.2.

Measurements by D. Alburger, of the Physics Department, made on an I^{126} sample with his lens-type beta ray spectrometer show the presence of two beta groups with end points at 1.24 ± 0.02 and 0.85 ± 0.03 Mev and conversion electrons of a 0.382 ± 0.004-kev gamma ray, in essential agreement with the results obtained by the Indiana group.[1] Beta absorption measurements were found also to be in agreement with these results.

For measurement of gamma ray energies, radiations from an I^{126} source were allowed to fall upon a scintillation counter covered by absorber to remove beta particles. The amplified pulses were displayed on an oscilloscope screen and photographed (Figure 2). A 640 ± 20-kev gamma ray line was found, low in intensity compared with the previously known 390-kev line. The energies of the two lines were established by comparison with the gamma rays of Cs^{137} (663 kev) and of Au^{198} (411 kev). In addition, a faint line was observed of energy corresponding to annihilation radiation. These scintillation spectrometer measurements were carried out in collaboration with E. der Mateosian, of the Physics Department.

With an I^{126} source, coincidences were observed between pulses from two NaI(Tl) scintillation counters placed at right angles and shielded from each other by 4 mm of lead. Measurements with copper and lead absorbers showed that approximately one-half the observed coincidence rate represented X-γ events and one-half γ-γ events. The half-thickness for absorption of the γ-γ coincidences was 5.6 g/cm^2 of lead, corresponding to a gamma ray energy of about 600 kev. A comparison of the coincidence rates at 180° and at 135° when both counters were covered with 3 g/cm^2 of lead absorber established the presence of annihilation radiation.

A preliminary estimate of 2% positron decay may be deduced from the data. Beta-gamma coincidences were measured with the use of a Geiger counter and a NaI scintillation counter. Comparison of the β-γ coincidence counts per β count for I^{126} and for Au^{198} (which has a 960-kev beta transition followed by a 411-kev gamma ray) and coincidence absorption measurement showed the decay scheme on the β^- side to be that shown in Figure 3. The observed γ-γ coincidences and the 640-kev gamma ray must therefore be in the electron capture branch. The coincidence work is being done in collaboration with A.W. Sunyar, of the Physics Department. Additional work is being done to elucidate the decay scheme of I^{126}.

With the data obtained on the decay schemes of Ni^{57},[5] and I^{126}, it is now possible to recalculate the (γ,n) yields for the production of these two nuclides[2,11] with 100-Mev X-rays. On a plot of (γ,n) yield vs. atomic number

---

[11] M.L. Perlman and G. Friedlander, Phys. Rev. 74, 442 (1948).

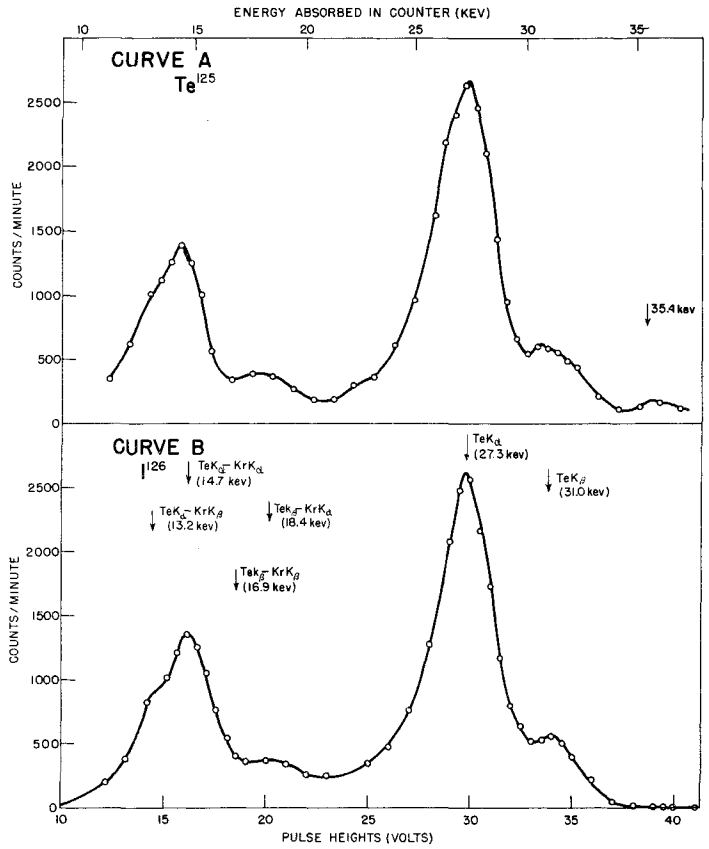

Figure 1 (Left). Pulse spectra from X-rays of Te^{125} and I^{126}.

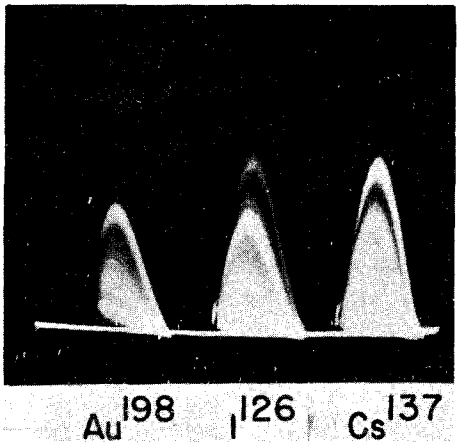

Figure 2. Pulse spectra from gamma rays of I^{126}, Cs^{137}, and Au^{198}.

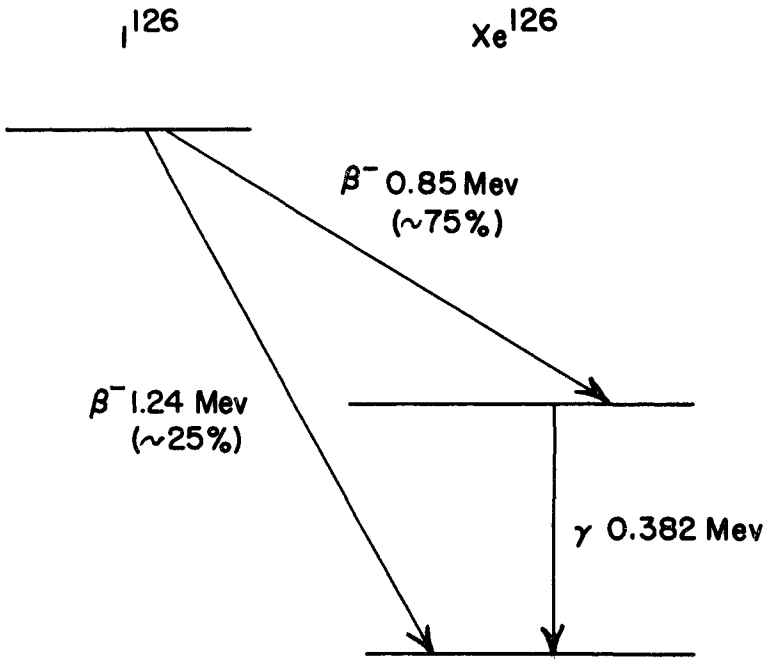

Figure 3. Negative beta decay of I^{126}. The electron capture and positron decay are not shown.

the new values along with other measured (γ,n) yields fall on a smooth curve. This brings the yields measured by the activation method into better agreement with the measured neutron yields.[12,13] It would also appear from such a plot that the reported (γ,n) yields[11] of Ag^{108} and Pd^{109} are low. This may well be due to unknown major features in the decay schemes of these nuclides. It should also be noted that the reported value for the Sb^{121} (γ,n) yield[11] is too low because it is based on the yield of only one of two isomers.[14]

We wish to thank J. Bulkley for the neutron irradiation of iodine at the M.I.T. cyclotron.

[12]G.A. Price and D.W. Kerst, Phys. Rev. 77, 806 (1950).
[13]G.C. Baldwin and F.R. Elder, Phys. Rev. 78, 76 (1950).
[14]M. Lindner and I. Perlman, Phys. Rev. 73, 1124 (1948).

NUCLEAR RECOIL FOLLOWING NEUTRINO EMISSION FROM Be^7

R. Davis

Introduction

An experiment to measure the nuclear recoil energy from neutrino emission in the electron capture decay of Be^7 was described in an earlier report.[1] In this experiment the recoil source was prepared by vacuum distillation of Be^7 onto a freshly distilled LiF surface, and the recoil spectrum was observed with a low-resolution electrostatic analyzer. The recoils observed exhibited a nearly continuous spectrum with a sharp cutoff on the high energy end. An additional experiment has been performed with an evaporated source in the same electrostatic analyzer set at a higher resolution with far more satisfactory results.

The isotope Be^7 decays according to the following scheme:

$$Be^7 + e_K \longrightarrow Li^7 + \nu + 0.864 \text{ Mev} \quad (90\%)$$

$$\left.\begin{aligned} Be^7 + e_K &\longrightarrow Li^{7*} + \nu + 0.384 \text{ Mev} \\ Li^{7*} &\longrightarrow Li^7 + \gamma\,(0.480 \text{ Mev}) \end{aligned}\right\} (10\%)$$

In 90% of the electron capture decays, 0.864 Mev of energy is emitted in the form of neutrinos, leaving the Li^7 nucleus in its ground state. If the energy

[1]BNL Quarterly Progress Report (BNL 64 (S-6)), p. 83.

is carried by a single neutrino, the momentum of the recoiling nucleus must be equal to the momentum of the emitted neutrino, with the result that all Li^7 nuclei should recoil with the same momentum. The energy of recoil based on the emission of a single neutrino of 0.864 Mev is 57.3 ev. However, if the energy is emitted in the form of several neutrinos in random directions, the momentum of the nucleus will be equal and opposite to the resultant of the momenta of the neutrinos; and the recoil energy of the nucleus will then vary from a maximum of 57.3 ev down to zero, exhibiting a continuous recoil spectrum. An experimental determination of the energy spectrum of the recoiling Li^7 atoms can thus distinguish between these two alternatives of a line or continuous spectrum.

Experimental

The electrostatic analyzer used in these experiments was described in the previous progress report.[1] The analyzer was modified for these experiments by the addition of two slits, one 3/16" wide at the entrance, and one 1/16" wide at the exit. This improved the resolution of the analyzer by a factor of about five over the previous arrangement. To test the resolution of the analyzer the tungsten ribbon source to be used in the experiment was set in place and heated to a temperature at which it emitted thermal ions (about 550°C). A fixed voltage was placed between the tungsten ribbon and the entrance slit, so that monoenergetic ions of known energy entered the analyzer. The peak was then measured in terms of the counting rate for various voltage settings on the analyzer plates. The half-width of these peaks was then taken as a measure of the resolution of the analyzer. The results are listed in Table 1.

Table 1

Energy of the Ion (V)	Half-Width of Peak (V)
8.24	0.62
46.05	1.02
92.59	1.86

The source used in the recoil experiment was prepared by evaporation of a hydrochloric acid solution of carrier-free Be^7 on the tungsten ribbon used above. The ribbon was installed in an auxiliary vacuum system and heated to 1560°C by means of a current passing through the ribbon. At this temperature most contaminating material was distilled from the ribbon along with about 90% of the Be^7, leaving the tungsten ribbon clean in appearance. The source, comprising the remaining Be^7, was then removed from the vacuum system and installed below the entrance slit of the electrostatic analyzer. Connections were made so that the ribbon could be heated in this position by a current passing through it. Measurements of the temperature of the ribbon were made with an optical pyrometer. A temperature versus current curve was prepared,

so that the temperature of the ribbon could be estimated from the heating current.

After a satisfactory vacuum (5×10^{-7} mm Hg) was obtained, the ribbon was heated to 1200°C to be outgassed. Prior to this operation no recoils could be observed. A series of measurements were made of the recoil spectrum, with the source at various temperatures, from room temperature to 300°C, and under a variety of preliminary heat treatments. The spectra showed a trend toward greater yields of high energy ions, with more and more vigorous thermal treatment of the source. Under these conditions, a strong peak was observed at the high energy end. To obtain the spectrum shown in Figure 1(a), the ribbon was flashed at 1000°C for 15 sec prior to each measurement, and then counts were taken immediately for a 3-min period at 300°C. The number of counts was recorded at 15, 30, 60, 90, 120, and 180 sec to note whether there was any change in the counting rate with time; however, there was no noticeable change within the statistical errors for the period observed. The points shown in the figure were 3-min averages.

The shape of the peak is consistent with a monoenergetic recoil ion of energy in the neighborhood of 55 v degraded in energy by collisions with surface contaminants. The curve is less steep on the low energy side, but at 30 v the counting rate is about 25% of the counting rate at the center of the peak. The curve is definitely in favor of the single neutrino hypothesis discussed in the introduction.

Since the aperture of the analyzer becomes narrower at low energies, as shown by the measured half-widths of the peaks obtained with monoenergetic thermal ion sources, it is clear that as one moves down the voltage scale the over-all geometry of the apparatus decreases. To reduce this effect, an accelerating potential V was placed between the tungsten ribbon source and the entrance slit. All ions entering the analyzer then have in addition to their recoil energy an energy of V electron volts, thus shifting the whole spectrum along the energy scale.

A number of spectra were observed at series of fixed accelerating potentials, 23, 46, and 92 v. The spectrum observed V = 46.4 v is reproduced in Figure 1(b). The shape of the spectrum is similar to that obtained without the accelerating potential, Figure 1(a), except that the low energy side is lifted, exhibiting a peak corresponding to nearly zero energy. There is some slope to the low energy side of the low peak, hence these ions are believed to have a few volts energy. The appearance of the high energy peak is about identical to that in Figure 1(a), only, of course, the over-all counting rate is higher. At other accelerating potentials, 23 and 92 v, respectively, similar spectra were obtained; the major effect was an over-all increase in counting rate with increasing accelerating potentials. In general, the low energy peak increases in height somewhat faster than the high energy peak. The low energy peak is not produced by thermal ions formed by holding the ribbon at about 300°C, since the height of the peak remains the same if the temperature is lowered to room temperature. It is, however, possible that the accelerating potential between the source and the entrance slit increases the geometry for low energy ions and thus exaggerates the height of the low energy peak. Experiments to test this point are in progress.

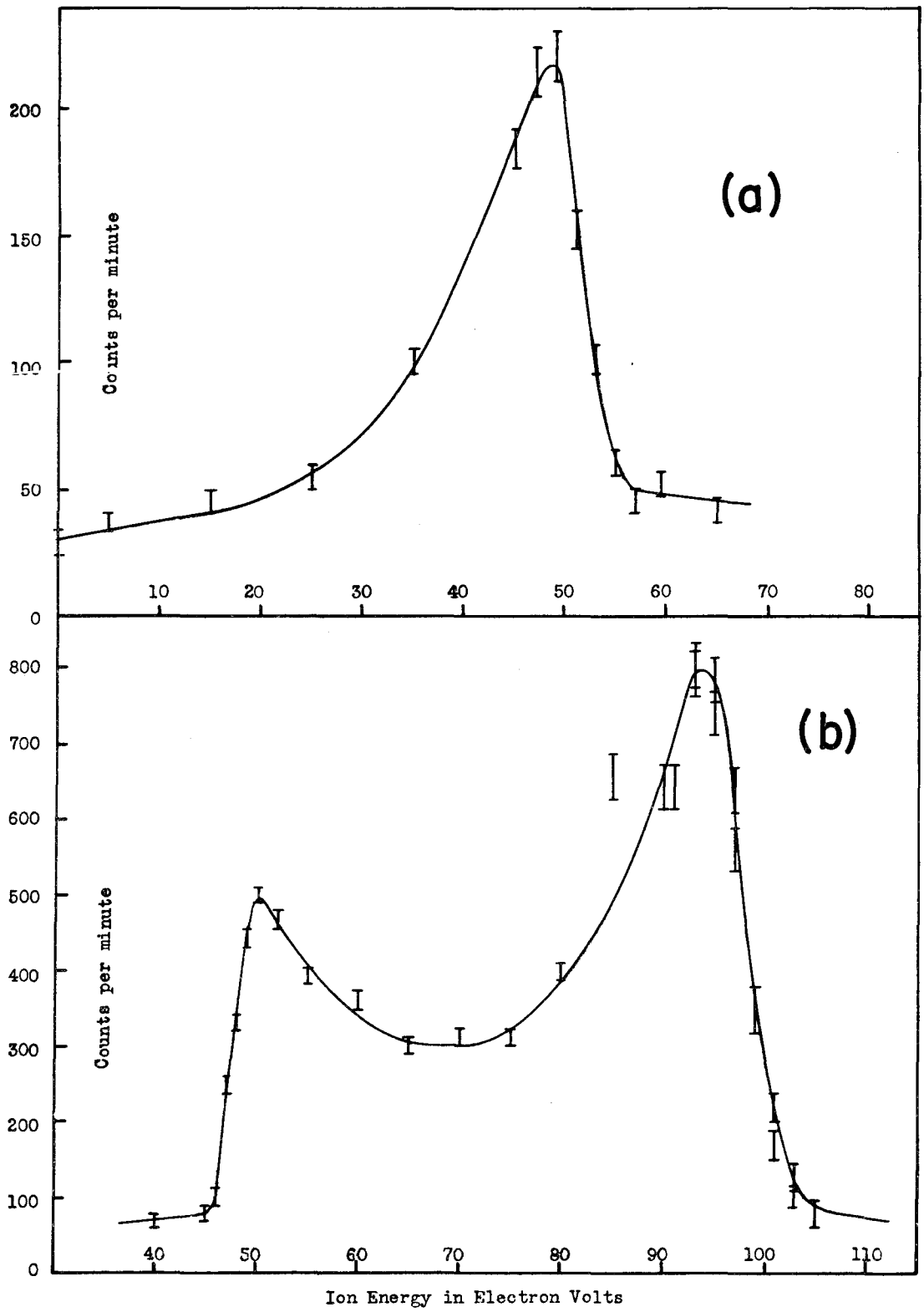

Figure 1. Nuclear recoil spectra from neutrino emission in Be^7 decay. (a) Curve obtained without accelerating voltage, and (b) Curve obtained with 46.4 accelerating voltage.

The energy scale in these experiments was established from the voltage on the plates of the analyzer and the radii of curvature of the plates. This was checked as described with thermal ion sources placed in the apparatus, or with the recoil source itself heated to a temperature sufficient to produce thermal ions in abundance far exceeding the feeble recoil ion current. The position of the peak was measured and was compared to the accelerating potential on the ions; these differ by a fixed voltage which corresponds to the difference in contact potential between the source and the brass analyzer. However, when a recoil spectrum was studied with a fixed accelerating potential between the source and the slit as in the case of the one represented in Figure 1(b), the maximum energy of the recoiling ions free of the contact potential can be read off directly as the difference in energy of the low and high energy sides of the spectrum. A subtractive correction must be applied to take into account the resolution of the apparatus. The spectrum in Figure 1(b) was analyzed in this manner and a value of 54.8 ± 1.0 ev was obtained for the maximum energy of the recoil ions. This value is to be compared to 57.3 ev minus the binding energy of the Li^7 ions to the surface. The measured value is reasonable since the binding energy to the surface is expected to be in the neighborhood of 1 or 2 ev.

Reactor Evaluation and Physics

On August 11, 1950, the reactor was turned over to Brookhaven National Laboratory by the H. K. Ferguson Co., the latter having finished their work of repair and construction. Loading was started immediately thereafter and criticality was achieved on August 21. The critical mass of the normal uranium fuel was substantially that of the design figures adjusted for the data taken in the subcritical experiments at the beginning of the year. The flux distribution was determined for various loadings and the temperature and barometric coefficients of reactivity was measured at low power operation (less than 500 watts). In addition, tests were made on the cooling air flow characteristics of the reactor in anticipation of high level operation. Further details of the preliminary tests on reactor operating characteristics will be found in the classified progress report of the Reactor Science and Engineering Department, as well as in forthcoming reports on the Brookhaven National Laboratory reactor start-up evaluation.

Radioisotope Production

During the early part of this report period, three tracer runs and a cold run were attempted. From these it was apparent that the sodium di-uranate precipitate obtained in the first step of the Te separation process was too difficult with which to work. The volume of precipitate was too large and the filtering time was much too long.

Accordingly, the process was changed. Instead of precipitating the uranium from the Te, the uranium was complexed and Te was precipitated as the first step. Several complexing agents were tried, among them ammonium carbonate, sodium carbonate, sodium peroxide, salicylic acid, and gallic acid. The agent chosen as the best is a mixture of sodium citrate and ammonium carbonate. This mixture permits the Te to be precipitated at a pH of approximately 6 using a combination of $NaHSO_3$ solution and SO_2 gas.

The idea was conceived of using slugs made of pressed uranium turnings rather than the pressed oxide, foil-wrapped slugs used heretofore. Pressing and canning is simpler and there is no danger of rupturing the slug during the jacket-dissolving step, as there was when the oxide slugs were used. The turnings are dense enough so that none are lost when the jacket solution is decanted. Dissolving time for the uranium turnings is about one hour, compared to about thirty minutes for the pressed oxide and several hours for the massive metal.

Both a cold run and a tracer run have been made successfully, using the new complexing step and the pressed turning slugs.

The present equipment will be placed in hot cell #1 and several cold and/or tracer runs will be made before going up to the high level.

The iodine generating vessel and the shipping shield and its accoutrements are well under way. The former is being built and the latter is in the mock-up stage.

Considerable time was spent in designing, building, and assembling the process equipment. Included in this equipment is a miniature diaphragm value, designed by the Hot Laboratory Operations Group. Arrangements are being made to have this valve manufactured.

(L. G. Stang, Jr., W. D. Tucker)

Shielding

Facilities

Those facilities required for the measurement of attenuation by the Brookhaven National Laboratory's shield of radiation from the slow reactor have been completed. Uranium bars for the source plate which simulates a fast reactor have been received. They have been straightened and are in the process of being milled for fitting together to form a solid plate. Design of the shielding tank and the associated water system of source plates and slow neutron shutters has been stabilized, and construction has begun. Additional mechanical equipment is in the process of design and construction.

Instrumentation

The instruments to be used in testing the Laboratory's shield have been decided on. Most have been obtained and others are expected daily. Victoreen ion chambers, health physics film, and G-M tubes will be used to measure gamma-ray attenuation. Indium and gold foils will be used to measure slow neutron attenuation. Use of sulfur and photographic plates impregnated with fissionable materials is planned for measurements of fast neutron attenuation. Because of possible ionization due to slow neutrons, aluminum cans to hold the Victoreen chambers have been made and coated with a B_4C and Glyptol mixture. Measurements made with a slow neutron source have shown that with this precaution, slow neutron effects will be negligible.

Measurements of attenuation by the Laboratory's shield are expected to begin by the middle of October.

(M. Fox, H. Kouts, A. Rand)

Permanent Disposal of Radioactive Wastes

The investigation of the use of clays of the montmorillonite group for the ultimate disposal of long-lived fission wastes is being continued. In a recent

report* we presented some values of the ion exchange capacities of certain montmorillonite clays. In addition, the effect of high temperature dehydration of the clay on the rate of release of exchangeable strontium was shown. Some of these release experiments have been continued for more than six months. The results show that high temperature treatment causes a decrease in the rate at which strontium ions are replaced by barium ions, the clay designated as R-2532* exhibiting the most favorable properties. A series of similar experiments using mixed fission products is now in progress.

Preliminary replacement tests on unheated active clay showed that the replacement of fission products by barium ions was not complete. Further tests were carried out using a sodium chloride solution and several solutions of nitric acid of different concentrations. It was found that 2M NaCl, 1M $BaCl_2$, and 2-8N HNO_3 removed, respectively, 20%, 60%, and 100% of the adsorbed activity. In addition, the efficiencies of removal of activity by distilled water and by a synthetic sea water were determined for each of the clays at several dehydration temperatures.

As a further step in the study of the interaction of fission products and well-characterized soil minerals, a study is in progress of the absorption of cesium from chloride solutions by montmorillonite clay (designated by the American Petroleum Institute as No. 23). According to P. F. Kerr and his collaborators,** this clay has approximately the composition given by the formula

$$(Al_{1.51}Fe_{0.13}Mg_{0.40})\ (Al_{0.07}Si_{3.93})\ O_{10}\ (OH)_2\ (Na_{0.02}\ \frac{Ca}{2}\ 0.37)$$

This formula implies a maximum exchange capacity of 1.05 milliequivalents/g. The present work points to a value of 1.036 meq/g. The agreement here is certainly as close as could be expected.

A considerable number of equilibrium experiments have been made, and the data have been correlated in various ways. However, no entirely satisfactory result has been obtained, although the summary given by the Rothmund-Kornfield equation** with $K = 32.85$ and $p = 0.917$, would produce better than qualitative predictions as do the results under various conditions of concentration.

(L. P. Hatch, W. S. Ginell)

Waste Concentration

During the past review period, the Waste Concentration Group has been carrying on the following tasks:

*BNL Conference Report, Waste Processing. I, March 27-28, 1950, pg. 19 (BNL 58 (C-11)).

**Kerr, P.F. et al., "Occurrence and Microscopic Examination of Reference Clay Mineral Specimens," Columbia University, N.Y., April, 1950.

1. Evaluation of experimental pilot plant data,
2. Installation, instrumentation, and shakedown of the semi-works compression distillation still,
3. Aiding contract negotiations for the process and mechanical design of the proposed low level waste concentration plant.

Pilot plant data are still being evaluated and are yielding much interesting information on the mechanism of the removal of fine liquid and solid particulates from vapor streams. A report covering this phase of investigation will be ready for publication shortly.

As reported in BNL I-10, BNL 49 (T-16), and BNL 59 (C-12), pilot plant data have indicated that the dilute, slightly contaminated liquid wastes expected by the Laboratory can be processed by either of two evaporative methods, with a decontamination factor of 10^6 from feed to product. An economic evaluation of the waste concentration project was reported in BNL 59 (C-12), and indicated that compressive distillation showed advantages over standard evaporative methods for conditions at this site.

Based on this and other considerations, an 85 gph compression distillation still, constructed of nonferrous materials, and modified to suit the Laboratory's requirements, was purchased and installed in the semi-works area of the hot laboratory. Plumbing, acceptance tests, and instrumentation are now complete; shakedown runs are now nearing completion, and heat and material balances are being calculated. Plans for the next quarter call for hot runs using 1) phosphorous, and 2) mixed fission product activity. Hot run semi-works data will then be available for process design of the full-scale waste concentrating plant.

Two brochures, entitled "Technical Information on a Waste Concentrating Plant," and "Economics of Liquid Waste Disposal" (B. Manowitz), have been made available to various engineering design and construction companies interested in the process design, mechanical design, and construction of the waste concentrating plant. Bids have been received and reviewed; contract negotiations are still in progress.

(B. Manowitz, R. H. Bretton, R. V. Horrigan)

Meteorology

Instrumentation

Two new smoke detection instruments have been completed by the Electronics and Instrumentation Department for the Meteorology Group. A new ground level densitometer embodies a number of improvements that provide greater sensitivity and stability than has been obtained with either of the earlier models. On its most sensitive scale, the instrument is capable of measuring 16×10^{-3} mg of oil-fog per cubic meter of air. In addition, a second model of the airborne densitometer has been used successfully to obtain measurements of oil-fog concentrations aloft under temperature inversion conditions.

The investigation of oil-fog particle size distribution (BNL-48, BNL-64) has continued. Samples from the calibration room and field generator have been compared, using both the cascade impactor and the "Owl." Preliminary results indicate that, although the particle size distribution is by no means homogeneous, the calibration oil-fog and that produced by the field generators are nearly identical.

Members of the Group have long felt the need of a simple, accurate method of determining oil-fog concentrations that requires neither a large staff nor extremely intricate equipment. The investigation of a fluormetric method of oil-fog concentration measurement was begun in July. This method involves the collection of oil-fog on a suitable filter and the comparison of its fluorescence with calibrated samples. Preliminary indications are that the method is superior to gravimetric measurements, at least where low concentrations and relatively short sampling periods are involved.

The bivane developed by the Meteorology Group (BNL-48, BNL-64) has been in continuous use at 355' above ground throughout the report period. The early records from the instrument indicated that when thermally induced turbulence was present, ascending gusts were of shorter duration and higher speed than the descending gusts. Although this agrees with observations made at higher levels in the atmosphere, it was felt that the difference might be induced by the aerodynamics of the boom, pipe support, and housing of the instrument. It was, therefore, operated in an inverted position for several weeks. A careful comparison of the normal and inverted records indicate that the vane is responding normally, and that the vertical gustiness is of this form.

Oil-Fog Tests

Eight additional oil-fog tests, in which the two new densitometers were used extensively, were completed during the Summer. On September 6, 1950, the new airborne instrument relayed the first accurate measurements of oil-fog concentration to the ground.

The other seven tests made use of the ground densitometers, and served to fill gaps in the existing data or to check earlier results that were of doubtful value.

Reactor Start-up

Considerable effort was devoted to the analysis and prediction of meteorological conditions important in the reactor start-up period. The Group was particularly active in the determination of barometric and temperature coefficients of reactivity. A Bendix-Friez microbarograph has been converted for use in future reactor tests. A new gearing system provides a chart speed of 0.8 in./hr; frictional drag of the pen is substantially reduced. Readings accurate to ± 0.1 millibar and ± 1 min are easily obtained.

In association with the Health Physics Division, detailed plans have been made for the initial measurements of ground-level radiation dosage from the reactor effluent. When the reactor begins operating at power levels greater than 1 megawatt, joint health physics-meteorology tests will be made to determine

the adequacy of the radiation dose-rate templates (BNL-48, BNL-64).

(M.E. Smith, P.H. Lowry, D.A. Mazzarella)

Geology

The principal progress made during this period was an increased realization of the complexity of the problem of setting up a network of water sampling points for routine ground water monitoring. Enough samples of ground and surface water have been taken and analyzed by this time to establish the background conditions, both for chemical content and for activity. The choice of sampling points for this purpose is relatively easy, but the sampling points for routine monitoring must be chosen so that they provide the maximum possible assurance that they will detect any contamination. This assurance can only be provided by knowledge of the pattern that the contaminated water will assume as it is carried through the ground, and in particular of the manner in which the width of the contamination will increase as it moves farther and farther from its point of origin.

To detect any possible leak from a point or area, the sampling wells must cover an arc that will include the direction of movement from the source, and must be spaced closer together than the width of the contamination when it passes the sampling wells. It was learned, partly from unsuccessful tracer experiments and partly from a review of theoretical considerations, that not enough is yet known to locate sampling wells to meet these conditions.

A review of the results of some of the earlier pumping tests has given a value for the transmissibility of the glacial outwash aquifer of about 300,000 gal/day/ft. In the area of the Laboratory, where the scope of the water table is about 5 ft to a mile, this would give a rate of flow of about 1.25 ft/day. This rate is higher than that obtained so far from tracer measurements, but less than that tentatively calculated from the annual average recharge to the water table. More work will be required to reconcile the results of these separate determinations of the same quantity.

(W. de Laguna)

BIOLOGY DEPARTMENT

Biological Effects of Radiations

Microchemical Analysis of Nucleic Acids in Normal and Irradiated Cells

Work is continuing in an effort to establish a method for the measurement of nucleic acids in fixed sections of cells. The method described in the last progress report has recently been questioned by several investigators. Consequently, a series of experiments has been undertaken on extracts from the cells of Lilium longiflorum. The extracts were analyzed by conventional methods for the determination of nucleic acids and also by the ultraviolet absorption method developed at the Laboratory. A preliminary analysis of the data indicates that there is little quantitative agreement between the different methods. Work is in progress to determine the origin of the discrepancies.

At the same time, work is in progress in conjunction with members of the Chemistry Department to perfect a recording spectrograph which will give a continuous absorption spectrum of a small portion of a single cell through the ultraviolet and visible portions of the spectrum. It is hoped that a number of the difficulties in nucleic acid determinations will be resolved when this apparatus is perfected.

The work on the cytochemical analysis of the effect of 20,000 r of X-rays on the nucleic acids of living and fixed Trillium pollen mother cell nuclei, as described in the last progress report, has continued. The analyses seem to indicate that there is virtually no change in the nucleic acid content of the nucleus following irradiation of either living or fixed cells. However, if the cells are subjected to a slow hydrolysis which brings about the degradation of the nucleic acid molecule, then it is found that the nucleic acids of the cells irradiated after fixation are hydrolyzed many times faster than the controls, while the cells which are irradiated in the living state are hydrolyzed much slower than the controls. This is quite a surprising result and would seem to indicate that the effect of radiation on the cell nucleus is not a destruction of the essential molecules, but rather a weakening of certain bonds which probably would impede the normal function of these molecules. Moreover, in the living cell, the insult of irradiation seems to be counteracted by a "repair reaction" which over-compensates and eventually leads to increased polymerization and resistance to degradation.

An attempt is being made to correlate these cytochemical changes with the morphological changes observed during cell division. It has been found that the normal pattern of changes in chromosomes which takes place during cell division is altered following irradiation of the cell. It appears now that it may be possible to explain this change in pattern by assuming that the effect of the radiation is to inhibit the synthesis of nucleic acids. An increased polymerization of the acids may well be responsible for the difficulty in synthesis.

Needless to say, these rather sweeping conclusions will have to be verified in many different ways before they can be accepted, and they are presented here only to indicate the trend of thinking relative to the problem of the fundamental action of radiation on cells.

(A.H. Sparrow, M.J. Moses, R. DuBow)

Action of X-Rays on Enzymes

Experiments have been done at the Laboratory in collaboration with Dr. A. Sussman, of the University of Michigan, on the effects of X-rays on tyrosinase, an enzyme obtained from potato tubers. Both whole potato tubers and the isolated enzyme were irradiated and in both cases an increase in enzyme activity was found.

(A.H. Sparrow)

Effects of Chronic Gamma Irradiation on Plant Growth

The 16-curie cobalt gamma irradiation field was used in studying the effects of various dose rates of chronic irradiation on regeneration in Tradescantia and the growth of the lily and the broad bean. Tradescantia, cut back to 2" above ground line at time of setting out, was allowed to make new growth at dosages of approximately 128 r, 82 r, 67 r, 55 r, 30 r, 22 r, 15 r, 10 r, 8 r, and 5 r per day. There was complete lack of regeneration at 128 r/day, with successively better growth as dosages decreased. Growth at 10 r/day was apparently normal. Within the affected range, there were foliar, floral, and shoot abnormalities in combinations unique to each dosage level. Histological studies are being carried out on this material by Dr. J.E. Gunckel of Rutgers University.

In the lily, growth and flower development were inhibited by dosages greater than 60 r/day, but no obvious structural abnormalities appeared in the plants. Broad bean seeds germinated, but growth and flower development were inhibited at dosages above 34 r/day. Plants growing at 22 r/day flowered but bore no fruit. At 5 r/day, growth and fruiting seemed normal. Leaves in a high dosage plant were thickened and abnormal in shape.

(A.H. Sparrow, E. Christensen)

Effects of X-Rays on Fibrinogen

In collaboration with Dr. H.A. Scheraga of the Chemistry Department at Cornell University, a study of the effects of X-rays on aqueous solutions of fibrinogen has begun. The problem has a two-fold interest: mechanisms by which ionizing radiations affect aqueous solutions of biological materials, and the identification of the changes in the structure of native fibrinogen and the correlation of such changes with the thrombin-induced clotting activity in irradiated solutions. The second aspect of such studies contributes

toward an understanding of the physiological function of fibrinogen, namely fibrin formation and the clotting mechanisms in blood.

Preliminary experiments have been done in which a solution of bovine fibrinogen has been irradiated with two-million volt X-rays. The X-rays were obtained from a gold target placed in the electron beam of the Chemistry Department's electrostatic generator; the irradiations were made possible through the courtesy of A.O. Allen of the Chemistry Department.

Solutions that had received doses up to 300,000 r units at dose rates up to 140 r/sec were assayed for fibrinogen activity, viscosity, ultracentrifuge patterns, and absorption spectra. The irradiation produced a marked increase in the viscosity of the solutions and there seems to be a linear increase in the log of the specific viscosity with dose. Along with this increase in viscosity, there is also an increase in turbidity. With very high doses the solutions formed a rigid gel 2 - 3 hr after irradiation, but there was no tendency toward a gel formation at dosages below 300,000 r.

Simultaneous studies of the total amount of protein clottable with thrombin seemed to indicate no loss in clotting activity, i.e., the irradiation at doses up to 300,000 r had not greatly altered the biological activity inherent in the native fibrinogen. However, the character of the clot changes somewhat. Up to doses of 130,000 r, the clots exhibit normal synergetic properties, but the solutions obtained from the higher doses produce clots that are more compact and that break up upon slight mechanical disturbance. This behavior is all the more remarkable since the ultracentrifuge examination shows that only 14% of the original fibrinogen was present after a dose of 300,000 r.

The ultraviolet absorption spectra of the irradiated solutions show a progressive decrease in transmission with increasing dose, the decrease being proportional to some reciprocal power of the wave length. However, at the present time, it is not possible to separate the effects of increased scattered light due to the turbidity of the solutions from possible changes in adsorptivity of the molecules.

The sedimentation velocity measurements show, in a striking fashion, some of the changes in the structure of the native fibrinogen with increasing dose. It is evident that aggregated, as well as low molecular weight fragments appear as a result of irradiation.

It is too early to give a complete interpretation of the results, but it appears that radical changes can be produced in the structure of the native fibrinogen molecule without changing its clottability. The observed increase in viscosity may be attributed either to uncoiling of peptide chains within the fibrinogen monomer, or else to a polymerization process that has been initiated which leads to higher degrees of asymmetry. The fact that material of higher sedimentation constant is formed indicates that polymerization processes are involved.

The native fibrinogen may be regarded as having a length of 700 Å and an axial ratio of 18 to 1, assuming that the bovine material is similar to human material. An end-to-end dimer formed from two fibrinogen molecules would have

a sedimentation constant of approximately 1.5 Svedberg units greater than the monomer in agreement with that found in the ultracentrifuge. By virtue of the increased asymmetry, such dimers, present to the extent indicated by the ultracentrifuge (16% at 130,000 r), could account for the increased viscosity. At higher doses where the clot character begins to change, the effects can not be accounted for by such a simple explanation. Careful examination of the ultracentrifuge picture indicates the presence of even higher polymers, produced in small amounts.

(L.F. Nims)

Radiation Effects in Mammals

It has previously been reported that there are two periods of polyuria occurring about the first and the fifth day after a single dose of X-rays to rats. A possible explanation of this phenomenon would be an inhibition of the pituitary, which would result in a decreased output of the antidiuretic substance. This possibility was tested in conjunction with Dr. W.J. Eversole of Syracuse University last Summer. Present results indicate that the serum of rats X-rayed with 600 r contains significantly smaller amounts of antidiuretic substance 24 hr after irradiation. However, 4 or 5 days after irradiation, the concentration of antidiuretic substance in the serum does not differ significantly from the controls. Furthermore, when irradiated rats are given a waterload about 24 hr after irradiation, they are able to eliminate this water at a significantly faster rate than are the controls. Again, this is not true at 4 or 5 days after irradiation. Thus, the early phase of diuresis after irradiation may be explained in part, at least, to decreased circulating antidiuretic substance. The later diuresis remains unexplained.

It has previously been shown that irradiation shortens the life span of adrenalectomized rats by about 50%. This fact is being used to determine the period after radiation when increased adrenal cortical secretion is required. Irradiated animals were adrenalectomized at various periods of time after irradiation, and survival time was noted. In another set of experiments, the adrenalectomized rat is being maintained on a minimum of adrenal cortical extract, and the amount of extract required to maintain body weight after irradiation is being determined. Preliminary results from these two experiments seem to indicate that adrenal cortical requirements are increased immediately after irradiation and remain high for about 3 days, after which they approach normal levels.

(A. Edelmann, S. Katsh)

Effects of Radiation on Seeds

In previous studies, it has been shown that X irradiation of corn seeds in amounts sufficient to stunt growth of the seedlings did not appear to result in a reduction in the staining of seeds in a solution of triphenoltetrazolium chloride (TPTZ). Thus, this dye which has been successfully used to test the heat and cold inactivation of seeds cannot be used for testing X-ray inactivation. At the present time, it is felt that this dye is a redox dye

which specifically stains the enzyme succinic dehydrogenase. Work is now in progress to test the succinic dehydrogenase activity by independent methods. Methods that seem satisfactory have been worked out and are now in the process of being tested.

(R. Van Reen)

Effects of Radiation on Bacteria

It has been found that bacteria grown in a solution containing P^{32} exhibit mutations more frequently than do the same bacteria grown in an equivalent irradiation field produced by X-rays. A double isotope experiment has been performed in an attempt to analyze this effect. It was shown that I^{131} was not taken up by the cells at all, and this isotope was then used to determine the amount of P^{32} which was actually taken up by the cells. The results of these experiments indicate definitely that the increased mutagenic effect is due to the presence of P^{32} within the cell.

(B.A. Rubin)

Effects of Radiation on Corn

The growing season of 1950 was almost ideal and many hand pollinations of corn were completed, as outlined in the previous quarterly progress report (BNL 64(S-6)). The hand-pollinated ears, as well as field-pollinated ears from crossing plots, are being harvested preparatory to making a genetic analysis of the mutations obtained. Preliminary observation on ears as they were harvested shows that many mutations were produced but the rate is yet to be determined.

One experiment was designed to determine what percentage of the "mutations" produced are really mutations and what percentage are chromosomal deletions. The recessive chromosome 9 stock c sh wx was pollinated by dominant pollen C Sh Wx from the Co^{60} gamma field. During the harvesting of the hand-pollinated ears, two kernels were found in which half of the seed had lost the C color factor. In both cases, the seeds were also recessive for sh (3.3 units from C), showing, in these two cases at least, the gene loss was a part of the greater loss of a piece of chromosome. Complete examination of the C losses will show how frequently losses of sh and wx accompany the loss of C, thus adding information on the nature of changes induced by gamma radiation from the Co^{60} source.

Several hundred plants of tall corn in the gamma field were pollinated by pollen from several of the various short genetic types growing in the clean field. Since tall is dominant, such pollinations will produce tall plants, with the exception of short types induced by the radiation. Enough seed is on hand for 15 to 20 acres of corn which will be examined for short plants. Arrangements have been made with the Suffolk County Home to grow this crop. They will do all the operations concerned with growing the crop and will harvest the grain produced. Laboratory personnel will go through the field and note the percentage of short corn of the different types. Through this

cooperative arrangement a much larger number of plants can be examined than if no outside facilities were used. Large numbers are essential in determining mutation rates of fairly low frequency.

A good crop of tobacco seed (N. rustica) was harvested from plants receiving different amounts of radiation in the Co^{60} field. This was grown for E.G. Beinhart of the U.S. Department of Agriculture, and a good supply of seed will be sent to him. Also, with Beinhart's permission, part of the seed produced will be sent to Dr. F.O. Holmes of the Rockefeller Institute for Medical Research, New York City. Dr. Holmes is also interested in mutations induced. In addition to the seed produced under continuous radiation in the field this Summer, seed of N. rustica and N. tabacum have been given comparatively high doses of 24,000, 48,000, and 99,000 r by exposing in the lucite box close to the source. By use of this apparatus, seeds are placed only a few cm from the source and receive approximately 6,000 r/hr.

Seeds of other crops grown in the gamma field will be harvested and sent to the different cooperators, as outlined in the last progress report.

(W.R. Singleton)

Tracer Studies of Biological Problems

The Mechanism of Glycolysis

A rather extensive investigation has been undertaken to prove the correctness of the Embden, Meyerhof, Parnas glycolysis scheme. It has been possible to produce glucose in which different carbon atoms were labeled. Following a degradation, the final products were isolated and, from the position of the label in the lactic acid or ethyl alcohol, the glycolysis scheme could be verified. The first part of the program involved an investigation of the synthesis of lactic acid by a homofermentative lactic acid bacterium, L. casei. An analysis of the degradation products confirmed the Embden, Meyerhof, Parnas glycolysis scheme for this bacterium, except for one point. About 3% of the label did not appear in the expected position. A similar result has also been reported recently for the case of yeast and the reason for this shift is now being investigated.

Next, the mold, Rhizopus oryzae, an organism which degrades glucose to lactic acid, ethyl alcohol, and CO_2, was investigated. An analysis of the labeled degradation products shows that this mold anaerobically forms lactic acid, ethyl alcohol, and carbon dioxide in a ratio 1:1:1. When glucose-1-C^{14} was fermented, about 50% of the label appeared in the methyl carbon of lactic acid and 50% in the methyl carbon of ethyl alcohol. A small amount appeared in the carboxyl carbon of the lactic acid, but this was found to be due to CO_2 fixation, presumably by the Wood-Werkman fixation reaction. When glucose-3,4-C^{14} was fermented, 50% of the activity appeared in the carboxyl carbon of the lactic acid and 50% in the produced CO_2 This organism did not show a shift of 3% of the label. Also, by comparing the specific activity of the lactic acid with the specific activity of the glucose -- which activities were

equal -- it could be shown for the first time that endogenous reserves were not entering the reaction. The next organism investigated (in conjunction with I.C. Gunsalus of the University of Illinois) was Luconostoc mesenteriodes. This organism produces lactic acid, ethyl alcohol, and CO_2 in a ratio 1:1:1 in the same way that R. oryzae does. However, an analysis of the degradation products shows that fermentation does not go according to the Embden, Meyerhof, Parnas scheme. The organism is the first one uncovered which lacks the enzyme isomerase that catalyzes the reaction between dihydroxyacetone phosphate and glyceraldehyde phosphate. The indications are that the dihydroxyacetone phosphate goes via acetate to alcohol. In this case, no 3% shift of the label occurred in the lactic acid. Thus, an entirely new scheme of enzymatic reactions have been uncovered; it will be investigated in the near future.

(M. Gibbs)

The Fate of Ingested and Injected Ascorbic Acid

A gas phase counting method for C^{14} has been developed which is 30 times as sensitive as the methane flow solid counter. This new method makes it possible to investigate the metabolism of uniformly tagged C^{14} ascorbic acid with the extremely small amounts of this material available. When labeled ascorbic acid was given to mice by stomach tube, about 75% of it was excreted within the first 24 hr and the remainder was presumably stored and excreted only very slowly. This material was excreted primarily by way of respiration, with the urine accounting for only about 10% of the first 24-hr excretion, and the feces about 20%. In contrast to this, when the ascorbic acid was given by intravenous injection, only about 55% was excreted in the first 24 hr and the rest was presumably stored and excreted rather slowly. In this case, almost all of the excretion was by way of the urine.

The results found for the excretion following intravenous injection are quite understandable. Here, the additional administered ascorbic acid should, to a considerable extent, be excreted in the urine in unaltered form. The results obtained in the feeding experiments were unexpected. It is believed that these may be ascribed to the action of intestinal microorganisms on the ascorbic acid prior to absorption through the intestinal wall so that the radiocarbon reaches the circulation to a large extent in some form other than as ascorbic acid. In order to establish this, it will be necessary to perfect a method for the separation of minute quantities of ascorbic acid. An attempt has been made to do this by means of two-dimensional chromatography, but the amount of activity is so small that a 2-month exposure leaves no spot on the film. It is planned to attempt to obtain larger quantities of labeled ascorbic acid and repeat the experiment.

(R. Steele)

Separation of Labeled Amino Acids

A column 4 cm in diameter and capable of accomodating the hydrolysate from at least 500 mg of protein has been set up for the chromatographic separation of amino acids. A fraction cutter has been devised with which it is

possible to separate about 16 amino acids from a hydrolysate. The method has been tested by quantitatively separating 14 labeled amino acids from a hydrolysate obtained by the sulfur bacteria technique.

(R. Steele)

Carbohydrate Metabolism in the Liver

Carbohydrate metabolism in the liver has been investigated in rats and mice made diabetic with alloxan. With respect to the composition of the acid-soluble phosphorus compounds, it is now clear that there is about 50% more inorganic phosphorus, and about 25% less ATP-ADP in the livers of the diabetics than in the normals. There is also significantly more free adenylic acid and less glucose-1- and glucose-6-phosphates in the liver of the diabetic rat.

So far as turnover data are concerned, the results show that there is no significant difference in the rate constant of the turnover of any of these phosphorus fractions between the normal and the diabetic animal.

These findings indicate, first, that the lesion in alloxan diabetes which prevents the liver from handling carbohydrate normally, cannot be ascribed to a defect in the operation of the phosphorylation cycle, and second, that they strengthen the indications furnished by previous experiments that there is an alternative pathway of carbohydrate metabolism in the intact normal cell -- one which does not involve the phosphorylation cycle.

(J. Sacks)

Iron Metabolism

It has been found that when duck blood is incubated with radioactive iron as the citrate, that part of the iron is incorporated in the hemin molecule. A series of experiments has been undertaken to determine whether or not the incorporation of the iron is a cellular process. Hemin was prepared from duck blood and incubated with radioactive iron for varying periods of time. It was found that the specific activity of the hemin reached a constant value relatively quickly, indicating that there was actual exchange of iron between that in the solution and that in the hemin molecule.

(J.R. Klein, L.M. Sharpe)

Iron Equilibrium in the Rat

Activity measurements on 8 tissues and the carcass from each of 8 rats transfused with tagged iron red cells and sacrificed periodically have now been collected and are in the process of being interpreted. It would appear that the specfic activity of the iron in heart muscle, spleen, liver, and leg muscle is similar to that in blood after 186 days. Consequently, it appears that the iron of these tissues does exchange with that of the blood. On the

other hand, the specific activity of bone and brain is about half that in blood, while that of kidney is about double.

(J.R. Klein, L.M. Sharpe)

The Influence of Blood Incompatibilities on the Measurement of Blood Volume

Work has been undertaken, in conjunction with Drs. Nickerson, Gregersen, and Root from Columbia University, in an effort to determine why the blood volume in animals as determined by the tagged red cell method is lower than when determined by the dye method. It was felt that this discrepancy could be accounted for, at least in certain cases, by blood incompatibilities. It is well known that if incompatible blood is injected into an animal there is a reaction between the injected blood cells and the circulating blood cells, resulting in a clumping of these cells. These clumped cells presumably would not be able to pass freely through blood capillaries and, therefore, there would not be a uniform distribution of these tagged red cells throughout the animal; one of the basic assumptions of the method would not be fulfilled. The attempt was made, in the case of a number of dogs, to estimate the degree of clumping which occurred between the injected cells and the circulating cells and to relate this to the discrepancy between the blood volume as measured by the tagged red cell method and by the dye method. It is difficult to put this on a quantitative basis, but indications are that this is a reasonable explanation of the discrepancy.

(L.M. Sharpe)

Mineral Metabolism

The metabolism of barium by *Drosophila* larvae has for some time been under investigation in the biology laboratory. The radioisotope tracer employed has been barium^{140}, which decays to lanthanum^{140}. Since the half-life of the barium is much greater than that of the lanthanum, an old sample of barium consists of an equilibrium mixture of activities, disappearing at the rate characteristic of the barium^{140} but actually consisting of more than 50% of lanthanum^{140} activity. Any deviation from this equilibrium composition will result in a changed shape of the decay curve that must be determined in these experiments if a given activity is to be assigned to one or the other isotope. Given good counting conditions, it proved possible to determine a 5% enrichment of either isotope.

In the course of the *Drosophila* studies, it was found that larvae on a barium^{140}-containing medium showed a lanthanum enrichment, if the medium had been inoculated with Texas Y-2 strain of yeast 24 hr before adding the larvae, but barium enrichment if the larvae had been placed directly on the sterile food. This appeared most explicable on the assumption that the yeasts were preferentially absorbing lanthanum, while the larvae, though preferring to feed on yeast cells, preferentially absorbed barium. In order to check this hypothesis, an investigation has been undertaken of the selective uptake by yeast cells of barium^{140} and lanthanum^{140}. The results of these experiments show a very positive discrimination in favor of lanthanum by this yeast, thus confirming the above explanation.

In an extension of this experiment, the effect of increasing concentrations of yttrium, aluminum, cerium, and neodymium on the uptake of lanthanum^{140} has been investigated in this strain of yeast. Preliminary results indicate that all of these trivalent ions increase the uptake of lanthanum.

A considerable amount of analytical work has been done on the accumulation by marine sponges of a wide variety of metallic ions. The data indicate that each different sponge has its own peculiarities with reference to accumulation to metallic ions. D. crawshayi is an accumulator of fluorine, potassium, and titanium, while D. etherea is not an accumulator of any of the common metallic ions. Chondrilla nucula is an accumulator of copper and sodium. Terpios fujax and Terpios zetaki are accumulators of titanium and, to a slight extent, of potassium, while the latter may also be an accumulator of manganese, tin, and vanadium. It was further found that one specimen of D. crawshayi is characterized by an extraordinary level of nickel accumulation. This is probably due to the activities of an irregularly occurring microfloral inhabitant. It is concluded that this sort of nickel accumulation is not of infrequent occurrence in several sponge species.

This type of information has important applications to the problems of radioisotope disposal.

(V.T. Bowen)

Publications

1. M.W. Holt, A semiautomatic injection apparatus for use with radioactive solutions, Science 112, 142-3 (1950)

2. L.M. Sharpe, G.G. Culbreth, and J.R. Klein, The blood and packed cell volume of the adult rat as measured by tagged cells, Proc. of Soc. for Biol. and Med. 74, 681-5 (1950)

3. M. Gibbs, On the mechanism of the chemical formation of lactic acid from glucose studied with C^{14}-labeled glucose, J. Am. Chem. Soc. 72, 3964-5 (1950)

4. S.A. Matthews, The effect of thiouracil on the uptake of radioactive iodine by the thyroid gland of summer frogs (Rana pipiens), Am. J. Physiol. 162, 590-7 (1950)

5. A.A. Bothner-By, M. Gibbs, and R.C. Anderson, The synthesis of L-ascorbic acid uniformly labeled with C^{14}, Science 112, 363 (1950)

6. B.A. Rubin, Radiation microbiology; problems and procedures, Nucleonics 7, 5-20 (1950)

MEDICAL DEPARTMENT

Division of the Hospital

During the report period, treatment of patients with thyroid carcinoma has continued. I^{131} has been used throughout. Patients with hyperthyroidism have also been treated with I^{131}. Sodium-24 has been used in tracer studies of extra-cellular fluid as detailed elsewhere in this report. Efforts are being made to better evaluate the maximum dose of iodine that can be tolerated by patients in an attempt to increase therapeutic efficiency of radioiodine.

(C. G. Foster, J. L. Gamble, Jr., J. S. Robertson, L. E. Farr)

Division of Pathology

Influence of Mechanical Injury, Radiation Injury, and Disease States on Body Protein Stores

The Division has continued work on the problems involving body protein metabolism during and following injury and other abnormal states, as presented in previous reports. The effects of radiation from the nuclear reactor will be investigated soon.

(S. C. Madden, J. A. Fancher, L. I. Gidez)

Division of Biochemistry

In further collaboration with the Biology Department, studies are being carried out on the metabolism of C^{14}-labeled compounds in mice.

(D. D. Van Slyke; R. Steele, Biology Department)

Chemical Anatomy of Body Fluids

During the review period, methods have been developed in the laboratory to determine antipyrine and sucrose in body fluids, to measure red cell mass *in vivo* with P^{32}-labeled red cells. Material for determination of total body water using deuterium has been obtained. Sodium space studies have been done on 12 different patients with more than one study being carried out on those patients whose body water status was changing.

(J. S. Robertson, C. G. Foster, J. L. Gamble, Jr., N. S. Deane, L. E. Farr)

Division of Bacteriology and Virology

Biological Effects of Radiation

Preliminary experiments with the recently established 72-curie source have been done on this problem; further biological calibration is presently under way.

(W. M. Hale, H. T. Gardner)

Homologous Tissue Immunity

Work is continuing on this problem with the main emphasis placed on whether or not active immunity against a spontaneous tumor is possible. The necessity of using spontaneous tumors makes the progress on this particular problem exceedingly slow. The spindle cell sarcoma, which grew with great rapidity in the other strain of mice, is not very satisfactory in the "infection-free" Swiss strain. We are attempting to find another transplantable tumor which will grow rapidly in the "infection-free" strain of mice so that these experiments may be resumed.

(W. M. Hale)

Immunology

Several experiments have been run on mice, using the new cobalt source of radiation, with very interesting results. Due to the preliminary nature of these experiments, however, it is not possible to make any definite statements at this time.

(W. M. Hale, H. T. Gardner)

Bacterial Metabolism

Considerable difficulty has been encountered in obtaining consistent results in the transformation of the pneumococcus. This seems to have been the experience of everyone who has worked with the transforming substance of the pneumococcus. Considerable work has been done in attempting to devise a method whereby the transformation will be consistent. A method, which holds some promise of solving the problem, is now being tried.

(Ruth M. Drew)